University of São Paulo
"Luiz de Queiroz" College of Agriculture

Coexpression network analysis of proteins and metabolites time-course of two contrasting *Eucalyptus grandis* reponses to *Austropuccinia psidii*

Ana Lúcia Mendes Pinheiro

Dissertation presented to obtain the degree of Master in Science. Area: Genetics and Plant Breeding

Piracicaba
2021

Ana Lúcia Mendes Pinheiro
Biotechnologist

Coexpression network analysis of proteins and metabolites time-course of two contrasting *Eucalyptus grandis* responses to *Austropuccinia psidii*

versão revisada de acordo com a resolução CoPGr 6018 de 2011

Advisor:
Prof. Dr. **CARLOS ALBERTO LABATE**

Dissertation presented to obtain the degree of Master in Science. Area: Genetics and Plant Breeding

Piracicaba
2021

Dados Internacionais de Catalogação na Publicação
DIVISÃO DE BIBLIOTECA – DIBD/ESALQ/USP

Pinheiro, Ana Lúcia Mendes

Coexpression network analysis of proteins and metabolites time-course of two contrasting Eucalyptus grandis responses to Austropuccinia psidii / Ana Lúcia Mendes Pinheiro- - versão revisada de acordo com a resolução CoPGr 6018 de 2011 - - Piracicaba, 2021.

100 p.

Dissertação (Mestrado) - - USP / Escola Superior de Agricultura “Luiz de Queiroz”.

1. interação planta-patógeno 2. *Eucalyptus grandis* 3. *Austropuccinia psidii* 4. metabolômica 5. proteômica 6. WGCNA ;I. Título

ACKNOWLEDGMENT

I would like to thank those who have helped and supported me during research process and my academic journey so far.

- Prof Dr. Carlos Labate, thank you for the oportunity of being part of your research group during the past two years. I am grateful for trusting my work and supporting me through the process;
- Conselho Nacional de Desenvolvimento Científico and Tecnológico (CNPq) for the scholarship (Process 132737/2019-1);
- Our laboratory specialist, Thaís Cataldi, thank you for all the knowledge shared on mass espectrometry, chromatography, extraction and for always being patient with my difficulties;
- Alline Sekiya and Fabricio Moraes for all the help with bioinformatics, statistics and different steps in this work;
- Mônica Labate and Juliana Fonseca, I am grateful for all the constant support and advices;
- I also would like to thank all the members of Max Feffer Laboratory of Plant Genetics/ESALQ-USP: to Andressa Ducatti, Hana, Thalita and Gustavo for good-fellowship; to Thiago Falda, Felipe Marques and Andressa Bini, who I didn't met, but established the basis and knowledge about eucalyptus rust in our laboratory.
- My gratitute to the extension groups GVENCK and GENt from ESALQ/USP and the science blog "Profissão Biotec" for the extra-academic skills and experiences.
- To all my friends from Brasília/DF, Piracicaba/SP, Alfenas/MG, São José dos Campos/SP, Araras/SP for all the happy moments and for always listening to my worries. Specially, thanks Isabella Tavares for the partnership during our master degree's process.
- I am grateful to my parents, Edna and Ezequiel, for always believing in me and encouraging me to move forward. My family, for understanding my absence at family events during the years I lived far from home and for supporting my decisions. My boyfriend, Tiago, for being the best partner in the past seven years

CONTENTS

RESUMO

Análise de redes de coexpressão de proteínas e metabólitos de dois genótipos contrastantes de *Eucalyptus grandis* infectados com *Austropuccinia psidii*

O desenvolvimento de técnicas ômicas, como a genômica, transcriptômica, proteômica e metabolômica auxiliaram no entendimento das respostas de plantas submetidas a diferentes estresses, incluindo estresse biótico, identificando mecanismos que determinam o sucesso do sistema imune de plantas ou a colonização e aquisição de nutrientes de maneira efetiva pelo patógeno. Entretanto, os rearranjos a nível molecular que ocorrem em espécies arbóreas em resposta a infecção por fungos, e como essas mudanças contribuem para o progresso da doença, especialmente envolvendo o metabolismo primário, ainda não são bem caracterizadas. No presente estudo, durante o período de 24h, plantas resistentes e suscetíveis a ferrugem de *Eucalyptus grandis* foram inoculadas e falsamente inoculadas com *Austropuccinia psidii,* fungo biotrófico de modo a caracterizar mudanças na abundância de proteínas e metabólitos nos dois genótipos selecionados. Metabolômica (GC-MS) e proteômica, utilizando o pacote WGCNA (Weighted Gene Coexpression Network Analysis) para integração dos dados, foram usados para contrastar as respostas dos genótipos resistentes e suscetíveis de *E. grandis* infectados com *A. psidii.* A análise integrada revelou potenciais diferenças temporais na fotossíntese e geração de espécies reativas de oxigênio, metabolismo de lipídeos, respostas pré-formadas e germinação dos esporos, metabolismo de aminoácidos, reforço da parede celular e produção de fitoalexinas. Os resultados indicam mecanismos moleculares chaves que caracterizam a interação entre *E. grandis* e *A. psidii*, conhecimento importante para o melhoramento da cultura a nível molecular.

Palavras-chave: Interação planta-patógeno, *Eucalyptus grandis*, *Austropuccinia psidii*, Metabolômica, Proteômica, WGCNA.

ABSTRACT

Coexpression network analysis of proteins and metabolites time-course of two contrasting *Eucalyptus grandis* responses to *Austropuccinia psidii*

The development of omics studies as genomics, transcriptomics, proteomics and metabolomics improved greatly our understanding of plant responses to different stresses, including biotic stress, providing insights on mechanisms that determine plant immune system success or pathogen invasion. However, molecular changes orchestrated by trees species in response to fungal infestation and how it is affecting disease outcome involving susceptibility or resistance responses, especially involving primary metabolism reconfigurations, remains poorly understood. Here, a 24h time-course of resistant and susceptible genotypes of *Eucalyptus grandis* were inoculated and mock-inoculated with *Austropuccinia psidii*, a biotrophic fungus responsible for rust disease in Eucalyptus, in order to characterize proteins and metabolites changes and divergences among the two selected genotypes. GC-MS based metabolomics and label-free proteomic analysis, were integrated using WGCNA package (Weighted Gene Co-Expression Analysis), to contrast resistant and susceptible responses in *Eucalyptus grandis* infected with *Austropuccinia psidii*. Integrated analysis revealed temporal divergences of protein-metabolites modules providing information of differences in photosynthesis and ROS generation, metabolism of lipids, spores germination, metabolism of amino acids, cell wall reinforcement, phytoalexins and defense responses. Our findings provide insights in key molecular mechanisms that underly the interactions between *Eucalyptus grandis* and *Austropuccinia psidii* and important features for enhancing molecular breeding efforts.

Keywords: plant-pathogen interaction, *Eucalyptus grandis*, *Austropuccinia psidii*, metabolomics, label-free proteomic analysis, WGCNA.

1. INTRODUCTION

Eucalyptus ssp. is a genus formed with more than 700 different species, widely planted due to the quality of its wood, accelerated growth, robustness and possibility of being used in many industrial agribusiness (e.g. pulp and paper, charcoal, fuel wood, wood panels and flooring, solid wood products). In Brazil, 77% of total area of 9 million hectares of cultivated trees are occupied with eucalyptus plantations, representing 1.2% of Brazil's Gross Domestic Product in 2019 with major contribution (46.5%) of paper and pulp industry (IBÁ, 2019).

Myrtle rust or eucalyptus rust is a fungal disease caused by *Austropuccinia psidii*, considered a major threat to Myrtaceae biodiversity and one of the most important diseases affecting *Eucalyptus* spp. (SILVA et al., 2020). *A. psidii* is a biotrophic fungus, which need to colonize and obtain nutrients from living host plant tissue, different from necrotrophs pathogens that kill and rot plant. Rust fungi mainly affects young tissues, being found in nursery seedlings, plants in clonal hedges, plants up to two years old in the field, and in young coppice, reducing productivity, causing losses of 30% in annual wood volume increase (BALINT-KURTI; HOLLAND, 2015; XAVIER et al., 2015). The main characteristic symptom of eucalyptus rust is the appearance of yellow pustules in infected leaves, which grows in diameter over infection time. In few days after spore release, initial infection spreads to younger tissues (MARQUES, 2016).

Due to its relevance, studies involving chemical control of *A. psidii* (BOAVA et al. 2010) and, mainly, genetic host resistance, with identification of rust-resistant genotypes and QTL identification (JUNGHANS et al, 2003; BRONDANI et al, 2006; MAMANI et al., 2010; ALVES et al., 2012; BUTLER et al., 2016) were performed. Several resistant materials were identified in years of research. However, little is known about the molecular mechanisms underlying resistance and susceptibility. To successfully colonize plant tissues, pathogens needs to overcome plant innate immune system, based on non-specific pre-formed defenses, including compounds with antimicrobial properties and a physical barrier composed of leaf waxes, and induced mechanisms of defense (MYSORE; RYU, 2004). Timely perception of pathogen attack are necessary for fast and efficient induced defense response, firstly as plant recognition of pathogen/microbe associated molecular patterns (PAMPs or MAMPS) using trans-membrane pattern recognition receptors (PRR) and proteins encoded by R genes, mostly containing important domains as nucleotide binding (NB) and leucine rich repeat (LRR), to recognize effector proteins produced by the pathogen (INRAM; YUN, 2020). After recognition, plants responses include early changes as cytoskeletal reorganization, cell wall fortification, generation of reactive oxygen species (ROS),

synthesis of metabolites and, later, development of programmed cell death khnown as hypersensitive response, responsible for limiting biotroph pathogen spread (ROJAS et al.., 2014).

Aiming to characterize the mechanisms involved in disease progression in resistant and susceptible *Eucalyptus grandis* genotypes infected by *A. psidii*., Leite (2012) and Xavier et al. (2001) analysed initial hours of infection, within 24 hours after inoculation (hai). Observing the germination of spores at 3 hai, apressorium development at 6 hai with penetration starting at 12hai in both resistant and susceptible genotypes. Xavier et al. (2001) observed haustorium development in susceptible (18hai) and resistant (24hai), while Leite (2012) observed only in the susceptible genotype at 24hai. Analysing structural aspects, Bini (2016) and Dos Santos et al. (2019) characterized wax composition in different genotypes and their involvement in defenses of *Eucalyptus* spp. Silva et al. (2020) analyzed essential oil composition of resistant and susceptible leaves with different ages, identifying limonene as an important metabolite involved in resistance to *A. psidii*. Santos et al. (2020) analyzed transcriptome profiles of 24hai infected E. *grandis* leafs with *A. psidii*, showing overexpression of photosynthesis and leucine-rich repeat (LRR) protein-related genes. Marques (2016) and Sekiya (2020) studied proteomic and secondary metabolite divergences among susceptible and resistant genotypes, indicating consistent activation of immunity-related proteins and metabolites involved in phenylpropanoids pathway after 12hai only in resistant genotype, while susceptible showed a suppression at the same time.

While progress has been made to characterize plant defenses, little is known about the role of primary metabolic pathways required for growth and development in supporting and regulating plant specialized responses (ROJAS et al, 2014). Focusing on primary metabolic changes, the present study performed metabolomics (GC-MS) and label-free protein analysis, to characterize two contrasting eucalyptus genotypes, resistant and susceptible, in response to *A. psidii.* Metabolite and proteomic data were integrated analysis using WGCNA (Weighted Gene Coexpression Analysis) R package (LANGFELDER; HORVATH, 2008), which relies on statistical correlations to assess the strength of relationship between two molecules, extensively used and originally developed for microarray or RNA-seq datasets. However, recently, the approach is also being applied to proteomic and metabolomic data analysis (PEI; CHEN; ZHANG, 2017; JAMIL et al, 2020). Co-expression networks provides information of groups of molecules, known as modules, whose expression or abundance profiles are highly correlated. Those modules are represented by eigengenes/eigenprotein, one principal molecule whose profile summarize module expression/abundance profile, providing a network reduction scheme, which can be used to correlate to external data in order to find important modules, clusters or

pathways involved in the studied disease or perturbation (LANGFELDER; HORVATH, 2007, JAMIL et al, 2020).

To complement previous studies in our laboratory, (LEITE, 2012; MARQUES, 2016; BINI, 2016; SEKIYA, 2020), the present work focus on proteomic and primary metabolism (metabolomics), analyzing the reconfiguration and alterations among susceptible and resistant genotypes, in a previously established infection time-course by Leite (2012). The current work provide the opportunity to evaluate cellular behaviors from a multi-level approach, identifying some potential metabolites and proteins involved in major biological processes affected by *E. grandis* rust infection, as photosynthesis, lipid metabolism, amino acid metabolism, cell wall reinforcement, proteasome and phenylpropanoids pathway and their differences between both genotypes.

REFERENCES

ALVES, A. A. et al. Genetic mapping provides evidence for the role of additive and non-additive QTLs in the response of inter-specific hybrids of Eucalyptus to Puccinia psidii rust infection. **Euphytica**, v. 183, n. 1, p. 27–38, jan. 2012.

BALINT-KURTI, P. J.; HOLLAND, J. B. New insight into a complex plant–fungal pathogen interaction. **Nature genetics**, v. 47, n. 2, p. 101, 2015.

BINI, Andressa Peres. **Estudo molecular do desenvolvimento de Puccinia psidii Winter in vitro e no processo de infecção em Eucalyptus grandis**. 2016. Tese de Doutorado. Universidade de São Paulo.

BOAVA, L. P. et al. Chitinase and peroxidase activity in different stages of eucalypt leaves after inoculation with Puccinia psidii and acibenzolar-S-metil. **Tropical Plant Pathology**, v. 35, n. 2, p. 124–128, 2010.

BUTLER, J. B. et al. Evidence for different QTL underlying the immune and hypersensitive responses of Eucalyptus globulus to the rust pathogen Puccinia psidii. **Tree Genetics and Genomes**, v. 12, n. 3, p. 1–13, 1 jun. 2016.

BRONDANI, R. et al. A microsatellite-based consensus linkage map for species of Eucalyptus and a novel set of 230 microsatellite markers for the genus. **BMC plant biology**, v. 6, n. 1, p. 20, 2006.

DOS SANTOS, I. B. et al. The Eucalyptus cuticular waxes contribute in preformed defense against Austropuccinia psidii. **Frontiers in plant science**, v. 9, p. 1978, 2019.

IBÁ. **Anual Report**. Available in: <https://iba.org/datafiles/publicacoes/relatorios/iba-relatorioanual2019.pdf>. Acessed: 12 jun. 2020.

IMRAN, Q.; YUN, B. Pathogen-induced Defense Strategies in Plants. **Journal of Crop Science and Biotechnology**, v. 23, n. 2, p. 97-105, 2020.

JAMIL, I. N. et al. Systematic Multi-Omics Integration (MOI) Approach in Plant Systems Biology. **Frontiers in Plant Science**, v. 11, p. 944, 2020.

JUNGHANS, D. T. et al. Resistance to rust (Puccinia psidii Winter) in Eucalyptus: mode of inheritance and mapping of a major gene with RAPD markers. **Theoretical and Applied Genetics**, v. 108, n. 1, p. 175-180, 2003.

LANGFELDER, P.; HORVATH, S. Eigengene networks for studying the relationships between co-expression modules. **BMC systems biology**, v. 1, n. 1, p. 54, 21 dez. 2007.

LANGFELDER, P.; HORVATH, S. WGCNA: An R package for weighted correlation network analysis. **BMC Bioinformatics**, v. 9, n. 1, p. 1–13, 29 dez. 2008.

LEITE, Thiago Falda. **Estabelecimento de um patossistema modelo e análise da interação molecular planta-patógeno entre Eucalyptus grandis e Puccinia psidii Winter por meio da técnica de RNA-Seq**. 2012. Tese de Doutorado. Universidade de São Paulo.

MAMANI, E. M. C. et al. Positioning of the major locus for Puccinia psidii rust resistance (Ppr1) on the Eucalyptus reference map and its validation across unrelated pedigrees. **Tree Genetics and Genomes**, v. 6, n. 6, p. 953–962, dez. 2010.

MARQUES, Felipe Garbelini. **Análise de metabólitos e proteínas totais em folhas de Eucalyptus grandis durante a infecção por Puccinia psidii**. 2016. Tese de Doutorado. Universidade de São Paulo.

MYSORE, Kirankumar S.; RYU, Choong-Min. Nonhost resistance: how much do we know?. **Trends in plant science**, v. 9, n. 2, p. 97-104, 2004

PEI, G.; CHEN, L.; ZHANG, W. WGCNA Application to Proteomic and Metabolomic Data Analysis. In: **Methods in Enzymology**. [s.l.] Academic Press Inc., 2017. v. 585p. 135–158.

ROJAS, C. M. et al. Regulation of primary plant metabolism during plant-pathogen interactions and its contribution to plant defense**. Frontiers in Plant Science**, v. 5, 17, 2014.

SANTOS, S. A. et al. Transcriptome analysis of Eucalyptus grandis genotypes reveals constitutive overexpression of genes related to rust (Austropuccinia psidii) resistance. **Plant Molecular Biology**, v. 1, p. 3, 2020.

SEKIYA, Alline. **Early responses of Eucalyptus grandis during rust infection**. 2020. Tese de Doutorado. Universidade de São Paulo.

SILVA, R. R. et al. Limonene, a Chemical Compound Related to the Resistance of Eucalyptus Species to Austropuccinia psidii. **Plant Disease**, v. 104, n. 2, p. 414–422, 16 fev. 2020.

XAVIER, A. A. et al. Infection of resistant and susceptible Eucalyptus grandis genotypes by urediniospores of Puccinia psidii. **Australasian Plant Pathology**, v. 30, n. 3, p. 277-281, 2001.

XAVIER, A. A. et al. Infection process of Puccinia psidii in Eucalyptus grandis leaves of different ages. **Tropical Plant Pathology**, v. 40, n. 5, p. 318–325, 1 out. 2015.

2. COEXPRESSION NETWORK ANALYSIS OF PROTEINS AND METABOLITES TIME-COURSE OF TWO CONTRASTING EUCALYPTUS GRANDIS RESPONSES TO AUSTROPUCCINIA PSIDII

ABSTRACT

Austropuccinia psidii is an obligate biotrophic fungus that infects *Eucalyptus* spp. leaves causing a disease called eucalyptus rust, affecting the wood productivity in the paper and pulp industry. Molecular changes orchestrated by plants in response to fungal infestation and how it is affecting disease outcome involving susceptibility or resistance responses, remains poorly understood, especially involving changes in primary metabolism. GC-MS based metabolomics and label-free proteomic data, correlated using WGCNA package (Weighted Gene Co-Expression Analysis), to contrast resistant and susceptible responses in *Eucalyptus grandis* infected with *Austropuccinia psidii*. A 24h time-course experiment was set, with leaves collection time-points chosen with the aid of epifluorescence microscopy. During time-course, 43 and 44 metabolites from different classes were significant by using ANOVA ($p < 0.05$) and 871 and 852 total proteins were obtained in resistant and susceptible genotypes, respectively. WGCNA generated seven protein modules for each genotype, correlating to 42 metabolites in the resistant network and 40 metabolites in the susceptible network. Integrated analysis revealed temporal divergences of protein-metabolites modules providing information of differences in photosynthesis and ROS generation, lipid metabolism, spores germination, amino acid metabolism, phytoalexins and defense responses. These findings provide useful information of different aspects involved in the establishment of efficient plant defenses and their contribution to susceptibility or resistance to *A. psidii*.

Keywords: plant-pathogen interaction, *Eucalyptus grandis*, *Austropuccinia psidii*, metabolomics, label-free proteomic analysis, WGCNA.

2.1. INTRODUCTION

Eucalyptus species are widely planted trees due to the quality of its wood, accelerated growth, robustness and possibility of being used in different industries (e.g., pulp and paper, charcoal, fuel wood, wood panels and flooring, solid wood products) (IBÁ, 2019). Eucalyptus production is constantly challenged by biotic stresses. Eucalyptus rust, also known as myrtle rust, is one of the most harmful diseases, caused by the biotrophic fungus *Austropuccinia psidii,* which affects young trees in field or nursery, causing deformation of the leaves, intense defoliation, reduced growth and even death of plants in severe cases, decreasing productivity (DOS SANTOS et al, 2019). *Eucalyptus grandis, E. cloeziana, E. phaeotricha, E. globulus* and *E. nitens* are the Eucalyptus species most susceptibles to rust. Among them, *E. grandis* and its hybrids are widely planted due to their suitability for paper and pulp industry. (ALFENAS et al, 2004).

Despite the importance of eucalyptus rust, the mechanisms of resistance to *A. psidii* are poorly understood. QTL mapping of resistance genes were performed in *E. grandis* (JUNGHANS et al, 2003a; BRONDANI et al, 2006; MAMANI et al., 2010), *E. globulus* (BUTLER et al., 2016) and interspecific hybrids of *E. grandis*, *E. globulus, E. urophylla* and *E. dunnii* (ALVES et al., 2012). These studies obtained important information to develop resistant varieties, introducing resistant alleles in elite lines on breeding programs. Although this strategy is effective at least in the short-term, they do not elucidate mechanisms behind disease development for the chosen plant-pathogen system (CASTRO-MORETTI et al, 2020). To identify molecular mechanisms, genomics, transcriptomics, proteomics, metabolomics and other omics studies have been conducted in the last decades. Proteomics analysis provides valuable information on the abundance profile of a large set of proteins in response to external stimulus, including abiotic and biotic stresses. Compared to the nature of genome, proteins are highly complex and dynamic structures, being an important part of the main signal transduction and biochemical pathways. (LI et al, 2019). Along with protein shifts, one of the major events occurring in biotic or abiotic stresses is metabolic reconfiguration. Metabolomics, the closest omics to phenotype, is an important part of systems biology, representing the end of regulatory circuits (FEUSSNER; POLLE, 2015). Numerous metabolomics and proteomics studies have been performed using different plant-pathogen systems. Karmakar et al. (2019) investigated metabolic and protein abundance divergences between transgenic NPR1 and non-transgenic rice infection with *Rhizoctonia solani,* identifying upregulated proteins related to energetic metabolism, with metabolites correlated to glycolysis and TCA cycle, stress and plant defense (e.g. phosphatase 2C1, trehalose-phosphate phosphatase 2). During compatible and incompatible interactions between chickpea and *Fusarium oxysporum,* Kumar et al. (2016) identified divergences in amino

acid metabolism, glycolysis/gluconeogenesis, TCA cycle, phenylpropanoid pathway and increased lignification. Ghosh et al. (2016), studying *Scleorotinia* sp. x Tomato pathosystem, used proteomics combined with metabolomics to uncover novel proteins and pathways potentially involved in defense mechanisms when tomato overexpresses oxalate decarboxylase.

Although commonly divided into primary and secondary metabolism, the metabolites that to these classes are intrinsically linked in plant-pathogen interactions. Metabolites from primary metabolism supports cellular energy requirements and serve, as building blocks for plant defense specialized responses (ROJAS et al, 2014; CASTRO-MORETTI et al, 2020). Not only important for plant responses, pathogen growth require nutrition from the host for successful colonization, which can be influenced by plant metabolism and availability of nutrients (FAGARD et al, 2014; WANG et al, 2019). Similar to other pathosystems, *Eucalyptus-A. psidii* molecular and metabolomic studies focus mainly in investigating secondary metabolites involved directly in disease progression or resistance mechanisms. Bini (2016) and Dos Santos et al (2019) investigated cuticular waxes composition of rust-resistant and rust-susceptible *Eucalyptus* species, identifying higher levels of Hexadecanoic acid in rust-susceptible species as *E. grandis* and *E. phaeotricha* . Silva et al. (2020) studied differences between young and old Eucalyptus leaves, with different susceptibilities to *A. psidii*, identifying the terpenoid limonene in old and resistant leaves. Santos et al. (2020) analyzed transcriptome profiles of 24 hours after inoculation (hai) infected E. *grandis* leafs with *A. psidii*, showing overexpression of photosynthesis and LRR protein-related genes. Sekiya (2020) investigated secondary metabolism and proteomic changes of rust resistant and susceptible genotypes during a time-course experiment, identifying temporal divergences in proteins and metabolites involved in phenylpropanoids pathway, oxidative stress and primary metabolism.

To improve our understanding of eucalyptus resistance mechanisms to rust, during the first 24 hpi, we decided to study protein and primary metabolic profiles that were altered during rust-resistant and rust-susceptible plants infection. In the current study, proteomic and GC-MS metabolomic analysis and data correlation utilizing WGCNA were used to characterize both genotypes. Proteins were grouped in modules with similar abundance over time and correlated with metabolites, providing insights into the *A. psidii-E. grandis* interaction and a basic understanding of the proteomic and primary metabolomic alternations in eucalyptus in order to confer resistance.

2.2. MATERIALS AND METHODS

2.2.1. Plant material and Inoculation with *Austropuccinia psidii*.

To study the changes in protein and primary metabolites linked to contrasting responses to eucalyptus rust, two half-siblings *Eucalyptus* derived from BRASUZ1 (*E. grandis*) were used. BRASUZ1 lineage was the one used for sequencing eucalyptus reference genome (MYBURG et al, 2014), and kindly provided by Suzano Papel e Celulose. R3 genotype (Resistant) and S4 genotype (Susceptible) were chosen due to their different response to *Austropuccinia psidii* monopustular isolate MF1 infection, R3 genotype is completely resistant (S0 response, with hypersensitive reaction HR) while S4 is sensitive (S3 response, with pustules > 1,6mm diameter), according to disease scale defined by Junghans; Alfenas; Maffia (2003b) (Figure S1), as described by Leite (2012). Six plants of each genotype were either mock-inoculated with 0.5% Tween 20 solution (v/v) or inoculated with 0.5% Tween 20 solution containing *A. psidii* spores (10^5 spores/mL). The experiment was conducted in growth chamber, with plants displayed into plastic bags to control the environmental effects and to obtain high humidity for fungal development. Photoperiod was set to 12 h dark, followed by 12h light (200 μmols m^{-2} s^{-1}). Leafs from both genotypes were collected at 0, 6, 12, 18 and 24 hai, and the samples were immediately frozen in liquid nitrogen. Sampling time points were chosen according to Leite (2012) after microscopy studies investigating penetration and *A. psidii* colonization in both plants used in this study.

After 48hai, plastic bags were opened and kept in growth chamber for pathogen absence or presence confirmation in mock-inoculated or inoculated, respectively, at 72hai. Pathogen confirmation we obtained using conventional PCR, according to Bini et al. (2018), utilizing markers IGS-7/IGS-9 specific for A. psidii detection.

2.2.2. GC-MS metabolomics

Frozen samples were grounded manually with liquid nitrogen and homogenized using a ball mill (Retch MM400) with tungsten beads for 1 min at 20Hz. Extraction was conducted according to Gullberg et al. (2004), using 20 mg of plant material and 400μL of extraction solution composed of chloroform/water/methanol (20%/20%/60%) containing succinic acid (D4, 98%), myristic acid (1,2,3-$^{13}C_3$, 99%) and palmitic acid (1,2,3,4-$^{13}C_4$, 98%) as internal standards, prepared with 1mg.ml^{-1} concentration.

The samples were sonicated (UltraCleaner 1600A – Unique) for 15 min in ice and centrifuged (Centrifuge 541R – Eppendorf) for 10 min, at 4ºC, at 16.000g. The supernatant was filtered (Millipore filter PVDF 0.22 μm). Aliquots of 100μL were dried in freeze dryer at -50ºC and derivatized as described in Budzinski et al. (2019), using 30 μl of methoxyamine hydrochloride (15 mg ml-1) in pyridine for 16h at room temperature, 30 μl of N-methyl-N-(trimethylsilyl) trifluoroacetamide (MSTFA) containing 1% trimethylchlorosilane (TMCS) for 1h at room temperatures. Then, 30 μl of heptane was added. Derivatized samples (1μL) were analyzed in Agilent 7890A gas chromatograph, equipped with DB-5 column (20m x 0.18mm i.d., 0.18μm) used as primary column (Agilent Technologies) and RX1-17 (Restek, Bellefonte, USA) (0.69 m x 0.1mm i.d., 0.10μm) used as secondary column, coupled to a Pegasus HT time-of-flight mass spectrometer (Leco Corporation). Injection temperature was 280ºC, with septum purge flow rate defined as 20 ml/min, turned on after 60s. Gas helium flow rate through the column was defined as 1 ml/min. When achieving 80ºC, the column stayed at the temperature for 2 min, then increased with a rate of 15°C/min to 305°C, and held at this final temperature for 10 min. The column effluent was introduced into the ion source of a GC×GC/TOF-MS (Pegasus 4D, Leco Corp., St. Joseph, USA). The transfer-line and the ion source temperatures were 280 and 250°C, respectively. Ions were generated by a 70-eV electron beam at an ionization current of 2.0 mA, and spectra were recorded in the mass range m/z 45–800.

Baseline correction, peak detection, retention time alignment (parameters set as baseline 1, peak width 2, s/n 250) and library matching, setting minimum similarity of 700, were performed with NIST Database v.11, using Leco ChromaTOF software (version 3.25). Metabolites intensities were normalized by TIC (sum of total ion count). Siloxans and metabolites absent in at least half of the samples in a group were excluded.

2.2.3. Statistical analysis

For statistical analysis, we needed to have the same number of biological samples for metabolomics and proteomics to construct WGCNA network. Metabolomics data were grouped, by calculating mean values of the same samples grouped in proteomic extraction preparation, obtaining three biological replicates. To access an overview of genotype-specific responses, differential abundance of metabolites was calculated by the ratio inoculated/false-inoculated and submitted to statistical analyses, for each genotype. Data were log-transformed, pareto-scaled and submitted to multivariate (Principal Component Analysis-PCA) to visualize group tendency and outliers presence and univariate analysis (ANOVA, FDR < 0.05) to determine metabolites with

statistical differences over infection time-course in each genotype, using MetaboAnalyst 4.0 (CHONG et al, 2018).

2.2.4. Proteomics Shotgun Label-free

For protein extraction, we pooled two samples to obtain necessary weight and conducted the analysis with three biological replicates. Total protein was extracted according to Hurkman; Tanaka (1986), with minor modifications. One hundred miligrams (100mg) of leaf samples were grounded using a ball mill (Retch MM400) with tungsten beads for 1min at 20Hz, and homogenized in 0.8mL of protein extraction buffer (0.5M Tris-HCl pH 7.5, 0.7M Sucrose, 0.1M Potassium Chloride, 50mM EDTA, 1mM PMSF, 2% (v/v), β- mercaptoethanol and 1% (w/v) PVPP. After, 800μL of Tris-HCl saturated phenol pH 8.5 solution was added to protein suspension. Samples were shaken for 30min and centrifuged at 10.000g for 30min at 4ºC. Supernatants were recovered and submitted to re-extraction three more times. Proteins were precipitated by adding 1.2 mL of 0.1 M ammonium acetate in methanol. The pellet was washed twice with the same solution and with acetone. After the last centrifugation, acetone was evaporated and proteins were resuspended in 0.4mL solubilization buffer (7M Urea, 2M Thiourea, 10mM DTT and 0.4% v/v Triton X-100). Supernatant containing proteins was desalinized in 50mM ammonium bicarbonate buffer (pH 8.5) using Amicon Ultra-0.5 ml 3K-NMWL filter devices (Millipore Corporation). Proteins were quantified according to Bradford (1976).

Fifty micrograms of proteins, were denatured using 25 μL 2% (v/v) RapiGest SF (Waters) at 80ºC for 15min. After, samples were reduced in 2.5μL 100mM dithiothreitol (DDT) for 30min at 60ºC and alkylated using 2.5μL 100Mm iodoacetamide (IAA) for 30 min in the dark. Trypsin digestion was performed with sequencing Grade Modified Trypsin (Promega) at a 1:100 (w/w) enzyme:protein ratio and proteins were incubated at 37°C overnight. After, 10 μl of 5% (v/v) trifluoroacetic acid (TFA) was added to the digested mixture to hydrolyze the RapiGest (Waters, USA).

The peptide mixture was centrifuged at 14.000g at 6ºC for 30min and desalted using ZipTip C18-columns (Millipore Corporation). The final volume of 40 μL was obtained by adding the solution of 20 mM pH10 ammonium formate with 8 μL of 100 fmol μL-1 internal standard (P00489. rabbit glycogen-phosphorylase) and analyzed in a Synapt G2 HDMS mass spectrometry (Waters, Manchester, UK) connected to UPLC M-class. Peptide separation was conducted as described in Budzinski et al. (2019). Peptides were separated in first dimension, using XBridge BEH C18 column with dimensions 5 μm, 300 μm x 50 mm (Waters, Manchester, UK), elution

parameters ranging 3–45% gradient of a solution of 0,1% (v/v) ammonium formate in ACN, at a flow rate of 2µl min^{-1}. Eluted peptides from first-dimension column were trapped in a Symmetry 2D column with dimensions 5µm, 180µm x 20mm. Second dimension separation was performed using an HSS T3 column (1.8 µm, 75 µm x 100 mm) (Waters, Manchester, UK) using a 7–40% binary gradient of acetonitrile in 0.1% (v/v) and formic acid, within 20 minuted at a flux rate of 350nL.min^{-1}.

Protein mass spectrometry data was acquired using Synapt G2 HDMS with a nanolockspray font in a positive mode (Waters, Manchester, UK). The equipament was calibrated with 200 fmol μL^{-1} of Glu1 ($[M+2H]^{2+}$ = 785,84206 Da). Mass spectra were processed with the ProteinLynx GlobalServer (PLGS) Program, version 3.0.3, using Phytozome *Eucalyptus grandis* database v.13 2.0 downloaded at 03/2020, containing 46280 proteins, as protein reference database (https://phytozome.jgi.doe.gov). Processing parameters included automatic tolerance of precursors and ion-products and required a minimum of three corresponding ion-fragments per peptide, minimum of seven corresponding ion-fragments per protein, minimum of two corresponding peptides per protein, possible cleavage error of trypsin, carbamidometilation of cysteine with fixed modification and methionine oxidation as variable modifying factors (FDR < 1%).

For protein identification and quantification, spectral intensities were calculated using the stoichiometric method, with an internal standard analyzed with MS^E and normalized with the PLGS auto-normalization function. The sequence and abundance of peptides were determined based on the mean values of the three most abundant peptides identified from data obtained from the three biological replicates assessed. Only proteins with confidence levels higher than 95% that were identified and quantified at least in two replicates were considered for subsequent analytical steps. Differential abundance of proteins was calculated by inoculated/false-inoculated ratio and submitted to further analysis.

2.2.5. WGCNA network analysis

Protein data was submitted to WGCNA analysis. The R package was used to build protein networks based on protein abundance during infection time course of both genotypes, separately, in order to identify modules, principal proteins of each module (eigenproteins) and analyze correlation with selected metabolites. WGCNA signed network was performed according to Langfelder; Horvath (2008), choosing soft thresholds by power numbers displayed in S3 and S4 Figures, generated with the package. Powers of 6 and 7, for susceptible and resistant genotypes, respectively, were chosen to suit maximum approximation of a scale free topology

distribution and small connectivity (Fig. S3, Fig. S4). Network was exported and visualized in Cytoscape (SHANNON et al, 2003). Modules correlated with the same metabolites and displaying similar eigenprotein abundance profile over time of infection were grouped into one major module (Fig. 6 and 7).

2.2.6. Functional analysis

To visualize biological processes, molecular functions or cellular components associated to proteins modules, each module was analyzed separately using gene ontology (GO). GO terms were obtained using AgriGO v.2, available at http://systemsbiology.cau.edu.cn/agriGOv2/ (TIAN et al, 2017) and *E. grandis* Phytozome database v. 11.0. Main results were obtained using REVIGO, with 0.04 similarity (SUPEK et al., 2011) and are displayed in tables S2-S15. Proteins were also characterized using KofamKOALA (ARAMAKI et al., 2020) available at http://www.genome.jp/tools/kofamkoala/, which uses HMMER (threshold set as default 0.01) and KEGG Orthologs (KOs) to link sequence data to KEGG database v. 96 and EC numbers in order to characterize interesting pathways and proteins (Tables 4 and 5).

2.3. RESULTS

2.3.1. Pathogen Growth within Plant Tissues

Eleven days after inoculation with *A. psidii*, the susceptible genotype showed yellow pustules containing spores on both adaxial and abaxial leaf surfaces. At the same time, resistant plants remained healthy, only showing fleck spots characteristic of hypersensitive response (HR). Controls (mock-inoculated) from both genotypes did not show any symptoms. Pathogen presence or absence was confirmed by conventional PCR, at 72hai (SEKIYA, 2020). (Figure S2).

2.3.2. GC-MS metabolomics

After manual inspection**,** GC-MS metabolomics analysis detected 115 different metabolites from all time points and genotypes, 105 obtained in resistant and 97 in susceptible. There were identified different classes of metabolites, mainly organic acids, sugars, amino acids, lipids and benzenoids (Supplementary Table 1). Some nucleosides, phenylpropanoids, amines, amides were also detected. To investigate samples group tendency and outliers, a PCA was performed (Figures 1A, 1B). No outliers were detected. All times from both genotypes were separated considering two principal components, explaining 45.8% and 44.6% of the total

variation found in resistant and susceptible genotype, respectively, and suggesting a metabolic reconfiguration in all time points in response to the infection of *A. psidii*. In resistant genotype PCA, 0hai was the most different time during infection, beeing well separated from other times by second principal component (19.5% of variance explained) while 12hai were the most divergent time of susceptible, well separated by first principal component (26.1% of variance explained), indicating divergences in genotypes profiles in response to *A. psidii*.

Using univariate analysis ANOVA - (FDR < 0.05), 44 metabolites were differentially abundant in resistant and 43 in susceptible, having 23 metabolites shared by them (Tables 1 and 2). The distribution of differentially abundant metabolites and their class were represented in heatmaps (Figures 2 and 3). The most abundant classes were amino acids and benzenoids for resistant genotype, while susceptible displayed more sugars during infection time-course. Sugars abundance during infection time course, were different between the genotypes, with a deacrease at later hours in resistant. Abundance of lipids, as linolenic acid (NIST ID 9100-replib), linoleic acid (NIST ID 9961-replib) and hexadecanoic acid (NIST ID 9118-replib) were abundant only at 0hai in resistant, differing from susceptible. The majority of amino acids and their derivatives (threonine NIST ID 38412-mainlib, proline NIST ID 20907-replib, γ-Aminobutyric acid (GABA) NIST ID 143908-mainlib, glutamic acid NIST ID 182910-mainlib) was abundant at 12hai in susceptible plants (57% of total amino acids), while at 18hai more amino acids (50%) were abundant in resistant (threonine NIST ID 38412-mainlib, methylleucine NIST ID 141919-mainlib, lysine NIST ID 39149-mainlib, GABA NIST ID143908-mainlib). Susceptible also displayed phenylpropanoids and benzenoids during time-course (p-coumaric acid NIST ID 39560-mainlib, Caffeic acid NIST ID 27526-replib, Alizarin NIST ID 207268-mainlib, Emodin NIST ID 211614-mainlib and others), possibly with a role in phytoalexins and defense metabolism, as the resistant genotype also presented, although displaying a divergent time pattern (Caffeic acid NIST ID 27526-replib, Embramine NIST ID 25951-mainlib, Alizarin NIST ID 207268-mainlib, Emodin NIST ID 211614-mainlib, Gallic acid NIST ID 39872-mainlib, and others).

2.3.3. Proteomics and WGCNA

Total proteomics analysis quantified 1006 proteins from all timepoints and genotypes, 871 belonging to resistant and 852 to susceptible plants. WGCNA was performed for resistant and susceptible genotypes, without any filter as recommended by developers, initially obtaining 13 and 14 protein modules, respectively (Figure S5). Proteins were grouped according to similar abundance profiles over time and distributed to color-named modules. Only 15 and 25

proteins of resistant and susceptible genotypes, respectively, did not fit in any module and were assigned as grey. Differentially abundant metabolites obtained from ANOVA analysis were correlated to eigenproteins module, the principal component representing all proteins of one group. All eigenproteins were correlated with at least one metabolite, showing positive or negative correlations (p-value < 0.05) (Figures 4 and 5).

Both WGCNA networks were exported to Cytoscape. They were visualized by representing proteins as nodes, modules as their respective color and strength of connections between nodes were indicated by the length of each edge, enabling visualization of related modules grouped as one major block-module (Figures 6 and 7). Related modules also responded to the same metabolites (Figures 4 and 5) and exhibited similar eigenprotein abundance pattern over time, initially grouped separately due to slightly differences in abundance. Then, connected modules were grouped into one major block module. For resistant, MagentaGreenPurpleSalmon, PinkYellowTan, BlackBownGreenyellow formed three new major modules. For susceptible, GreenGreenyellow, PurpleTurquoise, YellowPink, RedMagentaTanSalmon formed four new ones. In total, resistant and susceptible genotypes have 7 different modules. Most resistant modules showed more positive correlations than negative correlations with selected metabolites, except Turquoise. Susceptible showed more negative correlations than resistant, having Brown, PurpleTurquoise and GreenGreenyellow mostly negatively correlated to selected metabolites. Three metabolites from susceptible genotype (Xylitol, NIST ID 38261-mainlib, Xylanopyranose NIST ID 39372-mainlib, Caffeic acid NIST ID 27526-replib) and one metabolite from resistant (Adrenaline NIST ID 86262-mainlib) did not show statistical correlation with any module, although Caffeic acid from susceptible showed correlation with grey module eigenprotein (Figures 4 and 5). Significant ($p<0.05$) correlated modules and metabolites are summarized in table 3.

Protein modules or block-modules were mostly related at one specific time-point, except from Red resistant module, abundant at 12hai and 24hai. Resistant plants accumulated proteins from the MagentaGreenPurpleSalmon block-module at 0 hai; PinkYellowTan block-module at 6 hai; Blue and Cyan modules at 12 hai; Turquoise module proteins were less abundant at 18 hai; and BlackBrownGreenyellow block-modules accumulated at 24 hai. On the other hand, in susceptible plants, proteins from RedMagentaTanSalmon were abundant while proteins from PurpleTurquoise module were less abundant at 0hai; Blue module increased abundance at 6 hai; Black module was abundant while Brown module was less abundant at 12hai, YellowPink block-module increased abundance at 18 hai; and GreenGreenyellow block-module at 24 hai. To

differentiate modules from resistant and susceptible, they will be named with genotype first letter before module's name for further discussion.

2.3.4. Functional Analysis

The potential biological function for each module was acessed based on Gene Ontology enrichment analysis using AgriGO v. 2.0 and *E. grandis* database v.11 from Phytozome (TIAN et al, 2017). GO terms related to photosynthesis, oxido-reduction, and carbohydrate metabolism were major terms enriched during both genotypes time-courses, suggesting temporal divergences (Tables S2-S15).

Resistant genotype enriched terms related to photosynthesis (photosynthesis GO:0015979, photosystem GO:0009521) in R-MagentaGreenPurpleSalmon (0hai), Red (12hai) and R-BlackBrownGreenyellow (24hai) modules, while susceptible enriched in S-RedTanMagentaSalmon (0hai), S-PurpleTurquoise (0hai), S-Blue (6hai) and S-Brown (12hai) modules. In resistant, decreasing abundance was observed only at 0hai, while susceptible displayed deacresing pattern at 0hai and 12hai. S-Brown and R-BlackBrownGreenyellow enriched for light reaction in photosynthesis go term (GO:0019684), deacreasing in susceptible while increased in the resistant genotype. Oxido-reduction GO terms (cellular homeostasis GO:0019725, oxidoreductase activity GO:0016491) were enriched at 0hai (S-PurpleTurquoise and R-MagentaGreenPurpleSalmon), 6hai (S-Blue and R-PinkYellowTan), 12hai(R-Red and R-Blue), 18hai (S-PinkYellow) and 24hai (R- BlackBrownGreenyellow and S-GreenGreenyellow). In respect to carbohydrate metabolism GO terms, in both genotypes it was present at the earliest stages (0hai and 6hai), only were divergent at 12hai, when susceptible decreased proteins related to carbohydrate in Brown module and at 18hai, when resistant decreased proteins related to carbohydrate.

To characterize protein modules, Kegg analysis were also performed, using KofamKoala. The most abundant pathways, for resistant and susceptible genotypes, are summarized in tables 4 and 5, respectively. Enrichment analysis of GO terms and Kegg terms generated consistent and complementary results. Glicolysis/Gluconeogenesis, Photosynthesis, Translation (Involved in Ribosome constitution) and Glyoxylate and dicarboxylate metabolism were the main pathways abundant during time-course of resistant and susceptible genotypes. In respect to energetic metabolism, most abundant pathways were different between genotypes, with glycolysis/gluconeogenesis mainly present in susceptible and glyoxylate and dicarboxylate metabolism in resistant. Also, kegg analysis provided complementary information on proteasome and amino acid metabolism. Proteasome was one class important in R-Blue module (12hai) and

S-Brown module (12hai), presenting divergent profiles. Taken together GO and Kegg analysis, proteins involved in amino acid were present in R-PinkYellowTan (6hai) and R-BlackBrownGreenyellow (24hai), while in susceptible genotype were present S-RedTanMagentaSalmon (0hai), S-PurpleTurquoise (0hai) and S-YellowPink (18hai).

2.4. DISCUSSION

Metabolomics and proteomics are recognized as powerful tools to describe plant responses to several stimuli, providing a snapshot of metabolism and regulatory mechanisms of an organism at a given time (CASTRO-MORETTI et al., 2020). GC- MS analysis of primary metabolites and proteomics approaches, integrated in a time-course study using WGCNA, allowed us to identify a set of biological pathways and metabolites involved in several temporal aspects of *A. psidii* resistance or susceptibility of infected eucalyptus metabolism reconfiguration. Focusing on early metabolic and protein changes, initiated shortly after inoculation until full colonization of host tissue, we were able to differentiate pathogen growth on resistant and susceptible eucalyptus leaf tissues. Previous studies in our laboratory determined infection time-course of selected genotypes in response to *A. psidii* (LEITE, 2012). In both genotypes, disease progression started at 3hai with spore germination and production of primary germ tube (PGT). At 6hai appressorium spores germ tube (AGT) were visualized. At 12hai, penetration hyphae were visualized in both genotypes, but subepidermal vesicle were present only in susceptible. From 18hai, fungal development was impaired in resistant genotype. At 24hai, only susceptible showed development of haustorium, visualizing haustorial mother cells. Consistently, SHEN et al. (2017), also determines that the initial stages of plant-pathogen interactions usually occur in 24 hours post inoculation. Within this time, the efficiency of plant defenses determines whether plants will be susceptible or resistant to infection. These observation indicated that, in *Eucalyptus grandis* infection with *A. psidii*, the main molecular events determining resistance response occurred within 24h. Our analysis provided insights in respect to spore germination, photosynthesis and ROS generation, phytoalexins production, lipid, energetic and amino acid metabolism.

2.4.1. Spores germination

During the time interval of 0h-6h, spores started germinating in both genotypes, as observed in previous microcopy analysis using the same genotypes and pathogen inoculation (SEKIYA, 2020). R and S genotypes proteins and metabolites positively correlated with this time some may play a role in spore germination. Correlated to R genotype, Hexadecanoic acid (NIST

ID 9118-replib), also known as palmitic acid, is a lipid component of *Eucalyptus* cuticular waxes, absent in resistant Eucalyptus species and strongly related to the susceptibility of *Eucalyptus grandis* and *Eucalyptus phaeotricha* to *A. psidii*, according to Dos Santos (2019). Their absence is involved in pre-formed defenses in *Eucalyptus* species and, when present, this compound stimulated spore germination. In our work, Hexadecanoic acid deacreased in abundance in resistant genotype during the first hours of infection (R-MagentaGreenPurpleSalmon). Glycerol, another metabolite associated fungal spore germination, more specifically *A. nidulans* conidiospores, act as an osmoregulator in conidiospore swelling, according to Kalampokis et al. (2020). Glycerol (NIST ID 39414-mainlib) was present in both genotypes, although had different time signatures. In resistant, glycerol decreased in abundance 0-6hai (R-MagentaGreenPurpleSalmon , while susceptible only showed decreased at 18hai (S-PinkYellow). Early control of both metabolites can affect fungal full development in resistant genotype .

Putrescine (NIST ID 143937-mainlib), one of the most abundant polyamines (PA) found in plants, and Cadaverine (NIST ID 24430-replib), diamine synthesized by decarboxylation of lysine, are often linked to abiotic stress or insect resistance in different species, as reviewed by Masson; Takahashi; Angelini (2017), Jancewitz; Gibbs; Masson (2016), Minocha; Majumdar; Minocha (2014), while its role in plant-pathogen interactions remains poorly understood. In most cases, induction of PA synthesis has been reported during biotroph pathogen infection, with resistant cultivars accumulating higher putrescine and other polyamines levels than the susceptible after infection. (PAL; JANDA, 2017). These studies mainly involved later evaluation of host responses, with days after inoculation, often related with hypersensitive responses (HR). Evaluating early responses during *Puccinia coronate f. sp. Avenae* infection in resistant and susceptible oat cultivars, Montilla-Bascón et. al (2016) observed differential increases in polyamines, associated with increased pre-penetration and penetration resistance. In our study, susceptible genotype did not displayed any polyamines during time-course, while resistant displayed Cadaverine and Putrescine correlated positively to R-BlackBrownGreenyellow (24hai) and R-MagentaGreenPurpleSalmon (0-6hai), respectively. During 24hai, Cadaverine increased in abundance while Putrescine decreased, indicating some role in early defenses in *E. grandis-A. psidii* pathosystem.

2.4.2. Photosynthesis and ROS generation

The complex response of plant defenses during plant-pathogen interactions requires an abundant supply of energy, primarily derived from primary metabolic processes (BOLTON et al., 2009; ROJAS et al, 2014). Photosynthesis is a major energy producer in the form of ATP and

NADPH that can be utilized in the production of assimilates for various metabolic processes. However, decrease in photosynthesis is a widely observed phenomenon after a pathogen infection, including inhibition of photosystem II, reduction of CO_2 fixation and global down-regulation of photosynthetic genes and proteins. (BERGER; SINHA; ROITSCH, 2007; BILGIN et al, 2010; ZABALA et al, 2015, SERRANO; AUDRAN; RIVAS, 2016). Our findings are consistent to this observation, visualizing deacrese abundance in proteins related to photosynthesis in the first hours of infection in both genotypes, within R-MagentaGreenPurpleSalmon and S-RedMagentaTanSalmon modules and association to sugars as metabolites (galactose/glucose [NIST ID 164548-mainlib] and gluconic acid [NIST ID 9402-replib] with resistant module; talose [NIST ID 170819-mainlib] and metyl-glycoside [NIST ID 39358-mainlib] with susceptible module). Within R-MagentaGreenPurpleSalmon module, proteins are related to photosystem I (Eucgr.H00828.1.p), photosystem II (Eucgr.G02488.1.p, Eucgr.H02489.1.p, Eucgr.H01287.4.p, Eucgr.L03253.1.p, Eucgr.A01774.2.p), electron transport (Eucgr.I02744.1.p, Eucgr.E00291.1.p, Eucgr.I02340.1.p) and antenna (Eucgr.G03060.1.p) decreased in abundance (Table 6) S-RedMagentaTanSalmon, as well, displays proteins related to photosystem I (Eucgr.B01088.1.p, Eucgr.I00200.2.p, Eucgr.B02162.1.p, Eucgr.H00828.1.p), photosystem II (Eucgr.A00264.1.p, Eucgr.F01822.2.p, Eucgr.G02904.1.p), electron transport (Eucgr.E00291.1.p) and cytochrome b6/f (Eucgr.E01113.1.p) (Table 7)

Along with photosynthesis inhibition, upregulation of other pathways that provide the necessary energy are observed during plant-pathogen interactions (e.g. respiratory metabolism, cell wall invertase and carbohydrate transporters) (BOLTON et al, 2009; ROJAS et al, 2014; SU et al, 2018). During 0hai-6hai we observed a decrease in energetic metabolism in resistant genotype. R-MagentaGreenPurpleSalmon proteins also relates to glycolysis/gluconeogenesis and oxidative phosphorylation, decreasing at the initial hours of pathogen infection (Table 4). Pyruvic acid (NIST ID 119415-mainlib), metabolite product of glycolysis correlates with this module and deacreases at the time. Only after 6hai, resistant proteins increases in abundance and presents glycolysis/gluconeogenesis proteins (Table 8) and glyoxylate and dicarboxylate pathway present during whole infection time-course, in R-PinkYellowTan (6hai), R-Cyan (12hai), R-Red (12hai), R-BlackBrownGreenyellow (24hai), also with a role as energy provider, as in plants, glyoxylate cycle has a key role in conversion of acetyl coenzyme A (CoA) into oxaloacetate and subsequent conversion into sugar (MA et al., 2020).

S-RedMagentaTanSalmon module also enriched for glycolysis and carbon fixation with a decreasing pattern in the first hours of infection (Table 5). However, susceptible also displayed another module, S-Purple-Turquoise, related to an increasing pattern of photosynthetic proteins

(Table 7), pyruvate metabolism between 0hai-6hai time interval, providing energy. During the infection, susceptible mainly presented glycolysis/gluconeogenesis pathways as energy provider, with sugars abundant at later hours of infection, different from resistant genotype, as visualized in heatmap (Figures 2 and 3).

Not only important to plant-pathogen interactions as a source of energy to drive defense responses, energetic metabolism is also important as signaling molecules to directly or indirectly trigger defense responses (ROJAS et al, 2014). Chloroplasts is an important ROS generator, responsible for participating in hypersensitive response (HR) (ZURBRIGGEN; CARRILLO; HAJIREZAEI, 2010), synthesis of important hormones involved in plant defenses as salycilic acid (SA), jasmonic acid (JA) and abscisic acid (ABA), and signalling, making chloroplast one interesting target for pathogen-associated molecular patterns (PAMPs) or pathogen effectors (SERRANO; AUDRAN; RIVAS, 2016). Inhibition of photosynthesis by a biotrophic pathogen is potentially counter-intuitive, because it would reduce sugars available to the pathogen, remaining elusive if it is an active immune response of plants or a passive one (SU et al, 2018; ZABALA et al, 2015). Within 3hai, Zabala et al (2015) observed rapid downregulation of chloroplasts transcripts and non-estomatal inhibition of photosynthesis. At 6hai, chloroplast-targeted effectors collaborated to destabilize PSII and consequently inhibited photosynthetic electron transport decreasing the PAMP-induced ROS production in *Arabdopsis thaliana*/*Pseudomonas syringae* pathosystem. Recent studys, shows NLR-mediated MPK3/MPK6 signaling cascades activation induces global down-regulation of photosynthetic genes and, in the meantime, also accumulates ROS in chloroplasts under light and up-regulates numerous defense-related genes associated to ETI-triggered responses, HR cell death and pathogen resistance when working with A. thaliana-*P. syringae* pv *tomato* DC3000 pathosystem within 24hai (SU et al, 2018). In our work, susceptible did not fully impaired photosynthestic protein abundance in comparison to resistant genotype, as it also displayed S-PurpleTurquoise module, with an increasing pattern of photosynthesis-related proteins, involving maily photosystem II (Eucgr.H01287.4.p, Eucgr.G02488.1.p, Eucgr.F03186.8.p, Eucgr.G02593.1.p), correlating to Galactose/Glucose (NIST ID 164548-mainlib) and Mannose-6-Phosphate (NIST ID 39404-mainlib) increasing abundance (Table 7). Along infection, photosynthesis was also related to other modules in different time points. In Susceptible, at 6hai proteins enriched for photosynthesis in S-Blue module were abundant, related to Photosystem II (Eucgr.I01025.1.p, Eucgr.D00854.1.p), Cytochrome b6/f (Eucgr.A01769.1.p, Eucgr.B02878.1.p, Eucgr.C02765.1.p) and Antenna proteins (Eucgr.D00319.1.p, Eucgr.E02381.1.p). While at 12hai S-Brown module displayed a decreasing pattern in proteins related to light reactions (Eucgr.K01362.1.p, Eucgr.D00321.1,

Eucgr.K02983.1.p, Eucgr.I02677.1.p) and photosystem II (Eucgr.K00947.1.p, Eucgr.A02039, Eucgr.H01287, Eucgr.F03789.1.p), although Black module proteins had increased abundance mainly in electron transport (Table 7).

Divergently, photosynthetic proteins repression in resistant genotype lasted longer, being abundant only at 12hai in R-Red and R-Cyan Modules, involving photosystem I (Eucgr.B02162, Eucgr.I00200.2.p, Eucgr.K02362.3.p), II (Eucgr.K00947.1.p, Eucgr.A02039.1.p), electron transport (Eucgr.B03849.1.p, Eucgr.H02991.1.p) and light reactions (Eucgr.K01362.1.p, Eucgr.K02983.1.p). At 24hai, proteins from R-BlackBrownGreenyellow module were abundant and were related to photosystem II (Eucgr.A00264.1.p, Eucgr.D00854.1.p, Eucgr.F03186.8.p, Eucgr.F03789.1.p), photosystem I (Eucgr.B01088.1.p, Eucgr.K00389.1.p, Eucgr.F03646.1.p), Cytochrome b6/f (Eucgr.E02606.1.p), electron transport (Eucgr.I02340.2.p) and, mainly, light reactions (Eucgr.J01096.2.p, Eucgr.B00523.1.p, Eucgr.D00321.1.p, Eucgr.E02381.1.p, Eucgr.F04099.1.p, Eucgr.I02677.1.p, Eucgr.G00777.1.p).

During the time-course, photosynthesis partial decrease, timing divergences between susceptible and resistant along with impairment of light reactions after 12hai may be affecting ROS production and signaling in susceptible genotype, contributing to different plant responses.

2.4.3. Metabolism of Lipids

Lipids play vital roles in numerous physiological processes in living organisms, providing basic composition for cell membranes, waxes and signaling (ROJAS et al., 2014). Structurally, Hexadecanoic acid (NIST ID 37037-mainlib) plays a role in Eucalyptus cuticular waxes composition, as discussed previously. Related to signalling, Linolenic acid (18:3) (NIST ID 9100-replib) is less abundant in resistant genotype during all infection time course, as it was related to R-Magenta-Green-Purple-Salmon module. This fatty acid is the first component of octadecanoid (or oxylipin) pathway, involved in jasmonates, jasmonic acid (JA) and JA-Isoleucine biosynthesis. (CHRISTENSEN; KOLOMIETS, 2011). Jasmonic acid (JA), along with salicylic acid (SA), plays a major signaling role in defense against pathogens, combined with others hormones. JA combined with ethylene is associated to the activation of plant defense against necrotrophic pathogens and JA combined with ABA to the defense of insects, while SA induces defense against biotrophic and hemibiotrophic pathogens, during earliest stages of infection (ROBERT-SEILANIANTZ; GRANTS; JONES, 2011). Cross-talk between SA and JA hormones are reported, consisting in mainly antagonistic relationships, allowing plants to specialize its defense to the pathogen at the time and when challenged with multiple attackers, SA

is known to suppress JA-defense response (GLAZEBROOK, 2005; SPOEL; JOHNSON; DONG, 2007, CAARLS; PIETERSE; VAN WEES, 2015).

Another lipid involved in the same pathway, Linoleic acid (18:2) (NIST ID 9961-replib) can be converted in Linolenic acid directly by desaturation by enzyme 15-desaturase or modified by 13-lipoxygenases to produce different fatty acid monomers (ABU-NADA et al., 2007), and was significant in both genotypes. In susceptible, it is related to S-YellowPink module (increased abundance at 18hai) while in resistant displays correlation with R-MagentaGreenPurpleSalmon (decreasing pattern at 0hai-6hai). During infection time-course, enzymes related to jasmonic acid biosynthesis were also found in minor quantity. Eucgr.J00819.1 – Linoleate 13s-lipoxygenase (EC 1.13.11.12) was abundant at 6hai (R-PinkYellowTan) and Eucgr.J00820.1.p (EC 1.13.11.12) decreased at 18hai (R-Turquoise) in Resistant genotype. Susceptible displayed an increse in Eucgr.F02479.1.p - allene oxide cyclase (EC: 5.3.99.6) enzyme, involved in the production of 12-oxo-phytodienoic acid (OPDA), a precursor of jasmonic acid at 6 hai (S-Blue module).

As composition and timing of the hormonal blend and cross-communication between hormone signaling pathways are important to activation of effective over ineffective defenses (VOS et al, 2015), in our study, resistant plants showed earlier decrease of Jasmonates building blocks, possibly enhancing defense against biotrophic pathogens, as *Astropuccinia psidii*.

2.4.4. Phytoalexins and Defense Responses

After 12hai, phytoalexins intermediates associated with defense responses increased in resistant genotype, only flavonoid Catechin (NIST ID 207102-mainlib) related negatively to R-MagentaGreenPurpleSalmon was abundant during the whole infection time-course. Caffeic acid (NIST ID 27526-replib), at 12hai, and gallic acid (NIST ID 39872-mainlib), at 18hai, both intermediates of phenylpropanoids pathway, increased in abundance. Phenylpropanoids pathway is involved in biogenesis of various numbers of phenolics polymers as stilbenes, coumarins, flavonoids, phenolics acids displaying antimicrobial activities, and involved in lignin biosynthesis pathway with a role in cell wall reinforcement in order to restrain pathogen proliferation (DIXON et al., 2002; DENG; LU, 2017; YADAV et al., 2020). Anthraquinones derivatives, Alizarin (NIST ID 207268-mainlib), correlated to 24hai (R-BlackBrownGreenyellow), and Emodin (NIST ID 211614-mainlib), correlated to 12hai and 24hai (R-Blue and R-Red Modules), increased in abundance. Anthraquinone derivatives are the largest group of natural quinones, found in all plant organs as roots, rhizomes, flowers and leaves, showing antioxidant properties (IZHAKI, 2002; DUVAL et al., 2017), role in electron transport chain (DUVAL et al., 2017), and antifungal activities (BARROS et al, 2011). Barros et al. (2011) studied antifungical activity

of root and leaf extracts of *Coccoloba mollis,* identifying emodin as the most active compound of the extract, which caused inhibition of several phytopatogens. During grapevine infection with *Plasmopara viticola,* emodin alone was suficiente to stop fungus development through induction of HR and synthesis of phytoalexins (GODARD et al., 2009).

Sekiya (2020), studying secondary metabolism of *Eucalyptus grandis-A. psidii* pathosystem using metabolomics (LC-MS negative mode) and proteomics, observed major production of defense metabolites after 12hai in resistant genotype, while in susceptible plants they were repressed after 12hai. In proteomics analysis, Sekiya (2020) also identified protein-enzymes involved in Coumaric Acid branches and lignin biosynthesis with increased abundance after 12hai in resistant and decreasing at the same time in susceptible plants. Consistently, in our metabolomics study, susceptible displayed metabolites associated to phenylpropanoid pathway as well, exhibiting a decreasing pattern, differentiating from resistant. Caffeic acid (NIST ID 27526-replib) was one of the metabolites that did not correlated with any protein module, however, it was present in ANOVA metabolites and decreased abundance at 6hai as visualized in metabolite heatmap (Fig. 3). P-coumaric acid (NIST ID 39560-mainlib) negatively correlated to S-GreenGreenyellow module, decreasing at 24hai. Both metabolites are classified as hydroxycinnamic acids, which in the form of hydroxycinammic acid amides (HCAAs) are known for conferring thickening to cell walls due to their deposition (MACOY et al., 2015). Lyxose (NIST ID 39380-mainlib), major cell wall component, decreased and were negatively correlated to S-Blue Module at 6hai. Decrease abundance of lyxose and HCAAs identified may contribute to full fungal development in susceptible genotype, only visualizing subepidermal vesicle and haustorial mother cell development at 12hpi and 24hpi exclusively in this genotype (SEKIYA, 2020). Anthraquinones derivatives were also identified. Emodin, correlated to S-Blue module at 6hai, increased in abundance only at this time and Alizarin correlated to S-RedMagentaTanSalmon started to decrease at 0hai. Taken together these findings, anthraquinones, phenylpropanoids and cell wall reinforcement plays important roles during incompatible interactions.

2.4.5. Metabolism of Aminoacids and Protein Regulation

Amino acids play an important role in plant-pathogen interactions, being essential for host metabolism, participating in nitrogen assimilation and as precursors for hormones, pigments and defense metabolites. However, also important for the pathogen, which modulates host metabolism for its own advantage and nutrition. (CASTRO-MORETTI, 2020). During the present infection time-course, amino acids were abundant in both genotypes. At 12hai,

Susceptible genotype showed an increase in Proline (Pro) NIST ID 20907-replib, Threonine (Thre) NIST ID 38412-mainlib, Glutamic Acid (Glu) NIST ID 182910-mainlib and GABA NIST ID 143908-mainlib. Methylleucine NIST ID 141919-mainlib (S-Blue Module – 6hai), Alanine derivative NIST ID 127099-mainlib (S-RedTanMagentaSalmon-0hai) and Asparagine NIST ID 9234-replib (S-YellowPink Module – 18hai) were correlated at different times. R-Turquoise Module (18hai) negatively correlated to the increased abundance of GABA, Methylleucine, Threonine and Lysine NIST ID 39149-mainlib, presenting time divergence of aminoacid accumulation from susceptible. In resistant, Alanine derivatives (NIST IDs 86440-mainlib, 127099-mainlib) correlated to 6hai and 12hai, respectively, Proline to 6hai and Isoleucine (51164-mainlib) to 24hai. Proteins related to amino acids metabolism were present in S-RedTanMagentaSalmon (0hai) and S-PurpleTurquoise (0hai) module and S-YellowPink (18hai) module, while, in resistant were present in R-PinkYellowTan (6hai) and R-BlackBrownGreenyellow (24hai), also presenting timing differences. Proteins identification and their respective module are described in tables 12 and 13, for resistant and susceptible genotypes, respectively.

Proline, amino acid obtained in both genotypes, is known for increasing in abundance in plants during abiotic stress, acting as antioxidant, ROS detoxifier, redox buffering and osmotic adjuster (VERSLUES; SHARMA, 2010; LIANG et al., 2013). It is also associated to biotic stress, playing roles in programmed cell death. External application of proline on Arabidopsis plants produced HR-like cell death symptoms without pathogen inoculation (DEUSCHLE et al., 2004) and accumulation were also observed during infection time-course of others pathosysthems (SCHAKER et al., 2017), however, it is also linked to inducing fungal development by hyphae protection against damage caused by ROS produced by the plant (CHEN; DICKMAN, 2005; SCHAKER et al., 2017). In our study, proline was accumulated earlier in resistant plants, while susceptible showed an increased at 12hai, time when was able to visualize penetration hyphae of both genotypes, requiring further investigation of proline participation on fungal development. GABA is a non-proteic aminoacid involved in multiple functions in plants, as controling stress responses, pH regulation, redox regulation, energy production and maintenance of the carbon/nitrogen (C/N) balance, as reviewed by Ramos-Ruiz; Martinez; Knauf-Beiter (2019), also presenting timing divergence of accumulation. Increase in Glu, Thre, Asp, Lys may reflect a response in the nitrogen status of infected samples of both genotypes, although susceptible required nitrogen mobilization earlier, possibly for pathogen development, as Sekiya (2020) identified a repression in metabolites and proteins abundance involved in phytoalexins and defense responses after 12hai in susceptible genotype utilized in this study.

Another aspect involved in susceptible and resistant genotype response during infection was the proteasome regulation. Ths is a large protein complex responsible for intracellular proteins degradation in a controlled manner, found present in R-Blue (12hai) and S-Brown (12hai) modules more proeminently as one main altered pathway (Tables 4 and 5), time-point when was able to visualize defense responses from resistant genotype (SEKIYA, 2020). Targeted protein degradation by ubiquitin-proteasome system (UPS) are known for playing crucial roles on immunity regulation as ubiquitinated substrates can be degraded, often by 26S proteasome constituted with 20S proteolytic core particle, for protein abundance regulation (SOREL et al., 2018; COPELAND; LI, 2019). During our study, 20S subunits proteins were found in both resistant and susceptible genotypes, showing an increasing and a decreasing pattern at 12hai, respectively (Table 14, Table 15). As a multicomponent complex, perturbation of UPS can lead to either enhanced or reduced immune system. In respect to disruption of 26S proteasome function, the ability of plant to respond and resist to various environmental stressors, as oxidative, salinity and drought stress is also deacresed, as reviewed by ALI; BAEK (2020). In previous works, related to plant defenses against pathogens, ROS production efficient regulation and systemic acquired resistance induction is followed by an increasing abundance of 20s proteasome subunits, with pathogen effectors threatment (SUTY et al., 2003; LEQUEU et al, 2005). Consistently to literature, our work also presents proteasome participation in *E.grandis-A psidii* interaction, with increasing resistance associated to increased abundance of proteasome subunits.

2.4.6. CONCLUSION

Highlighting the importance of primary metabolism knowledge during plant-pathogen interactions, the present study unveiled possible causes associated with susceptibility or resistance. Identifying some potential metabolites and proteins involved in spore germination and pathogen-triggered defense responses, providing insights into major biological processes affected by *E. grandis* rust infection, as photosynthesis, lipid metabolism, amino acid metabolism, cell wall reinforcement, proteasome and phenylpropanoids pathway and their differences between both genotypes. Diferrent regulation of proteins associated to photosynthesis and light reactions, early decrease in lipids involved in jasmonates synthesis, presence of polyamines and early decrease with metabolites associated with spore germination, divergent amino acid metabolism, increasing pattern of phenylpropanoids intermediates with involvement in cell wall straightening and anthraquinones after 12hai were the major advantages identified from resistant genotype during *A. psidii* infection. Taken together, the present data shows candidate mechanisms, metabolites

and proteins to be further explored among genotypes with different responses to rust disease, enhancing knowledge of molecular mechanisms involved in eucalyptus *A. psidii* infection.

REFERENCES

ABU-NADA, Y. et al. Temporal dynamics of pathogenesis-related metabolites and their plausible pathways of induction in potato leaves following inoculation with Phytophthora infestans. **European Journal of Plant Pathology**, v. 118, n. 4, p. 375–391, 2007.

ALFENAS, A. C. et al. Clonagem e doenças do eucalipto. 2004.

ALI, M. S.; BAEK, K. H. Protective roles of cytosolic and plastidal proteasomes on abiotic stress and pathogen invasion. **Plants**, v. 9, n. 7, p. 1–17, 2020.

ALVES, A. A. et al. Genetic mapping provides evidence for the role of additive and non-additive QTLs in the response of inter-specific hybrids of Eucalyptus to Puccinia psidii rust infection. **Euphytica**, v. 183, n. 1, p. 27–38, 2012.

ARAMAKI, T. et al. KofamKOALA: KEGG ortholog assignment based on profile HMM and adaptive score threshold. **Bioinformatics**, v. 36, n. 7, p. 2251-2252, 2020.

BARROS, I. B. de et al. Phytochemical and antifungal activity of anthraquinones and root and leaf extracts of Coccoloba mollis on phytopathogens. **Brazilian Archives of Biology and Technology**, v. 54, n. 3, p. 535-541, 2011.

BERGER, S.; SINHA, A. K.; ROITSCH, T. Plant physiology meets phytopathology: plant primary metabolism and plant pathogen interactions. **Journal of Experimental Botany**, v. 58, n. 15–16, p. 4019–4026, 2007.

BINI, A. P. **Estudo molecular do desenvolvimento de Puccinia psidii Winter in vitro e no processo de infecção em Eucalyptus grandis**. Tese de Doutorado. Universidade de São Paulo. 2016.

BINI, A. P. et al. Development of a quantitative real-time PCR assay using SYBR Green for early detection and quantification of Austropuccinia psidii in Eucalyptus grandis. **European Journal of Plant Pathology**, v. 150, n. 3, p. 735–746. 2018.

BILGIN, D. D. et al. Biotic stress globally downregulates photosynthesis genes. **Plant, Cell and Environment**, v. 33, n. 10, p. 1597–1613, 2010.

BOLTON, M. D. Primary Metabolism and Plant Defense-Fuel for the Fire. **MPMI**, v. 22, n. 5, p. 487–497, 2009.

BRADFORD, M. M. A rapid and sensitive method for the quantitation of microgram quantities of protein utilizing the principle of protein-dye binding. **Analytical biochemistry**, v. 72, n. 1-2, p. 248-254, 1976.

BRONDANI, R. et al. A microsatellite-based consensus linkage map for species of Eucalyptus and a novel set of 230 microsatellite markers for the genus. **BMC plant biology**, v. 6, n. 1, p. 20, 2006.

BUDZINSKI, I. G. F. et al. Network Analyses and Data Integration of Proteomics and Metabolomics From Leaves of Two Contrasting Varieties of Sugarcane in Response to Drought. **Frontiers in Plant Science**, v. 10, p. 1524, 2019.

BUTLER, J. B. et al. Evidence for different QTL underlying the immune and hypersensitive responses of Eucalyptus globulus to the rust pathogen Puccinia psidii. **Tree Genetics and Genomes**, v. 12, n. 3, p. 1–13. 2016.

CAARLS, L.; PIETERSE, C. M. J.; VAN WEES, S. C. M. How salicylic acid takes transcriptional control over jasmonic acid signaling. **Frontiers in Plant Science**, v. 6, n. MAR, p. 170, 2015.

CASTRO-MORETTI, F. R. et al. Metabolomics as an emerging tool for the study of plant–pathogen interactions. **Metabolites**, v. 10, n. 2, p. 1–23, 2020.

CHEN, C.; DICKMAN, M. B. Proline suppresses apoptosis in the fungal pathogen Colletotrichum trifolii. **Proceedings of the National Academy of Sciences of the United States of America**, v. 102, n. 9, p. 3459–3464, 2005.

CHONG, J. et al. MetaboAnalyst 4.0: towards more transparent and integrative metabolomics analysis. **Nucleic acids research**, v. 46, n. W1, p. W486-W494, 2018.

CHRISTENSEN, S. A.; KOLOMIETS, M. V. The lipid language of plant-fungal interactions. **Fungal Genetics and Biology**. V. 48, 1, p. 4-14. 2011.

COPELAND, C.; LI, X. Regulation of plant immunity by the proteasome. In: **International review of cell and molecular biology**. Academic Press, p. 37-63. 2019.

DENG, Y.; LU, S. Biosynthesis and Regulation of Phenylpropanoids in Plants. **Critical Reviews in Plant Sciences**, v. 36, n. 4, p. 257–290, 2017.

DEUSCHLE, K. et al. The role of 1-pyrroline-5-carboxylate dehydrogenase in proline degradation. **Plant Cell**, v. 16, n. 12, p. 3413–3425, 2004.

DIXON, R. A. et al. The phenylpropanoid pathway and plant defence - A genomics perspective**. Molecular Plant Pathology. Molecular Plant Pathology**, v. 3, 5, p. 371-390. 2002

DOS SANTOS, I. B. et al. The Eucalyptus cuticular Waxes contribute in preformed defense against austropuccinia psidii. **Frontiers in Plant Science**, v. 9, 2019.

DUVAL, J. et al. Research advances for the extraction, analysis and uses of anthraquinones: A review. **Industrial Crops and Products**, v. 94, p. 812–833, 2017.

FAGARD, M. et al. Nitrogen metabolism meets phytopathology. **Journal of experimental botany**, v. 65, n. 19, p. 5643-5656, 2014.

FEUSSNER, I.; POLLE, A. What the transcriptome does not tell — proteomics and metabolomics are closer to the plants' patho-phenotype. **Current Opinion in Plant Biology**, v. 26, p. 26–31. 2015.

GHOSH, S. et al. Proteometabolomic analysis of transgenic tomato overexpressing oxalate decarboxylase uncovers novel proteins potentially involved in defense mechanism against Sclerotinia. **J Proteomics**, v. 143, p. 242–253. 2016.

GLAZEBROOK, J. Contrasting mechanisms of defense against biotrophic and necrotrophic pathogens. **Annual Review of Phytopathology**, v. 43, p. 205–227, 2005.

GODARD, S. et al. Induction of defence mechanisms in grapevine leaves by emodin- and anthraquinone-rich plant extracts and their conferred resistance to downy mildew. **Plant Physiology and Biochemistry**, v. 47, n. 9, p. 827–837, 2009.

GULLBERG, J. et al. Design of experiments: an efficient strategy to identify factors influencing extraction and derivatization of Arabidopsis thaliana samples in metabolomic studies with gas chromatography/mass spectrometry. **Analytical Biochemistry**, v. 331, n. 2, p. 283–295, 2004.

HURKMAN, W. J.; TANAKA, C. K. Solubilization of plant membrane proteins for analysis by two-dimensional gel electrophoresis. **Plant physiology**, v. 81, n. 3, p. 802-806, 1986.

IBÁ. **Anual Report**. Available in: <https://iba.org/datafiles/publicacoes/relatorios/iba-relatorioanual2019.pdf>. Acessed: 12 jun. 2020.

IZHAKI, I. Emodin - A secondary metabolite with multiple ecological functions in higher plants**.** **New Phytologist,** v. 155, 2, p. 205-217, 2002.

JANCEWICZ, A. L.; GIBBS, N. M.; MASSON, P. H. Cadaverine's Functional Role in Plant Development and Environmental Response. **Frontiers in Plant Science**, v. 7, p. 870, 2016.

JUNGHANS, D. T. et al. Resistance to rust (Puccinia psidii Winter) in Eucalyptus: mode of inheritance and mapping of a major gene with RAPD markers. **Theoretical and Applied Genetics**, v. 108, n. 1, p. 175-180, 2003a.

JUNGHANS, D. T.; ALFENAS, A. C.; MAFFIA, L. A. Escala de notas para quantificação da ferrugem em Eucalyptus. **Fitopatologia Brasileira**, v. 28, n. 2, p. 184-188, 2003b.

KALAMPOKIS, I. F. et al. Untargeted metabolomics as a hypothesis-generation tool in plant protection product discovery: Highlighting the potential of trehalose and glycerol metabolism of fungal conidiospores as novel targets. **Metabolomics**, v. 16, n. 7, p. 79. 2020.

KARMAKAR, S. et al. Proteo-metabolomic investigation of transgenic rice unravels metabolic alterations and accumulation of novel proteins potentially involved in defence against Rhizoctonia solani. **Scientific Reports**, v. 9, n. 1. 2019.

KUMAR, Y. et al. *Fusarium oxysporum* mediates systems metabolic reprogramming of chickpea roots as revealed by a combination of proteomics and metabolomics. **Plant Biotechnology Journal**, v. 14, n. 7, p. 1589–1603, 2016.

LANGFELDER, Peter; HORVATH, Steve. WGCNA: an R package for weighted correlation network analysis. **BMC bioinformatics**, v. 9, n. 1, p. 559, 2008.

LEITE, T. F. **Estabelecimento de um patossistema modelo e análise da interação molecular planta-patógeno entre Eucalyptus grandis e Puccinia psidii Winter por meio da técnica de RNA-Seq**. Tese de Doutorado. Universidade de São Paulo. 2012

LEQUEU, J. et al. Proteasome comprising a β1 inducible subunit acts as a negative regulator of NADPH oxidase during elicitation of plant defense reactions. **FEBS letters**, v. 579, n. 21, p. 4879-4886, 2005.

LI, S. et al. Differential Proteome Analysis of Hybrid Bamboo (Bambusa pervariabilis × Dendrocalamopsis grandis) Under Fungal Stress (Arthrinium phaeospermum). **Scientific Reports**, v. 9, n. 1, 2019.

LIANG, X. et al. Proline mechanisms of stress survival. **Antioxidants and Redox Signaling**, v. 19, n. 9, p. 998–1011, 2013.

MA, H. et al. A comparative proteomic approach to identify defence-related proteins between resistant and susceptible rice cultivars challenged with the fungal pathogen Rhizoctonia solani. **Plant Growth Regulation**, v. 90, n. 1, p. 73–88, 2020.

MACOY, D. M. et al. Biosynthesis, physiology, and functions of hydroxycinnamic acid amides in plants. **Plant Biotechnology Reports**, v. 9, n. 5, p. 269-278, 2015.

MAMANI, E. M. C. et al. Positioning of the major locus for Puccinia psidii rust resistance (Ppr1) on the Eucalyptus reference map and its validation across unrelated pedigrees. **Tree Genetics and Genomes**, v. 6, n. 6, p. 953–962, 2010.

MASSON, P. H.; TAKAHASHI, T.; ANGELINI, R. Editorial: Molecular Mechanisms Underlying Polyamine Functions in Plants. **Frontiers in Plant Science**, v. 8, p. 14, 2017.

MINOCHA, R.; MAJUMDAR, R.; MINOCHA, S. C. Polyamines and abiotic stress in plants: A complex relationship. **Frontiers in Plant Science**, v. 5, n. MAY, p. 175, 2014.

MONTILLA-BASCÓN, G. et al. Free polyamine and polyamine regulation during pre-penetration and penetration resistance events in oat against crown rust (*Puccinia coronata* f. sp. *avenae*). **Plant Pathology**, v. 65, n. 3, p. 392–401, 2016.

MYBURG, A. A. et al. The genome of Eucalyptus grandis. **Nature**, v. 510, n. 7505, p. 356–362, 11 jun. 2014.

PAL, M.; JANDA, T. Role of polyamine metabolism in plant pathogen interactions. **Journal of Plant Sciences and Phytopathology**, v. 1, p. 095–0100, 2017.

RAMOS-RUIZ, R.; MARTINEZ, F.; KNAUF-BEITER, G. The effects of GABA in plants. **Cogent Food & Agriculture**, v. 5, n. 1, p. 1670553, 2019.

ROBERT-SEILANIANTZ, A.; GRANT, M.; JONES, J. D. G. Hormone crosstalk in plant disease and defense: More than jasmonate-salicylate antagonism. **Annual Review of Phytopathology**, v. 49, p. 317–343, 2011.

ROJAS, C. M. et al. Regulation of primary plant metabolism during plant-pathogen interactions and its contribution to plant defense**. Frontiers in Plant Science**, v. 5, 17, 2014.

SANTOS, S. A. et al. Transcriptome analysis of Eucalyptus grandis genotypes reveals constitutive overexpression of genes related to rust (Austropuccinia psidii) resistance. **Plant Molecular Biology**, v. 1, p. 3, 2020.

SCHAKER, P. D. C. et al. Metabolome dynamics of smutted sugarcane reveals mechanisms involved in disease progression and whip emission. **Frontiers in Plant Science**, v. 8, 2017.

SEKIYA, A. **Early responses of Eucalyptus grandis during rust infection.** Tese de Doutorado. Universidade de São Paulo. 2020

SERRANO, I.; AUDRAN, C.; RIVAS, S. Chloroplasts at work during plant innate immunity. **Journal of Experimental Botany**, v. 67, n. 13, p. 3845–3854, 2016.

SHANNON, P. et al. Cytoscape: A software Environment for integrated models of biomolecular interaction networks. **Genome Research**, v. 13, n. 11, p. 2498–2504, 2003.

SHEN, Y. et al. The early response during the interaction of fungal phytopathogen and host plant. **Open biology**, v. 7, n. 5, p. 170057, 2017.

SILVA, R. R. et al. Limonene, a Chemical Compound Related to the Resistance of Eucalyptus Species to Austropuccinia psidii. **Plant Disease**, v. 104, n. 2, p. 414–422, 16 fev. 2020.

SOREL, M. et al. Ubiquitin/Proteasome System in Plant Pathogen Responses. **Annual Plant Reviews online**, p. 65-116, 2018.

SPOEL, S. H.; JOHNSON, J. S.; DONG, X. Regulation of tradeoffs between plant defenses against pathogens with different lifestyles. **Proceedings of the National Academy of Sciences of the United States of America**, v. 104, n. 47, p. 18842–18847, 20 nov. 2007.

SU, J. et al. Active photosynthetic inhibition mediated by MPK3/MPK6 is critical to effector-triggered immunity. **PLoS Biology**, v. 16, n. 5, p. e2004122–e2004122, 2018.

SUPEK, F. et al. REVIGO Summarizes and Visualizes Long Lists of Gene Ontology Terms. **PLoS ONE**, v. 6, n. 7, p. e21800, 2011.

SUTY, L. et al. Preferential induction of 20S proteasome subunits during elicitation of plant defense reactions: towards the characterization of "plant defense proteasomes". **The international journal of biochemistry & cell biology**, v. 35, n. 5, p. 637-650, 2003.

TIAN, T. et al. agriGO v2.0: a GO analysis toolkit for the agricultural community, 2017 update. **Nucleic Acids Research**, v. 45, 2017.

VERSLUES, P. E.; SHARMA, S. Proline Metabolism and Its Implications for Plant-Environment Interaction. **The Arabidopsis Book**, v. 8, p. e0140, 2010.

VOS, I. A. et al. Impact of hormonal crosstalk on plant resistance and fitness under multi-attacker conditions. **Frontiers in Plant Science**, v. 6, n. AUG, p. 639, 2015.

WANG, M. et al. Plant Primary Metabolism Regulated by Nitrogen Contributes to Plant-Pathogen Interactions. **Plant and Cell Physiology**, v. 60, n. 2, p. 329–342, 2019.

YADAV, V. et al. Phenylpropanoid pathway engineering: An emerging approach towards plant defense**. Pathogens,** v.9, 4, p. 4, 2020.

ZABALA, M. T. et al. Chloroplasts play a central role in plant defence and are targeted by pathogen effectors. **Nature Plants**, v. 1, n. 6, p. 15074, 1 jun. 2015.

ZURBRIGGEN, M. D.; CARRILLO, N.; HAJIREZAEI, M. ROS signaling in the hypersensitive response. **Plant Signaling & Behavior**, v. 5, n. 4, p. 393–396, abr. 2010.

TABLES

Table 1. List of 44 metabolites with significant differences among time-course infection, obtained with univariate analysis ANOVA (FDR < 0.05) for resistant genotype. Metabolites are represented by NIST ID, common name and respectively class obtained utilizing Human metabolome database (HMDB).

ID	Metabolite Name	Class	F-Value	P-Value	-log10(p)	FDR
38436-mainlib	1,2,3-Butanetriol	Alcohols or Polyols	81423	1.64E-22	21.786	1.72E-20
115954-mainlib	3-Buten-2-one, 3-trimethylsilyloxy- (Derivatized name)	Alcohols or Polyols	19981	1.84E-19	18.736	6.43E-18
9311-replib	Ethylene glycol	Alcohols or Polyols	5948	7.85E-17	16.105	1.65E-15
39414-mainlib	Glycerol	Alcohols or Polyols	11.468	0.00093762	3.028	0.002983
143937-mainlib	Putrescine	Amines	48.365	1.65E-06	5.7824	9.12E-06
24430-replib	Cadaverine	Amines	16.413	0.00021544	3.6667	0.00087
86442-mainlib	Alanine, N-methyl-N-methoxycarbonyl-, undecyl ester	Aminoacid derivative	21.28	7.03E-05	4.153	0.000321
141919-mainlib	Methylleucine	Aminoacid derivative	14.354	0.00037758	3.423	0.001416
86440-mainlib	Alanine, N-methyl-N-methoxycarbonyl-, hexyl ester	Aminoacid derivative	10.801	0.0011869	2.9256	0.003514
127099-mainlib	Butyl 2-[methyl(trifluoroacetyl)amino]propanoate	Aminoacid derivative	9.2872	0.00212	2.6737	0.005565
51164-mainlib	Isoleucine	Aminoacids	7593	2.32E-17	16.635	6.08E-16
20907-replib	Proline	Aminoacids	16.97	0.00018702	3.7281	0.000786
143908-mainlib	4-Aminobutyric acid (GABA)	Aminoacids	16.234	0.00022568	3.6465	0.000878
38412-mainlib	Threonine	Aminoacids	13.059	0.0005566	3.2545	0.001996
39149-mainlib	Lysine	Aminoacids	10.76	0.0012047	2.9191	0.003514
21693-replib	diisobutyl phthalate	Benzenoids	1087	3.81E-13	12.419	4.96E-12
180080-mainlib	3,4-Dimethoxymandelic acid	Benzenoids	65.606	3.88E-07	6.4116	2.39E-06
86262-mainlib	Adrenaline	Benzenoids	52.84	1.09E-06	5.964	6.34E-06
180295-mainlib	di(3-methylphenyl) phthalic acid	Benzenoids	17.235	0.00017507	3.7568	0.000766
25951-mainlib	Embramine	Benzenoids	12.31	0.00070681	3.1507	0.002394

ID	Metabolite Name	Class	F-Value	P-Value	-log10(p)	FDR
207268-mainlib	Alizarin	Benzenoids	9.7782	0.0017435	2.7586	0.004818
180294-mainlib	Methyl (3,4-dimethoxyphenyl)(hydroxy)acetate	Benzenoids	9.5153	0.0019341	2.7135	0.005207
211614-mainlib	Emodin	Benzenoids	8.5604	0.0028731	2.5416	0.007183
39872-mainlib	Gallic acid	Benzenoids	6.8367	0.0064154	2.1928	0.015665
207102-mainlib	Catechine	Flavonoids	29590	2.58E-20	19.588	1.36E-18
9961-replib	Linoleic acid	Lipids	828.31	1.48E-12	11.831	1.41E-11
9118-replib	Hexadecanoic acid	Lipids	662.46	4.49E-12	11.347	3.93E-11
9100-replib	Linolenic acid	Lipids	487.46	2.07E-11	10.685	1.45E-10
38643-mainlib	Levulinic acid enol	Organic acids	546.4	1.17E-11	10.931	8.79E-11
38429-mainlib	Lactic acid	Organic acids	480.8	2.21E-11	10.655	1.45E-10
9526-replib	Arabinonic acid, 1,4-lactone,	Organic acids	25.884	2.95E-05	4.5306	0.000141
119415-mainlib	Pyruvic acid	Organic acids	11.804	0.00083604	3.0778	0.002743
119441-mainlib	Succinic acid	Organic acids	10.169	0.0015001	2.8239	0.004257
1348-mainlib	Hydroxy-acetic acid	Organic acids	4.952	0.018369	1.7359	0.043835
37089-mainlib	2-(3-Bromo-5,5,5-trichloro-2,2-dimethylpentyl)-1,3-dioxolane	Other	3193.7	1.76E-15	14.756	2.63E-14
29786-mainlib	3-Octadecyne	Other	42.227	3.12E-06	5.5057	1.64E-05
36897-mainlib	1-Ethenyl-3-(1-hexenyl)-cyclopentane	Other	35.374	7.10E-06	5.1485	3.55E-05
27526-replib	Caffeic acid	Phenylpropanoids	12.981	0.00057029	3.2439	0.001996
38761-mainlib	Sorbose	Sugars	5145.8	1.62E-16	15.791	2.83E-15
38809-mainlib	Glyceric acid	Sugars	1063.4	4.25E-13	12.371	4.96E-12
9402-replib	Gluconic acid	Sugars	896.37	9.96E-13	12.002	1.05E-11
9299-replib	Erythronic acid	Sugars	647.47	5.04E-12	11.298	4.07E-11
38732-mainlib	2-Deoxy-erythro-pentonic acid	Sugars	10.762	0.001204	2.9194	0.003514
164548-mainlib	Glucose, Galactose, linear form	Sugars	9.1173	0.0022725	2.6435	0.00582

Table 2. List of 43 metabolites with significant differences among time-course infection, obtained with univariate analysis ANOVA (FDR <0.05) for susceptible genotype. Metabolites are represented by NIST ID, common name and respectively class obtained utilizing Human metabolome database (HMDB).

ID	Metabolite Name	Class	F-Value	P-Value	-log10(p)	FDR
9311-replib	Ethylene glycol	Alcohols or Polyols	3549.6	1.04E-15	14.985	3.35E-14
9203-replib	Ribitol	Alcohols or Polyols	43.885	2.61E-06	5.584	1.94E-05
39414-mainlib	Glycerol	Alcohols or Polyols	8.2273	0.0033238	2.4784	0.009212
38436-mainlib	1,2,3-Butanetriol	Alcohols or Polyols	7.2485	0.005233	2.2812	0.013358
26040-mainlib	N-Methyltrifluoroacetamide	Amides	629.83	5.78E-12	11.238	7.00E-11
141919-mainlib	Methylleucine	Aminoacid derivative	1142.1	2.98E-13	12.526	4.13E-12
127099-mainlib	Butyl 2-[methyl(trifluoroacetyl)amino]propanoate	Aminoacid derivative	10.292	0.001432	2.8441	0.005145
143908-mainlib	4-Aminobutyric acid (GABA)	Aminoacids	5420	1.25E-16	15.903	6.06E-15
9234-replib	Asparagine	Aminoacids	13.281	0.00051963	3.2843	0.0024
38412-mainlib	Threonine	Aminoacids	12.603	0.0006428	3.1919	0.002834
20907-replib	Proline	Aminoacids	8.8612	0.0025279	2.5972	0.00743
182910-mainlib	Glutamic acid	Aminoacids	4.6726	0.0219	1.6595	0.049403
37244-mainlib	4-tolyl isocyanate	Benzenoids	1597.1	5.59E-14	13.253	1.36E-12
211614-mainlib	Emodin	Benzenoids	289.5	2.74E-10	9.5622	2.42E-09
180081-mainlib	2,5-Dimethoxymandelic acid	Benzenoids	105.57	3.90E-08	7.4092	3.15E-07
207268-mainlib	Alizarin	Benzenoids	34.553	7.92E-06	5.1014	5.12E-05
146504-mainlib	2-Allyl-1,4-dimethoxybenzene	Benzenoids	15.927	0.0002446	3.6115	0.001318
180294-mainlib	Methyl (3,4-dimethoxyphenyl)(hydroxy)acetate	Benzenoids	13.409	0.0004997	3.3013	0.0024
86262-mainlib	Adrenaline	Benzenoids	10.807	0.0011844	2.9265	0.004596
9961-replib	Linoleic acid	Lipids	9.9802	0.0016122	2.7926	0.005443
40201-mainlib	Glycerophosphoric acid (BGA)	Lipids	6.8621	0.006334	2.1983	0.01536
39649-mainlib	Adenosine	Nucleoside	31.282	1.25E-05	4.9032	7.58E-05
38907-mainlib	Tartaric acid	Organic acids	1160.4	2.75E-13	12.561	4.13E-12

ID	Metabolite Name	Class	F-Value	P-Value	-log10(p)	FDR
38813-mainlib	Acetic acid, bis[(trimethylsilyl)oxyl]-, trimethylsilyl ester (derivatized name)	Organic acids	17.531	0.00016281	3.7883	0.000929
38695-mainlib	Oxalic acid	Organic acids	14.075	0.00040953	3.3877	0.002091
38766-mainlib	Ribonic acid	Organic acids	10.867	0.0011589	2.9359	0.004596
38643-mainlib	Levulinic acid enol	Organic acids	9.3773	0.0020441	2.6895	0.006196
38429-mainlib	Lactic acid	Organic acids	8.7506	0.0026488	2.577	0.007557
29786-mainlib	3-Octadecyne	Other	7.6608	0.004301	2.3664	0.011276
36897-mainlib	1-Ethenyl-3-(1-hexenyl)-cyclopentane	Others	9.9562	0.0016272	2.7886	0.005443
37089-mainlib	2-(3-Bromo-5,5,5-trichloro-2,2-dimethylpentyl)-1,3-dioxolane	Others	9.5352	0.0019188	2.717	0.006004
39560-mainlib	p-Coumaric acid	Phenylpropanoids	390.65	6.21E-11	10.207	6.02E-10
27526-replib	Caffeic acid	Phenylpropanoids	12.281	0.00071355	3.1466	0.003009
39380-mainlib	Lyxose, Linear form	Sugars	9550.8	7.36E-18	17.133	7.14E-16
39404-mainlib	Mannose 6-Phosphate	Sugars	1501.6	7.60E-14	13.119	1.47E-12
38809-mainlib	Glyceric acid	Sugars	585.31	8.32E-12	11.08	8.97E-11
170819-mainlib	Talose, furanose form	Sugars	43.234	2.80E-06	5.5536	1.94E-05
164548-mainlib	Glucose, Galactose, linear form	Sugars	10.432	0.0013591	2.8667	0.005071
38732-mainlib	2-Deoxy-erythro-pentonic acid	Sugars	9.7963	0.0017312	2.7616	0.005598
38261-mainlib	Xylitol	Sugars	7.737	0.0041511	2.3818	0.011185
39372-mainlib	Xylose, pyranose form	Sugars	7.0909	0.0056519	2.2478	0.014057
9299-replib	Erythronic acid	Sugars	6.4715	0.0077406	2.1112	0.018313
39358-mainlib	Methyl glycoside	Sugars	5.9061	0.0105	1.9788	0.02425

Table 3. List of metabolites and their respective correlated modules (p-value <0.05), with negative or positive correlations, obtained with WGCNA analysis from both genotypes.

Metabolite Name	Metabolite ID	Correlated Modules	Correlation type
Glucose/Galactose	164548-mainlib	R-MagentaGreenPurpleSalmon / S- PurpleTurquoise / S-Blue	Positive/ Positive / Negative
Glycerol	39414-mainlib	R-MagentaGreenPurpleSalmon / S-YellowPink	Positive / Negative
Putrescine	143937-mainlib	R-MagentaGreenPurpleSalmon	Positive
Linoleic acid	9961-replib	R-MagentaGreenPurpleSalmon/ S-YellowPink	Positive / Positive
Linolenic acid	9100-replib	R-MagentaGreenPurpleSalmon	Positive
Gluconic acid	9402-replib	R-MagentaGreenPurpleSalmon	Positive
Hexadecanoic acid	9118-replib	R-MagentaGreenPurpleSalmon	Positive
Lactone-Arabinonic acid	9526-replib	R-MagentaGreenPurpleSalmon	Positive
Pyruvic acid	119415-mainlib	R-MagentaGreenPurpleSalmon	Positive
Diisobutyl phthalate	21693-replib	R-MagentaGreenPurpleSalmon	Negative
Catechine	207102-mainlib	R-MagentaGreenPurpleSalmon	Negative
Sorbose	38761-mainlib	R-MagentaGreenPurpleSalmon	Negative
Proline	20907-replib	R-YellowPinkTan / S-Black	Positive / Positive
1-Ethenyl-3-(1-hexenyl)-cyclopentane	36897-mainlib	R-YellowPinkTan / S- Brown	Positive / Negative
Alanine derivative	86440-mainlib	R-YellowPinkTan, R-Blue	Positive
Levulinic acid enol	38643-mainlib	R-YellowPinkTan / S-Black / S-Brown	Positive / Positive / Negative
2-(3-Bromo-5,5,5-trichloro-2,2-dimethylpentyl)-1,3-dioxolane	37089-mainlib	R-YellowPinkTan	Negative
di(3-methylphenyl) phthalic acid	180295-mainlib	R-Blue	Positive
Alanine derivative	127099-mainlib	R-Blue/ R-Cyan / S-PurpleTurquoise/ S-RedTanMagentaSalmon	Positive/Positive/Negative/Positive
3-Octadecyne	29786-mainlib	R-Blue/ R-Red/ S-YellowPink	Positive/Positive/Positive
Caffeic acid	27526-replib	R-Blue	Positive
Emodin	211614-mainlib	R-Blue/ R-Red/ S-Blue	Positive/Positive/Positive
Succinic acid	119441-mainlib	R-Cyan/ R-BlackBrownGreenyellow	Positive/Positive

Metabolite Name	Metabolite ID	Correlated Modules	Correlation type
Hydroxy-acetic acid	1348-mainlib	R-Cyan	Positive
Alanine derivative	86442-mainlib	R-Cyan	Positive
3-Buten-2-one, 3-trimethylsilyloxy- (derivatized name)	115954-mainlib	R-Turquoise	Positive
L-Threonine	38412-mainlib	R-Turquoise/ S-Brown/ S-Black	Negative/ Negative/ Positive
Ethylene glycol	9311-replib	R-Turquoise / S-Blue	Negative/Positive
Lactic acid	38429-mainlib	R-Turquoise/ S-Brown/ S-GreenGreenyellow	Negative/ Positive/ Positive
N-methylleucine	141919-mainlib	R-Turquoise/ S-Blue	Negative/Positive
L-Lysine	39149-mainlib	R-Turquoise	Negative
Erythronic acid	9299-replib	R-Turquoise/ S-RedTanMagentaSalmon / S-Brown	Negative/Positive/Positive
4-Aminobutyric acid (GABA)	143908-mainlib	R-Turquoise/ S-Black / S-Brown	Negative/Positive/Negative
Glyceric acid	38809-mainlib	R-Turquoise/ S-Black / S-Brown	Negative/Negative/Positive
Gallic acid	39872-mainlib	R-Turquoise	Negative
Alizarin	207268-mainlib	R-BlackBrownGreenyellow / S-RedTanMagentaSalmon / S-PurpleTurquoise	Positive/ Positive /Negative
Cadaverine	24430-replib	R-BlackBrownGreenyellow	Positive
L-Isoleucine	51164-mainlib	R-BlackBrownGreenyellow	Positive
Embramine	25951-mainlib	R-BlackBrownGreenyellow	Positive
3,4-Dimethoxymandelic acid	180080-mainlib	R-BlackBrownGreenyellow	Negative
1,2,3-Butanetriol	38436-mainlib	R-BlackBrownGreenyellow / S-GreenGreenyellow	Negative/ Negative
2-Deoxy-erythro-pentonic acid	38732-mainlib	R-BlackBrownGreenyellow / S-PurpleTurquoise	Negative/Negative
Methyl glycoside	39358-mainlib	S-RedTanMagentaSalmon / S-PurpleTurquoise	Positive/ Negative
Methyl (3,4-dimethoxyphenyl)(hydroxy)acetate	180294-mainlib	R-MagentaGreenPurpleSalmon/ S-RedTanMagentaSalmon/S-PurpleTurquoise	Positive/ Positive/ Negative
Talose, furanose form	170819-mainlib	S-RedTanMagentaSalmon	Positive
Adenosine	39649-mainlib	S-RedTanMagentaSalmon / S-PurpleTurquoise	Positive / Negative
2-Deoxy-erythro-pentonic acid	38732-mainlib	S-RedTanMagentaSalmon	Positive
Mannose 6-Phosphate	39404-mainlib	S-RedTanMagentaSalmon / S-PurpleTurquoise	Negative / Positive

Metabolite Name	Metabolite ID	Correlated Modules	Correlation type
Oxalic acid	38695-mainlib	S-Blue	Positive
Acetic acid, bis[(trimethylsilyl)oxyl]-, trimethylsilyl ester (Derivatized name)	38813-mainlib	S-Blue	Positive
Lyxose	39380-mainlib	S-Blue	Negative
2-Allyl-1,4-dimethoxybenzene	146504-mainlib	S-Black / S-Brown	Positive/ Negative
Glycerophosphoric acid (BGA)	40201-mainlib	S-Black / S-Brown	Positive / Negative
2,5-Dimethoxymandelic acid	180081-mainlib	S-Black / S-Brown	Positive / Negative
Ribonic acid	38766-mainlib	S-Black / S-Brown	Positive / Negative
Glutamic acid	182910-mainlib	S-Black / S-Brown	Positive / Negative
N-Methyltrifluoroacetamide	26040-mainlib	S-Black / S-Brown	Negative
Adrenaline	86262-mainlib	S-Brown	Negative
Tartaric acid	38907-mainlib	S-YellowPink	Positive
L-Asparagine	9234-replib	S-YellowPink	Positive
Ribitol	9203-replib	S-YellowPink	Positive
4-tolyl isocyanate	37244-mainlib	S-GreenGreenyellow	Negative
p-Coumaric acid	39560-mainlib	S-GreenGreenyellow	Negative

Table 4. Main KEGG pathways, with more K accessions mapped, for each resistant module. Main pathways were accessed using KofamKoala (E-value < 0.01).

Module	Main Pathways	Number of K acessions mapped	K acessions
MagentaGreenPurpleSalmon	03010 Translation - Ribosome	13	K02891,K02895,K02931,K02937,K02940,K02942,K02943,K02946,K02947,K02966,K02978,K02981,K02985
	00010 Glicolysis/Gluconeogenesis	10	K00002,K00121,K00162,K00850,K01568,K01623,K01803,K01835,K03841,K15633
	00195/00196 Photosynthesis	8	K02113,K02115,K02639,K02641,K02693,K02717,K08901,K08915
	00190 Oxidative Phosphorilation	8	K00417,K01507,K02113,K02115,K02134,K02145,K02147,K03942
PinkYellowTan	03010 Translation - Ribosome	14	K02867,K02870,K02888,K02891,K02933,K02940,K02941,K02943,K02951,K02951,K02968,K02981,K02985,K02987,K02993
	00010 Glycolysis / Gluconeogenesis	11	K00128,K00131,K00134,K00161,K00873,K00895,K00927,K01623,K01803,K01913,K03841
	00630 Glyoxylate and dicarboxylate metabolism	9	K00600,K01602,K01681,K01913,K01915,K11517,K15893,K18121,K19269
Blue	00030 Pentose phosphate pathway	5	K00616,K01623,K01807,K01835,K03841,K03841
	00710 Carbon fixation in photosynthetic organisms	4	K00026,K01623,K01807,K03841
	03050 Proteasome	4	K02727,K02729,K02732,K02738
	00500 Starch and sucrose metabolism	4	K00963,K00975,K01835,K05349
Cyan	00630 Glyoxylate and dicarboxylate metabolism	5	K00600,K00626,K01602,K01915,K02437
	00195 Photosynthesis	3	K02109,K02639,K02699

Module	Main Pathways	Number of K acessions mapped	K acessions
Red	00710 Carbon fixation in photosynthetic organisms	8	K00025,K00134,K00134,K00615,K00927,K01100,K01602,K01803,K05298
	00195 Photosynthesis	7	K02636,K02693,K02701,K02717,K08902,K08909,K08915
	00630 Glyoxylate and dicarboxylate metabolism	4	K00025,K00830,K01602,K03781
Turquoise	03010 Translation - Ribosome	7	K02871,K02876,K02881,K02906,K02945,K02997,K02998
	00010 Glycolysis / Gluconeogenesis	5	K00162,K00627,K00927,K01623,K01792
	00710 Carbon fixation in photosynthetic organisms	4	K00814,K00927,K01623,K01783
BlackBrownGreenyellow	001950/0196 Photosynthesis	16	K02109,K02112,K02634,K02641,K02692,K02694,K02704,K03541,K03542,K08901,K08905,K08907,K08910,K08912,K08916,K08917
	03010 Translation - Ribosome	11	K02868,K02870,K02871,K02904,K02908,K02909,K02951,K02961,K02985,K02989,K02993
	00630 Glyoxylate and dicarboxylate metabolism	9	K00026, K00281, K00284, K00382, K00600, K00605, K01602, K01681, K01915

Table 5. Main KEGG pathways, with more K accessions mapped, for each susceptible module. Main pathways were accessed using KofamKoala (E-value < 0.01).

Module	Main Pathways	Number of K acessions mapped	K acessions
RedTanMagentaSalmon	00010 Glicolysis/Gluconeogenesis	11	K00128,K00134,K00162,K00627,K00873,K00895,K00927,K01623,K01803, K01835,K01913
	00710 Carbon fixation in photosynthetic organisms	10	K00051,K00134,K00615,K00927,K01602,K01623,K01783,K01803,K01807, K05298
	03010 Translation - Ribosome	10	K02871,K02891,K02937,K02941,K02942,K02955,K02962,K02989,K02993, K02998
	00195/00196 Photosynthesis	7	K02634,K02639,K02692,K02693,K02701,K02704,K02717
PurpleTurquoise	03010 Translation -Ribosome	10	K02895,K02931,K02940,K02947,K02958,K02966,K02978,K02985,K02987, K02993
	00630 Glyoxylate and dicarboxylate metabolism	9	K00026,K00382,K00626,K00830,K01091,K01915,K02437,K07130,K11517
	00620 Pyruvate metabolism	9	K00026,K00101,K00128,K00161,K00382,K00626,K00873,K01649,K02160
Blue	03010 Translation - Ribosome	8	K02863,K02868,K02873,K02906,K02945,K02951,K02961,K02981
	00195 Photosynthesis	5	K02109,K02112,K02636,K02716,K08901,K08912
	00010 Glycolysis / Gluconeogenesis	5	K00002,K00162,K01623,K01810,K15633
Brown	00195 Photosynthesis	8	K02634,K02717,K03542,K08902,K08909,K08912,K08915,K08917
	03050 Proteasome	5	K02728,K02732,K02738,K03061,K03066
	00710 Carbon fixation in photosynthetic organisms	5	K00134,K01100,K01623,K01803,K05298

Module	Main Pathways	Number of K acessions mapped	K acessions
Black	00630 Glyoxylate and dicarboxylate metabolism	8	K00382,K01602,K01681,K01915,K02437,K11517,K15893,K18121
	00195 Photosynthesis	7	K02113,K02115,K02636,K02639,K02981,K08907,K08913
	03010 Translation - Ribosome	4	K02891,K02943,K02981,K02998
YellowPink	03010 Translation - Ribosome	10	K02863,K02867,K02870,K02891,K02898,K02930,K02933,K02943,K02946, K02985
	00270 Cysteine and methionine metabolism	7	K00025,K00058,K00549,K00789,K00811,K01738,K16843
	00010 Glycolysis / Gluconeogenesis	6	K00131,K00134,K00927,K01623,K01835,K03841
GreenGreenyellow	00710 Carbon fixation in photosynthetic organisms	5	K00026,K00855,K01623,K01783,K03841
	00010 Glycolysis / Gluconeogenesis	5	K00121,K01623,K01792,K03841,K18857
	03010 Ribosome	5	K02888,K02904,K02957,K02968,K02984

Table 6. All proteins from resistant genotype mapped with Photosynthesis GO terms ($p < 0.05$), using AgriGO, or associated to Photosynthesis Kegg pathway, using KofamKoala.

Protein ID	Related Module	Protein Name	Kegg pathway	GO Terms
Eucgr.F04149.1.p	MagentaGreenPurpleSalmon	ATP synthase delta-subunit gene	00195 [1]	
Eucgr.E04053.1.p	MagentaGreenPurpleSalmon	ATPase, F1 complex, gamma subunit protein	00195	
Eucgr.I02744.1.p	MagentaGreenPurpleSalmon	2Fe-2S ferredoxin-like superfamily protein	00195	
Eucgr.E00291.1.p	MagentaGreenPurpleSalmon	2Fe-2S ferredoxin-like superfamily protein	00195	
Eucgr.I02340.1.p	MagentaGreenPurpleSalmon	ferredoxin-NADP(+)-oxidoreductase 1 [EC:1.18.1.2]	00195	
Eucgr.H00828.1.p	MagentaGreenPurpleSalmon	photosystem I subunit E-2	00195	GO:0015979 [3]
Eucgr.G02488.1.p	MagentaGreenPurpleSalmon	PsbQ-like 2	00195	GO:0015979
Eucgr.G03060.1.p	MagentaGreenPurpleSalmon	light harvesting complex photosystem II	00196 [2]	GO:0009765 [4]
Eucgr.H02489.1.p	MagentaGreenPurpleSalmon	Mog1/PsbP/DUF1795-like photosystem II reaction center PsbP family protein		GO:0015979
Eucgr.H01287.4.p	MagentaGreenPurpleSalmon	Photosystem II reaction center PsbP family protein	00195	GO:0015979
Eucgr.A01774.2.p	MagentaGreenPurpleSalmon	photosystem II reaction center PSB29 protein		GO:0015979
Eucgr.L03253.1.p	MagentaGreenPurpleSalmon	PsbP-like protein 2	00195	GO:0015979
Eucgr.A01769.1.p	Red	photosynthetic electron transfer C		
Eucgr.B02162.1.p	Red	photosystem I subunit E-2		GO:0015979
Eucgr.I00200.2.p	Red	photosystem I reaction center subunit PSI-N, chloroplast, putative / PSI-N, putative (PSAN)		GO:0015979
Eucgr.A02039.1.p	Red	photosystem II subunit P-1		GO:0015979
Eucgr.K00947.1.p	Red	photosystem II family protein		GO:0015979
Eucgr.K01362.1.p	Red	photosystem I light harvesting complex gene 3	00196	GO:0009765
Eucgr.K02983.1.p	Red	light harvesting complex photosystem II	00196	GO:0009765
Eucgr.H02991.1.p	Cyan	ATPase, F0 complex, subunit B/B\', bacterial/chloroplast	00195	
Eucgr.B03849.1.p	Cyan	ferredoxin 3	00195	
Eucgr.K02362.3.p	Cyan	photosystem I subunit l	00195	

Protein ID	Related Module	Protein Name	Kegg pathway	GO Terms
Eucgr.C02765.1.p	BlackBrownGreenyellow	ATPase, F0 complex, subunit B/B\', bacterial/chloroplast	00195	
Eucgr.B02878.1.p	BlackBrownGreenyellow	ATP synthase alpha/beta family protein [EC:7.1.2.2 7.2.2.1]	00195	
Eucgr.E02606.1.p	BlackBrownGreenyellow	photosynthetic electron transfer A	00195	GO:0015979
Eucgr.I02340.2.p	BlackBrownGreenyellow	ferredoxin-NADP(+)-oxidoreductase 1 [EC:1.18.1.2]	00195	
Eucgr.B01088.1.p	BlackBrownGreenyellow	photosystem I subunit D-2	00195	GO:0015979
Eucgr.K00389.1.p	BlackBrownGreenyellow	photosystem I subunit F	00195	GO:0015979
Eucgr.A00264.1.p	BlackBrownGreenyellow	photosystem II reaction center protein B	00195	GO:0015979
Eucgr.F03186.8.p	BlackBrownGreenyellow	photosystem II subunit R	00195	GO:0015979
Eucgr.F03789.1.p	BlackBrownGreenyellow	Chlorophyll A-B binding family protein	00195	
Eucgr.D00854.1.p	BlackBrownGreenyellow	photosystem II subunit Q-2	00195	GO:0015979
Eucgr.F03646.1.p	BlackBrownGreenyellow	photosystem I subunit G	00195	GO:0015979
Eucgr.J01096.2.p	BlackBrownGreenyellow	photosystem I light harvesting complex gene 1	00196	GO:0009765
Eucgr.B00523.1.p	BlackBrownGreenyellow	light-harvesting chlorophyll-protein complex I subunit A4	00196	GO:0009765
Eucgr.D00321.1.p	BlackBrownGreenyellow	light-harvesting chlorophyll-protein complex II subunit B1	00196	GO:0009765
Eucgr.E02381.1.p	BlackBrownGreenyellow	light-harvesting chlorophyll-protein complex II subunit B1	00196	GO:0009765
Eucgr.F04099.1.p	BlackBrownGreenyellow	light harvesting complex of photosystem II 5	00196	GO:0009765
Eucgr.I02677.1.p	BlackBrownGreenyellow	Thioesterase superfamily protein	00196	GO:0009765
Eucgr.G00777.1.p	BlackBrownGreenyellow	light harvesting complex photosystem II subunit 6	00196	GO:0009765
Eucgr.F01822.1.p	BlackBrownGreenyellow	Photosystem II reaction center PsbP family protein		GO:0015979

[1]00195 – Photosynthesis [2]00196 – Photosynthesis (Antenna proteins) [3]GO:0015979 Photosynthesis [4]GO:0009765 – Photosynthesis, light harvesting

Table 7. All proteins from susceptible genotype mapped with Photosynthesis GO terms ($p<0.05$), using AgriGO, or associated to Photosynthesis Kegg pathway, using KofamKoala.

Protein ID	Related Module	Protein Name	Kegg Pathway	GO Terms
Eucgr.E01113.1.p	RedTanMagentaSalmon	photosynthetic electron transfer A	00195 [1]	GO:0015979 [3]
Eucgr.E00291.1.p	RedTanMagentaSalmon	2Fe-2S ferredoxin-like superfamily protein	00195	
Eucgr.B01088.1.p	RedTanMagentaSalmon	photosystem I subunit D-2	00195	GO:0015979
Eucgr.B02162.1.p	RedTanMagentaSalmon	photosystem I subunit E-2	00195	GO:0015979
Eucgr.H00828.1.p	RedTanMagentaSalmon	photosystem I subunit E-2	00195	GO:0015979
Eucgr.I00200.2.p	RedTanMagentaSalmon	photosystem I reaction center subunit PSI-N, chloroplast, putative / PSI-N, putative (PSAN)	00195	GO:0015979
Eucgr.A00264.1.p	RedTanMagentaSalmon	photosystem II reaction center protein B	00195	GO:0015979
Eucgr.G02904.1.p	RedTanMagentaSalmon	PsbP-like protein 1	00195	GO:0015979
Eucgr.F01822.2.p	RedTanMagentaSalmon	Photosystem II reaction center PsbP family protein		GO:0015979
Eucgr.G02593.1.p	PurpleTurquoise	Mog1/PsbP/DUF1795-like photosystem II reaction center PsbP family protein		GO:0015979
Eucgr.H01947.1.p	PurpleTurquoise	photosystem II reaction center protein D		GO:0015979
Eucgr.F03186.8.p	PurpleTurquoise	photosystem II 10kDa protein subunit R		GO:0015979
Eucgr.H01287.4.p	PurpleTurquoise	Photosystem II reaction center PsbP family protein		GO:0015979
Eucgr.G02488.1.p	PurpleTurquoise	PsbQ-like 2		GO:0015979
Eucgr.C02765.1.p	Blue	ATPase, F0 complex, subunit B/B\', bacterial/chloroplast	00195	
Eucgr.J02731.1.p	Blue	ATP synthase epsilon chain	00195	
Eucgr.A01769.1.p	Blue	photosynthetic electron transfer C	00195	
Eucgr.I01025.1.p	Blue	photosystem II subunit O-2	00195	GO:0015979
Eucgr.D00854.1.p	Blue	photosystem II subunit Q-2	00195	GO:0015979
Eucgr.D00319.1.p	Blue	chlorophyll A/B binding protein 1	00196 [2]	GO:0009765 [4]
Eucgr.E02381.1.p	Blue	light-harvesting chlorophyll-protein complex II subunit B1	00196	GO:0009765
Eucgr.D00551.1.p	Blue	magnesium chelatase i2		GO:0015979
Eucgr A02039.1.p.	Brown	photosystem II subunit P-1	00195	GO:0015979

Protein ID	Related Module	Protein Name	Kegg Pathway	GO Terms
Eucgr.H01287.1.p	Brown	Photosystem II reaction center PsbP family protein	00195	GO:0015979
Eucgr.F03789.1.p	Brown	Chlorophyll A-B binding family protein	00195	
Eucgr.K00947.1.p	Brown	photosystem II family protein	00195	GO:0015979
Eucgr.K01362.1.p	Brown	photosystem I light harvesting complex gene 3	00196	GO:0009765
Eucgr.D00321.1.p	Brown	light-harvesting chlorophyll-protein complex II subunit B1	00196	GO:0009765
Eucgr.K02983.1.p	Brown	light harvesting complex photosystem II	00196	GO:0009765
Eucgr.I02677.1.p	Brown	light harvesting complex photosystem II subunit 6	00196	GO:0009765
Eucgr.F04149.1.p	Black	ATP synthase delta-subunit gene	00195	
Eucgr.E04053.1.p	Black	ATPase, F1 complex, gamma subunit protein	00195	
Eucgr.F01067.2.p	Black	photosynthetic electron transfer C	00195	
Eucgr.F01067.3.p	Black	photosynthetic electron transfer C	00195	
Eucgr.B03849.1.p	Black	ferredoxin 3	00195	
Eucgr.F03646.1.p	Black	photosystem I subunit G	00195	
Eucgr.J01096.2.p	Black	photosystem I light harvesting complex gene 1	00196	
Eucgr.A01047.1.p	Black	photosystem II light harvesting complex gene 2.2	00196	

[1]00195 – Photosynthesis [2]00196 – Photosynthesis (Antenna proteins) [3]GO:0015979 Photosynthesis [4]GO:0009765 – Photosynthesis, light harvesting

Table 8. All proteins from resistant genotype associated to Glycolysis/Gluconeogenesis (00010) Kegg pathway, using KofamKoala.

Protein ID	Related Module	Protein Name	Kegg Pathway
Eucgr.B02711.1.p	MagentaGreenPurpleSalmon	alcohol dehydrogenase (NADP+) [EC:1.1.1.2]	00010
Eucgr.B01499.1.p	MagentaGreenPurpleSalmon	alcohol dehydrogenase (NADP+) [EC:1.1.1.2]	00010
Eucgr.K01401.1.p	MagentaGreenPurpleSalmon	S-(hydroxymethyl)glutathione dehydrogenase [EC:1.1.1.284]	00010
Eucgr.E01909.2.p	MagentaGreenPurpleSalmon	pyruvate dehydrogenase E1 component beta subunit [EC:1.2.4.1]	00010
Eucgr.C03703.1.p	MagentaGreenPurpleSalmon	6-phosphofructokinase 1 [EC:2.7.1.11]	00010
Eucgr.K02969.1.p	MagentaGreenPurpleSalmon	pyruvate decarboxylase [EC:4.1.1.1]	00010
Eucgr.K02073.1.p	MagentaGreenPurpleSalmon	fructose-bisphosphate aldolase, class I [EC:4.1.2.13]	00010
Eucgr.J02049.1.p	MagentaGreenPurpleSalmon	triosephosphate isomerase (TIM) [EC:5.3.1.1]	00010
Eucgr.B02942.1.p	MagentaGreenPurpleSalmon	phosphoglucomutase [EC:5.4.2.2]	00010
Eucgr.K00185.2.p	MagentaGreenPurpleSalmon	phosphoglucomutase [EC:5.4.2.2]	00010
Eucgr.B02755.3.p	MagentaGreenPurpleSalmon	fructose-1,6-bisphosphatase I [EC:3.1.3.11]	00010
Eucgr.A00868.1.p	MagentaGreenPurpleSalmon	2,3-bisphosphoglycerate-independent phosphoglycerate mutase [EC:5.4.2.12]	00010
Eucgr.C03858.1.p	PinkYellowTan	aldehyde dehydrogenase (NAD+) [EC:1.2.1.3]	00010
Eucgr.C02594.1.p	PinkYellowTan	glyceraldehyde-3-phosphate dehydrogenase (NADP+) [EC:1.2.1.9]	00010
Eucgr.F04466.1.p	PinkYellowTan	glyceraldehyde 3-phosphate dehydrogenase [EC:1.2.1.12]	00010
Eucgr.J02288.1.p	PinkYellowTan	glyceraldehyde 3-phosphate dehydrogenase [EC:1.2.1.12]	00010
Eucgr.B03379.1.p	PinkYellowTan	pyruvate dehydrogenase E1 component alpha subunit [EC:1.2.4.1]	00010
Eucgr.K02074.2.p	PinkYellowTan	pyruvate kinase [EC:2.7.1.40]	00010
Eucgr.E03983.1.p	PinkYellowTan	diphosphate-dependent phosphofructokinase [EC:2.7.1.90]	00010
Eucgr.F04463.1.p	PinkYellowTan	phosphoglycerate kinase [EC:2.7.2.3]	00010
Eucgr.A01538.1.p	PinkYellowTan	fructose-bisphosphate aldolase, class I [EC:4.1.2.13]	00010
Eucgr.J02049.2.p	PinkYellowTan	triosephosphate isomerase (TIM) [EC:5.3.1.1]	00010
Eucgr.J00008.1.p	PinkYellowTan	triosephosphate isomerase (TIM) [EC:5.3.1.1]	00010

Protein ID	Related Module	Protein Name	Kegg Pathway
Eucgr.A00203.1.p	PinkYellowTan	acetate-CoA ligase [EC:6.2.1.1]	00010
Eucgr.F02711.2.p	PinkYellowTan	fructose-1,6-bisphosphatase I [EC:3.1.3.11]	00010
Eucgr.F02506.1.p	Turquoise	pyruvate dehydrogenase E1 component beta subunit [EC:1.2.4.1]	00010
Eucgr.F03161.3.p	Turquoise	pyruvate dehydrogenase E2 component (dihydrolipoamide acetyltransferase) [EC:2.3.1.12]	00010
Eucgr.F04463.3.p	Turquoise	phosphoglycerate kinase [EC:2.7.2.3]	00010
Eucgr.B02864.2.p	Turquoise	fructose-bisphosphate aldolase, class I [EC:4.1.2.13]	00010
Eucgr.K02073.2.p	Turquoise	fructose-bisphosphate aldolase, class I [EC:4.1.2.13]	00010
Eucgr.H03316.3.p	Turquoise	glucose-6-phosphate 1-epimerase [EC:5.1.3.15]	00010

Table 9. All proteins from susceptible genotype associated to Glycolysis/Gluconeogenesis GO terms ($p<0.05$) or kegg pathway.

Protein ID	Related Module	Protein Name	Kegg Pathway	GO Terms
Eucgr.C03858.1.p	RedTanMagentaSalmon	aldehyde dehydrogenase (NAD+) [EC:1.2.1.3]	00010 [1]	
Eucgr.I01564.1.p	RedTanMagentaSalmon	glyceraldehyde 3-phosphate dehydrogenase [EC:1.2.1.12]	00010	
Eucgr.F04466.1.p	RedTanMagentaSalmon	glyceraldehyde 3-phosphate dehydrogenase [EC:1.2.1.12]	00010	
Eucgr.E01909.2.p	RedTanMagentaSalmon	pyruvate dehydrogenase E1 component beta subunit [EC:1.2.4.1]	00010	
Eucgr.F03161.3.p	RedTanMagentaSalmon	pyruvate dehydrogenase E2 component (dihydrolipoamide acetyltransferase) [EC:2.3.1.12]	00010	
Eucgr.D02166.1.p	RedTanMagentaSalmon	pyruvate kinase [EC:2.7.1.40]	00010	GO:0006096 [2]
Eucgr.E03983.1.p	RedTanMagentaSalmon	diphosphate-dependent phosphofructokinase [EC:2.7.1.90]	00010	GO:0006096
Eucgr.F01476.1.p	RedTanMagentaSalmon	phosphoglycerate kinase [EC:2.7.2.3]	00010	GO:0006096
Eucgr.I01326.2.p	RedTanMagentaSalmon	fructose-bisphosphate aldolase, class I [EC:4.1.2.13]	00010	GO:0006096
Eucgr.K02073.1.p	RedTanMagentaSalmon	fructose-bisphosphate aldolase, class I [EC:4.1.2.13]	00010	GO:0006096
Eucgr.J02049.2.p	RedTanMagentaSalmon	triosephosphate isomerase (TIM) [EC:5.3.1.1]	00010	
Eucgr.B02942.2.p	RedTanMagentaSalmon	phosphoglucomutase [EC:5.4.2.2]	00010	
Eucgr.A00203.1.p	RedTanMagentaSalmon	acetate-CoA ligase [EC:6.2.1.1]	00010	
Eucgr.B01499.1.p	Blue	alcohol dehydrogenase (NADP+) [EC:1.1.1.2]	00010	
Eucgr.F02506.1.p	Blue	pyruvate dehydrogenase E1 component beta subunit [EC:1.2.4.1]	00010	
Eucgr.A01538.2.p	Blue	fructose-bisphosphate aldolase, class I [EC:4.1.2.13]	00010	
Eucgr.F02133.1.p	Blue	glucose-6-phosphate isomerase [EC:5.3.1.9]	00010	
Eucgr.A00868.1.p	Blue	2,3-bisphosphoglycerate-independent phosphoglycerate mutase [EC:5.4.2.12]	00010	
Eucgr.C02594.1.p	YellowPink	glyceraldehyde-3-phosphate dehydrogenase (NADP+) [EC:1.2.1.9]	00010	
Eucgr.H04673.1.p	YellowPink	glyceraldehyde 3-phosphate dehydrogenase [EC:1.2.1.12]	00010	
Eucgr.F04463.1.p	YellowPink	phosphoglycerate kinase [EC:2.7.2.3]	00010	
Eucgr.A01538.1.p	YellowPink	fructose-bisphosphate aldolase, class I [EC:4.1.2.13]	00010	
Eucgr.B02864.1.p	YellowPink	fructose-bisphosphate aldolase, class I [EC:4.1.2.13]	00010	
Eucgr.K02073.2.p	YellowPink	fructose-bisphosphate aldolase, class I [EC:4.1.2.13]	00010	

Protein ID	Related Module	Protein Name	Kegg Pathway	GO Terms
Eucgr.K00185.2.p	YellowPink	phosphoglucomutase [EC:5.4.2.2]	00010	
Eucgr.B02755.1.p	YellowPink	fructose-1,6-bisphosphatase I [EC:3.1.3.11]	00010	
Eucgr.K01401.1.p	GreenGreenyellow	S-(hydroxymethyl)glutathione dehydrogenase [EC:1.1.1.284]	00010	
Eucgr.G01726.1.p	GreenGreenyellow	fructose-bisphosphate aldolase, class I [EC:4.1.2.13]	00010	
Eucgr.B02864.2.p	GreenGreenyellow	fructose-bisphosphate aldolase, class I [EC:4.1.2.13]	00010	
Eucgr.H03316.1.p	GreenGreenyellow	glucose-6-phosphate 1-epimerase [EC:5.1.3.15]	00010	
Eucgr.H03316.5.p	GreenGreenyellow	glucose-6-phosphate 1-epimerase [EC:5.1.3.15]	00010	
Eucgr.B02755.3.p	GreenGreenyellow	fructose-1,6-bisphosphatase I [EC:3.1.3.11]	00010	
Eucgr.F02711.2.p	GreenGreenyellow	fructose-1,6-bisphosphatase I [EC:3.1.3.11]	00010	
Eucgr.I00224.1.p	GreenGreenyellow	alcohol dehydrogenase class-P [EC:1.1.1.1]	00010	

[1]00010 – Glycolysis/Gluconeogenesis [2]GO:0006096 – glycolytic process

Table 10. All proteins from resistant genotype associated to glyoxylate and dicarboxylate metabolism (00630) kegg pathway.

Protein ID	Related Module	Protein Name	Kegg Pathway
Eucgr.F02167.5.p	PinkYellowTan	glycine hydroxymethyltransferase [EC:2.1.2.1]	00630
Eucgr.J01502.2.p	PinkYellowTan	ribulose-bisphosphate carboxylase small chain [EC:4.1.1.39]	00630
Eucgr.I02307.1.p	PinkYellowTan	aconitate hydratase [EC:4.2.1.3]	00630
Eucgr.A00203.1.p	PinkYellowTan	acetate-CoA ligase [EC:6.2.1.1]	00630
Eucgr.B01163.2.p	PinkYellowTan	glutamine synthetase [EC:6.3.1.2]	00630
Eucgr.F02872.2.p	PinkYellowTan	glutamine synthetase [EC:6.3.1.2]	00630
Eucgr.K02283.1.p	PinkYellowTan	glutamine synthetase [EC:6.3.1.2]	00630
Eucgr.F01413.2.p	PinkYellowTan	(S)-2-hydroxy-acid oxidase [EC:1.1.3.15]	00630
Eucgr.I01423.2.p	PinkYellowTan	glycerate dehydrogenase [EC:1.1.1.29]	00630
Eucgr.F03139.1.p	PinkYellowTan	glyoxylatesemialdehyde reductase [EC:1.1.1.79]	00630
Eucgr.K02346.1.p	PinkYellowTan	glyoxylatesemialdehyde reductase [EC:1.1.1.79]	00630
Eucgr.B01439.1.p	PinkYellowTan	phosphoglycolate phosphatase [EC:3.1.3.18 3.1.3.48]	00630
Eucgr.H02679.1.p	Cyan	glycine hydroxymethyltransferase [EC:2.1.2.1]	00630
Eucgr.I00580.3.p	Cyan	glycine hydroxymethyltransferase [EC:2.1.2.1]	00630
Eucgr.H00090.2.p	Cyan	acetyl-CoA acyltransferase 1 [EC:2.3.1.16]	00630
Eucgr.B03013.1.p	Cyan	ribulose-bisphosphate carboxylase small chain [EC:4.1.1.39]	00630
Eucgr.F02872.3.p	Cyan	glutamine synthetase [EC:6.3.1.2]	00630
Eucgr.D02179.2.p	Cyan	glycine cleavage system H protein	00630
Eucgr.H03047.1.p	Red	malate dehydrogenase [EC:1.1.1.37]	00630
Eucgr.B03720.1.p	Red	alanine-glyoxylate transaminase [EC:2.6.1.44]	00630
Eucgr.K02223.1.p	Red	ribulose-bisphosphate carboxylase small chain [EC:4.1.1.39]	00630
Eucgr.F01776.1.p	Red	catalase [EC:1.11.1.6]	00630
Eucgr.F03557.1.p	Red	catalase [EC:1.11.1.6]	00630
Eucgr.B00511.1.p	BlackBrownGreenyellow	malate dehydrogenase [EC:1.1.1.37]	00630
Eucgr.F03251.1.p	BlackBrownGreenyellow	malate dehydrogenase [EC:1.1.1.37]	00630

Protein ID	Related Module	Protein Name	Kegg Pathway
Eucgr.H02358.5.p	BlackBrownGreenyellow	malate dehydrogenase [EC:1.1.1.37]	00630
Eucgr.F01209.1.p	BlackBrownGreenyellow	malate dehydrogenase [EC:1.1.1.37]	00630
Eucgr.C03047.1.p	BlackBrownGreenyellow	glycine dehydrogenase [EC:1.4.4.2]	00630
Eucgr.A02249.1.p	BlackBrownGreenyellow	glutamate synthase (ferredoxin) [EC:1.4.7.1]	00630
Eucgr.H04086.1.p	BlackBrownGreenyellow	dihydrolipoamide dehydrogenase [EC:1.8.1.4]	00630
Eucgr.I00580.1.p	BlackBrownGreenyellow	glycine hydroxymethyltransferase [EC:2.1.2.1]	00630
Eucgr.L02773.1.p	BlackBrownGreenyellow	aminomethyltransferase [EC:2.1.2.10]	00630
Eucgr.J01502.1.p	BlackBrownGreenyellow	ribulose-bisphosphate carboxylase small chain [EC:4.1.1.39]	00630
Eucgr.A01129.1.p	BlackBrownGreenyellow	aconitate hydratase [EC:4.2.1.3]	00630
Eucgr.I02307.2.p	BlackBrownGreenyellow	aconitate hydratase [EC:4.2.1.3]	00630
Eucgr.F02872.1.p	BlackBrownGreenyellow	glutamine synthetase [EC:6.3.1.2]	00630

Table 11. All proteins from susceptible genotype associated to glyoxylate and dicarboxylate metabolism (00630) kegg pathway.

Protein ID	Related Module	Protein Name	Kegg Pathway
Eucgr.B00511.1.p	PurpleTurquoise	malate dehydrogenase [EC:1.1.1.37]	00630
Eucgr.A00348.1.p	PurpleTurquoise	dihydrolipoamide dehydrogenase [EC:1.8.1.4]	00630
Eucgr.H00849.1.p	PurpleTurquoise	acetyl-CoA C-acetyltransferase [EC:2.3.1.9]	00630
Eucgr.B03720.1.p	PurpleTurquoise	alanine-glyoxylate transaminase [EC:2.6.1.44]	00630
Eucgr.H03302.1.p	PurpleTurquoise	phosphoglycolate phosphatase [EC:3.1.3.18]	00630
Eucgr.F02872.1.p	PurpleTurquoise	glutamine synthetase [EC:6.3.1.2]	00630
Eucgr.B01163.1.p	PurpleTurquoise	glutamine synthetase [EC:6.3.1.2]	00630
Eucgr.E04249.1.p	PurpleTurquoise	glycine cleavage system H protein	00630
Eucgr.D00982.1.p	PurpleTurquoise	glycine cleavage system H protein	00630
Eucgr.E02953.1.p	PurpleTurquoise	arylformamidase [EC:3.5.1.9]	00630
Eucgr.E02420.1.p	PurpleTurquoise	L-lactate dehydrogenase (cytochrome) [EC:1.1.2.3]	00630
Eucgr.F01413.1.p	PurpleTurquoise	(S)-2-hydroxy-acid oxidase [EC:1.1.3.15]	00630
Eucgr.H04086.1.p	Black	dihydrolipoamide dehydrogenase [EC:1.8.1.4]	00630
Eucgr.J01502.2.p	Black	ribulose-bisphosphate carboxylase small chain [EC:4.1.1.39]	00630
Eucgr.I02307.1.p	Black	aconitate hydratase [EC:4.2.1.3]	00630
Eucgr.B01163.2.p	Black	glutamine synthetase [EC:6.3.1.2]	00630
Eucgr.D02179.2.p	Black	glycine cleavage system H protein	00630
Eucgr.F01413.2.p	Black	(S)-2-hydroxy-acid oxidase [EC:1.1.3.15]	00630
Eucgr.I01423.1.p	Black	glycerate dehydrogenase [EC:1.1.1.29]	00630
Eucgr.F03139.1.p	Black	glyoxylate reductase [EC:1.1.1.79]	00630

Table 12. All proteins from resistant genotype associated to amino acid metabolism (GO:0006520) kegg pathway.

Protein ID	Related Module	Protein Name	GO Term
Eucgr.A02126.1.p	PinkYellowTan	5-methyltetrahydropteroyltriglutamate--homocysteine methyltransferase [EC:2.1.1.14]	GO:0006520 [1]
Eucgr.K02283.1.p	PinkYellowTan	glutamine synthetase [EC:6.3.1.2]	GO:0006520
Eucgr.F02872.2.p	PinkYellowTan	glutamine synthetase [EC:6.3.1.2]	GO:0006520
Eucgr.J00613.1.p	PinkYellowTan	5-methyltetrahydropteroyltriglutamate--homocysteine methyltransferase [EC:2.1.1.14]	GO:0006520
Eucgr.B03437.1.p	PinkYellowTan	aspartate-semialdehyde dehydrogenase [EC:1.2.1.11]	GO:0006520
Eucgr.C02720.1.p	PinkYellowTan	aspartate aminotransferase, chloroplastic [EC:2.6.1.1]	GO:0006520
Eucgr.C02721.1.p	PinkYellowTan	aspartate aminotransferase, chloroplastic [EC:2.6.1.1]	GO:0006520
Eucgr.F01880.1.p	PinkYellowTan	ornithine carbamoyltransferase [EC:2.1.3.3]	GO:0006520
Eucgr.B01163.2.p	PinkYellowTan	glutamine synthetase [EC:6.3.1.2]	GO:0006520
Eucgr.K01508.1.p	BlackBrownGreenyellow	5-methyltetrahydropteroyltriglutamate--homocysteine methyltransferase [EC:2.1.1.14]	GO:0006520
Eucgr.A02126.4.p	BlackBrownGreenyellow	5-methyltetrahydropteroyltriglutamate--homocysteine methyltransferase [EC:2.1.1.14]	GO:0006520
Eucgr.C03047.1.p	BlackBrownGreenyellow	glycine dehydrogenase [EC:1.4.4.2]	GO:0006520
Eucgr.L02773.1.p	BlackBrownGreenyellow	aminomethyltransferase [EC:2.1.2.10]	GO:0006520
Eucgr.F02872.1.p	BlackBrownGreenyellow	glutamine synthetase [EC:6.3.1.2]	GO:0006520
Eucgr.A02249.1.p	BlackBrownGreenyellow	glutamate synthase (ferredoxin) [EC:1.4.7.1]	GO:0006520
Eucgr.A00394.1.p	BlackBrownGreenyellow	methylenetetrahydrofolate reductase (NADPH) [EC:1.5.1.20]	GO:0006520

[1]GO:0006520 cellular amino acid metabolic process

Table 13. All proteins from susceptible genotype associated to amino acid metabolism GO terms ($p<0.05$) or kegg pathways.

Protein ID	Related Module	Protein Name	Kegg Pathway	GO Terms
Eucgr.K01508.1.p	RedTanMagentaSalmon	5-methyltetrahydropteroyltriglutamate--homocysteine methyltransferase [EC:2.1.1.14]		GO:1901607 [2]
Eucgr.L02175.1.p	RedTanMagentaSalmon	glutamine synthetase [EC:6.3.1.2]		GO:1901607
Eucgr.A02126.4.p	RedTanMagentaSalmon	5-methyltetrahydropteroyltriglutamate--homocysteine methyltransferase [EC:2.1.1.14]		GO:1901607
Eucgr.K02283.1.p	RedTanMagentaSalmon	glutamine synthetase [EC:6.3.1.2]		GO:1901607
Eucgr.F02872.2.p	RedTanMagentaSalmon	glutamine synthetase [EC:6.3.1.2]		GO:1901607
Eucgr.A01927.2.p	PurpleTurquoise	aspartate aminotransferase, mitochondrial [EC:2.6.1.1]		GO:0006520 [3]
Eucgr.C02894.1.p	PurpleTurquoise	aspartate aminotransferase [EC:2.6.1.1]		GO: 0006520
Eucgr.F02872.1.p	PurpleTurquoise	glutamine synthetase [EC:6.3.1.2]		GO: 0006520
Eucgr.F02952.1.p	PurpleTurquoise	bifunctional aspartokinase / homoserine dehydrogenase 1 [EC:2.7.2.4 1.1.1.3]		GO: 0006520
Eucgr.H04482.1.p	PurpleTurquoise	seryl-tRNA synthetase [EC:6.1.1.11]		GO: 0006520
Eucgr.A00249.1.p	PurpleTurquoise	2-isopropylmalate synthase [EC:2.3.3.13]		GO: 0006520
Eucgr.A00394.3.p	PurpleTurquoise	methylenetetrahydrofolate reductase (NADPH) [EC:1.5.1.20]		GO: 0006520
Eucgr.B01163.1.p	PurpleTurquoise	glutamine synthetase [EC:6.3.1.2]		GO: 0006520
Eucgr.H03047.1.p	YellowPink	malate dehydrogenase [EC:1.1.1.37]	00270 [1]	
Eucgr.F04000.1.p	YellowPink	D-3-phosphoglycerate dehydrogenase [EC:1.1.1.95]	00270	
Eucgr.J00613.1.p	YellowPink	5-methyltetrahydropteroyltriglutamate--homocysteine methyltransferase [EC:2.1.1.14]	00270	
Eucgr.K00588.1.p	YellowPink	S-adenosylmethionine synthetase [EC:2.5.1.6]	00270	
Eucgr.H04112.1.p	YellowPink	S-adenosylmethionine synthetase [EC:2.5.1.6]	00270	
Eucgr.C02720.1.p	YellowPink	aspartate aminotransferase, chloroplastic [EC:2.6.1.1]	00270	
Eucgr.L00009.1.p	YellowPink	cysteine synthase [EC:2.5.1.47]	00270	

[1]00270 – Cysteine and methionine metabolism [2]GO:1901607 alpha-amino acid biosynthetic process [3]GO:0006520 celullar amino acid metabolic process

Table 14. All proteins from resistant genotype associated to proteasome kegg pathways.

Protein ID	Related Module	Protein Name	Kegg Pathway
Eucgr.B03771.1.p	Blue	20S proteasome subunit alpha 7 [EC:3.4.25.1]	03050 Proteasome
Eucgr.J02596.2.p	Blue	20S proteasome subunit alpha 5 [EC:3.4.25.1]	03050 Proteasome
Eucgr.E01416.1.p	Blue	20S proteasome subunit beta 6 [EC:3.4.25.1]	03050 Proteasome
Eucgr.C02133.1.p	Blue	20S proteasome subunit beta 1 [EC:3.4.25.1]	03050 Proteasome

Table 15. All proteins from susceptible genotype associated to proteasome kegg pathways.

Protein ID	Related Module	Protein Name	Kegg Pathway
Eucgr.H04776.2.p	Brown	20S proteasome subunit alpha 3 [EC:3.4.25.1]	03050 Proteasome
Eucgr.E01416.1.p	Brown	20S proteasome subunit beta 6 [EC:3.4.25.1]	03050 Proteasome
Eucgr.C02133.2.p	Brown	20S proteasome subunit beta 1 [EC:3.4.25.1]	03050 Proteasome
Eucgr.J02583.2.p	Brown	26S proteasome regulatory subunit T1	03050 Proteasome
Eucgr.C04160.1.p	Brown	26S proteasome regulatory subunit T6	03050 Proteasome

FIGURES

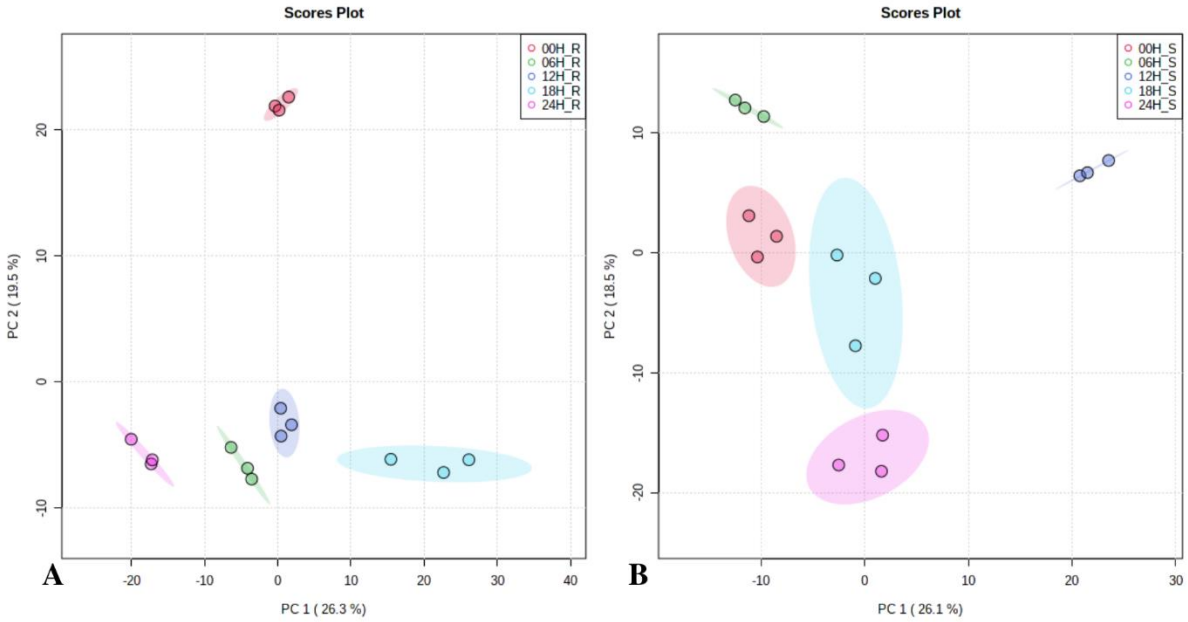

Figura 1. Principal Component Analysis (PCA) of metabolites identified along time points, which correspond to the different times of leaves collection after inoculation, including (A) resistant genotypes score plot of samples 00H_R (collected at 0hai),06H_R (collected at 6hai), 12H_R (collected at 12hai), 18H_R (collected at 18hai) and 24H_R (collected at 24hai) (B) susceptible genotypes score plot of samples 00H_S (collected at 0hai),06H_S (collected at 6hai), 12H_S (collected at 12hai), 18H_S (collected at 18hai) and 24H_S (collected at 24hai).

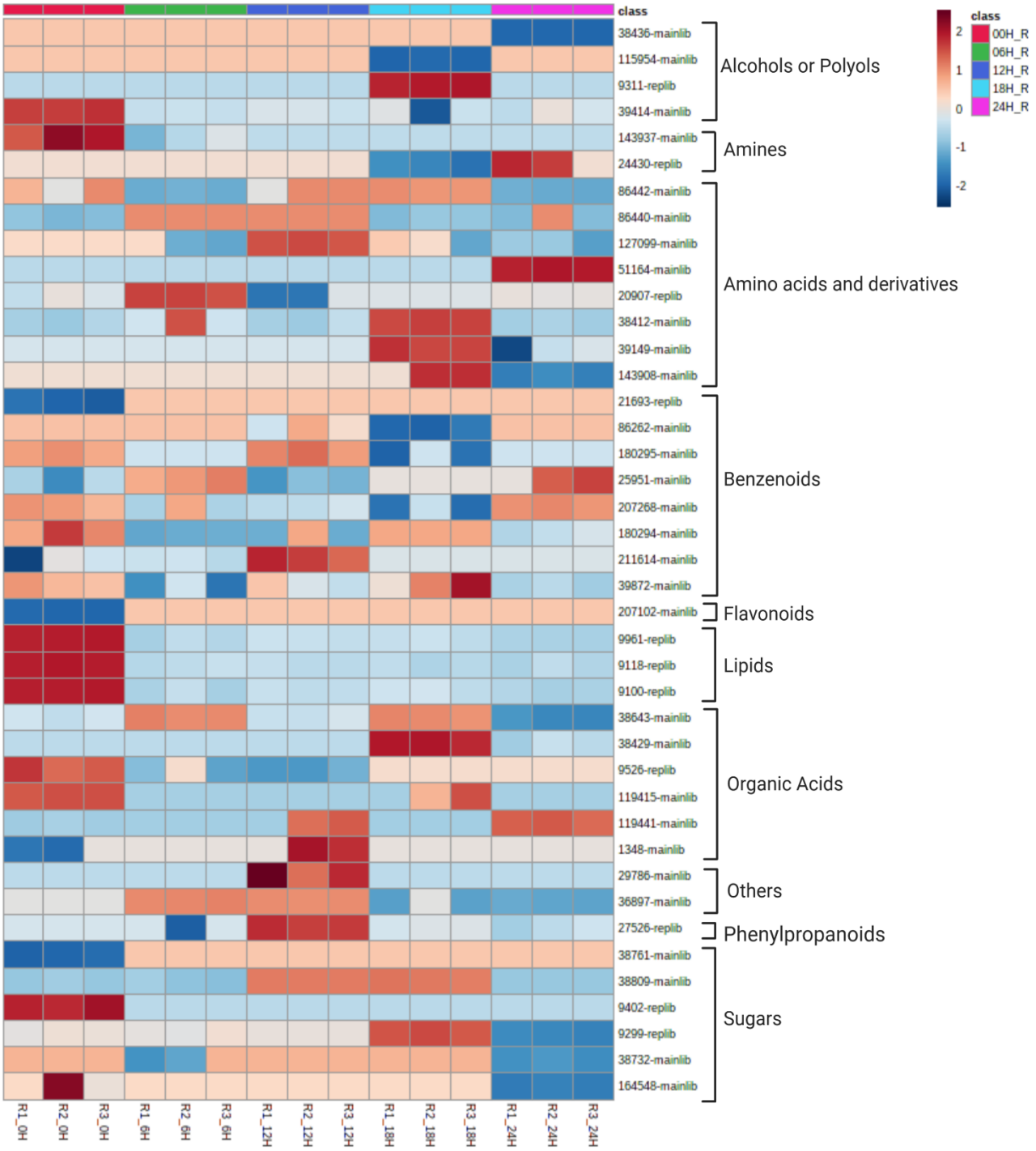

Figura 2. Heatmap of selected ANOVA metabolites (FDR < 0.05), represented by their NIST ID number and respective class according to HMDB from resistant genotype. Each time-point is represented as 00H (represented by color red), 06H (green), 12H (dark blue), 18H (light bue) and 24H (pink) . 44 metabolites had statistical difference over time.

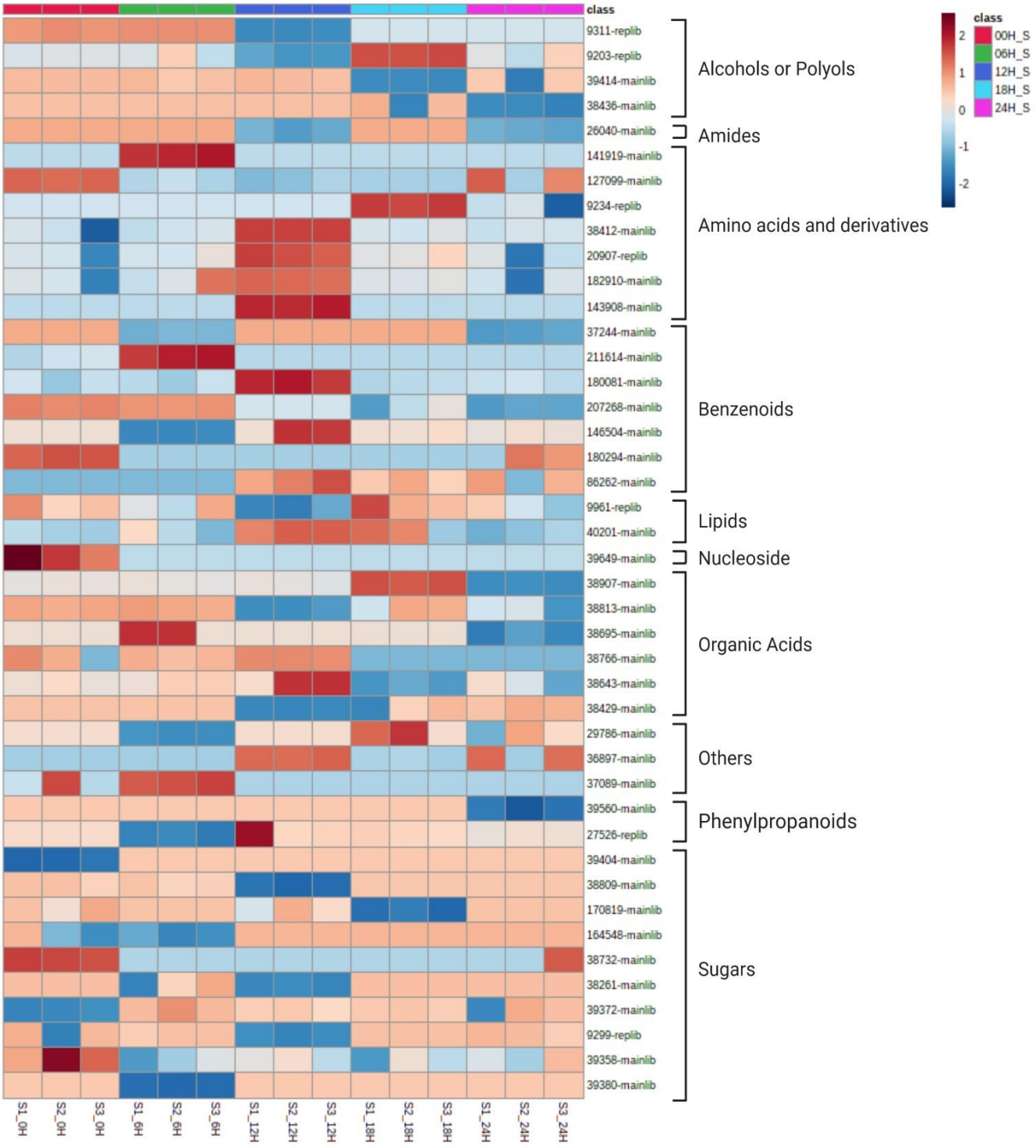

Figura 3. Heatmap of selected ANOVA metabolites (FDR < 0.05), represented by their NIST ID number and respective class according to HMDB from susceptible genotype. Each time-points is represented as 00H (represented by color red), 06H (green), 12H (dark blue), 18H (light bue) and 24H (pink). 43 metabolites had statistical difference over time.

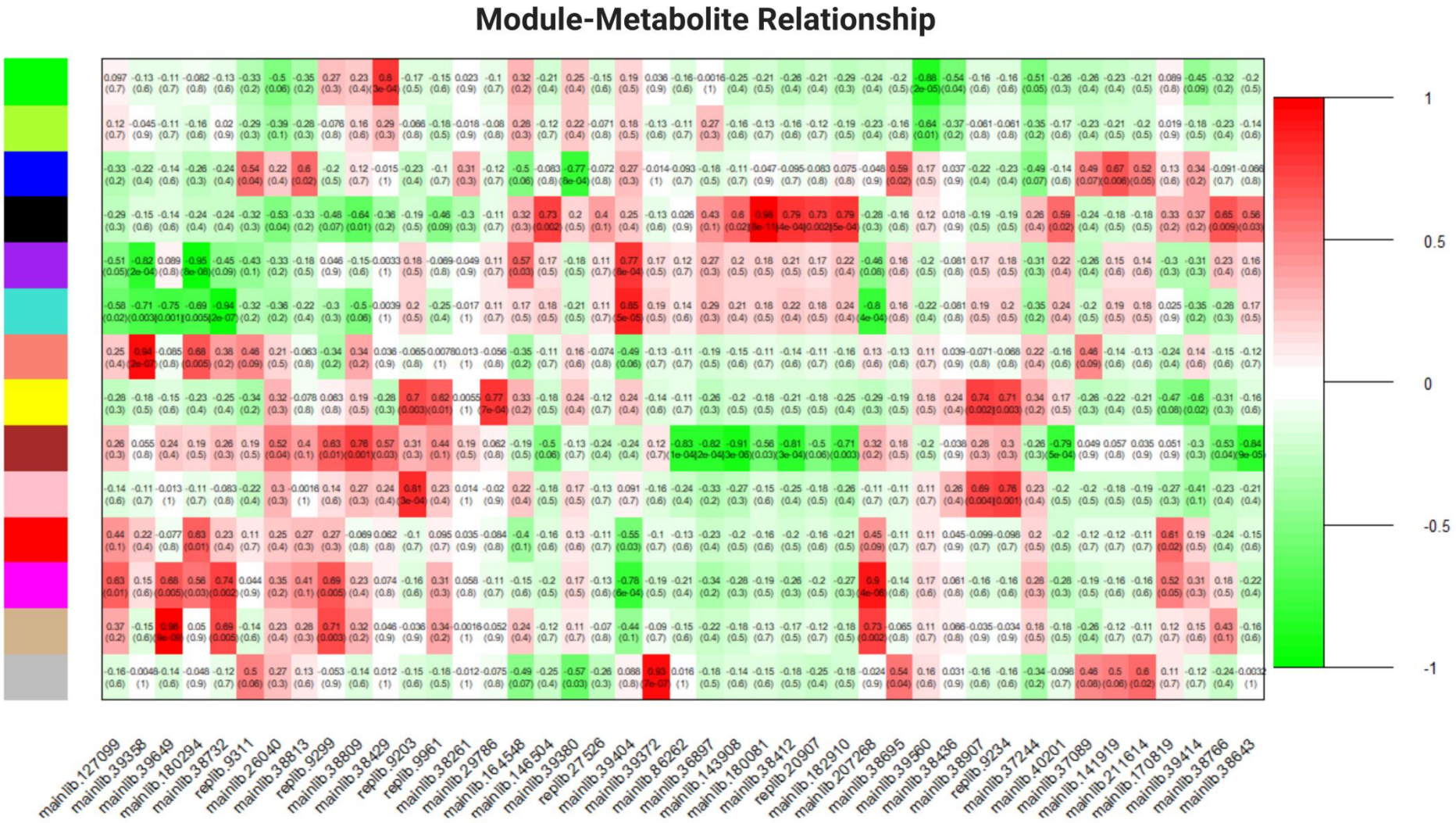

Figura 4. Susceptible genotype correlation of protein modules and selected metabolites, generated by WGCNA analysis. Protein modules are represented by colors, in the left, and selected metabolites are represented by their ID NIST numbers. Correlation values and p-values are presented. Red and green colors indicate positive and negative correlations, respectively.

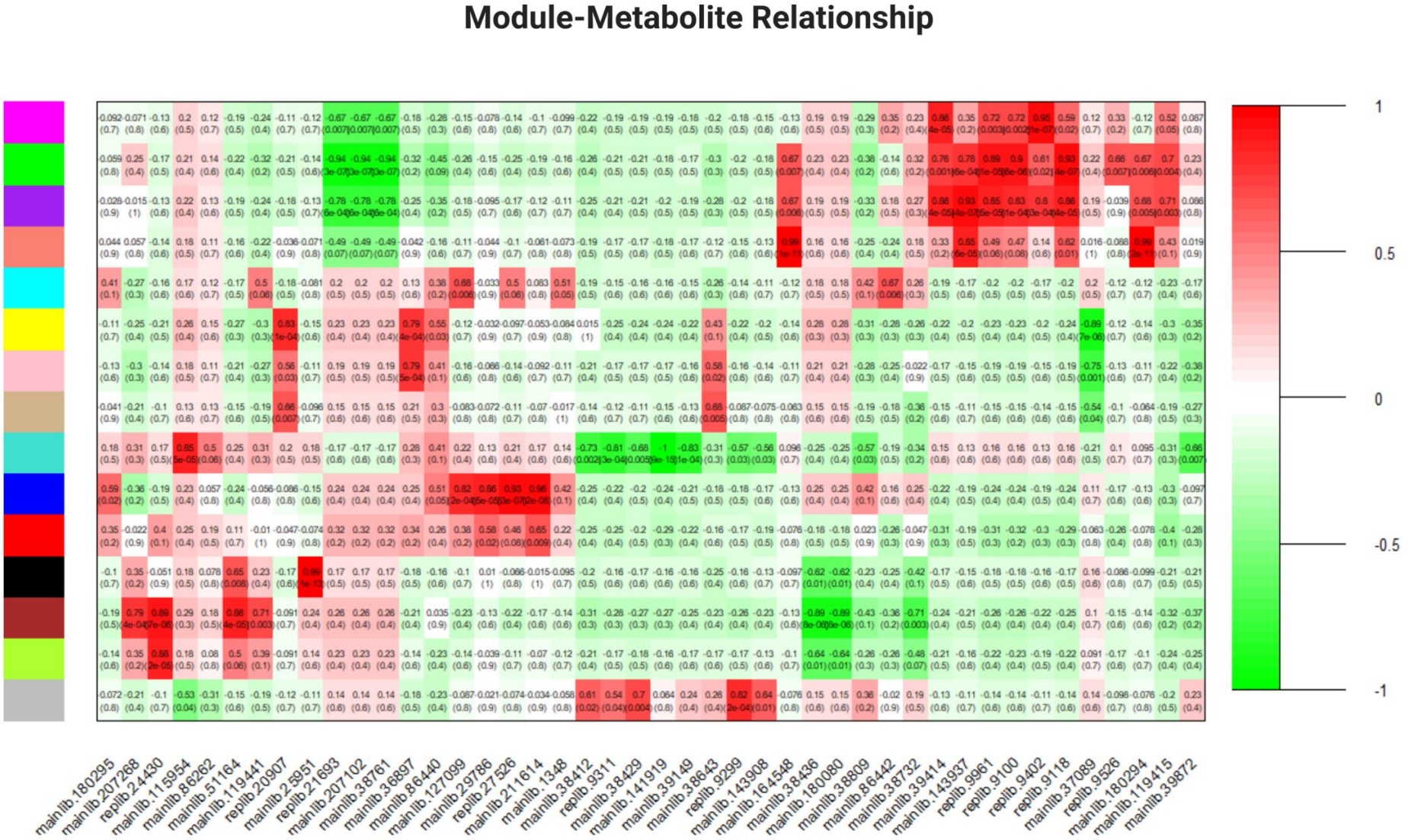

Figura 5. Resistant genotype correlation of protein modules and selected metabolites, generated by WGCNA analysis. Protein modules are represented by colors and selected metabolites are represented by their ID NIST numbers. Correlation values and p-values are presented. Red and green colors indicate positive and negative correlations, respective.

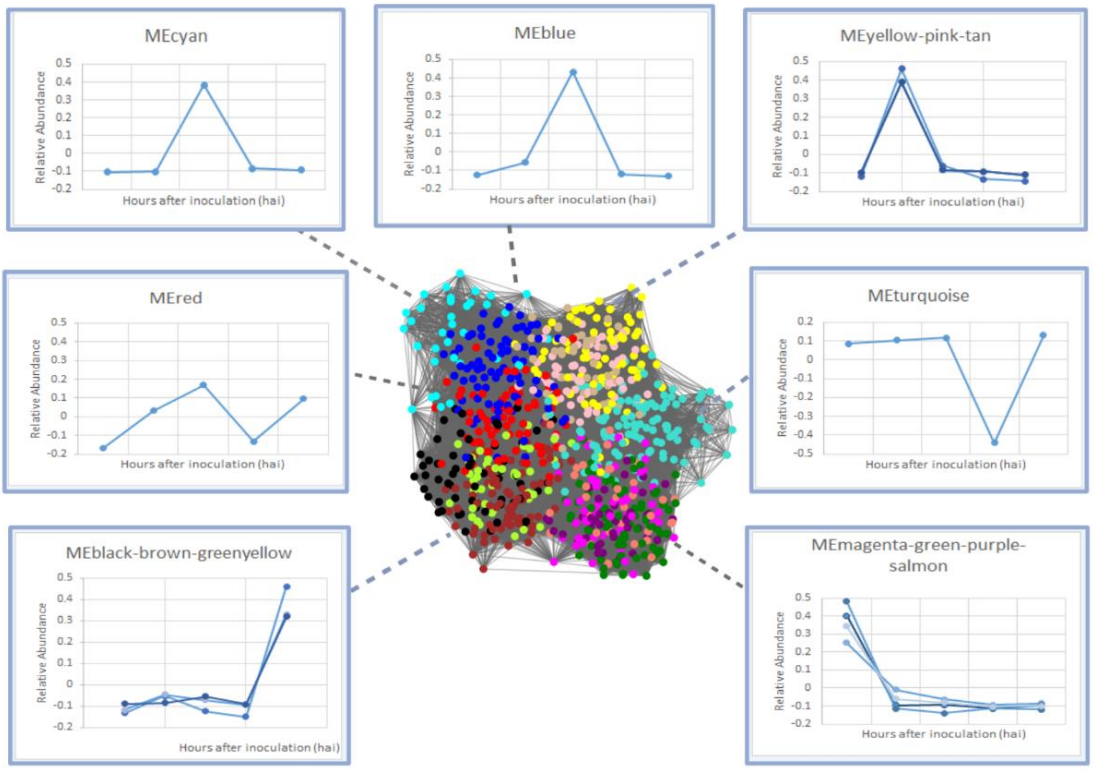

Figura 6. Resistant network visualization, represented by their respective color-names, and respective correlated modules, grouped into one major module when responded similarly to the same metabolites and presented similar abundance pattern over time. Graphics of relative abundance over time were generated according to module eigenproteins values. (Image created using BioRender)

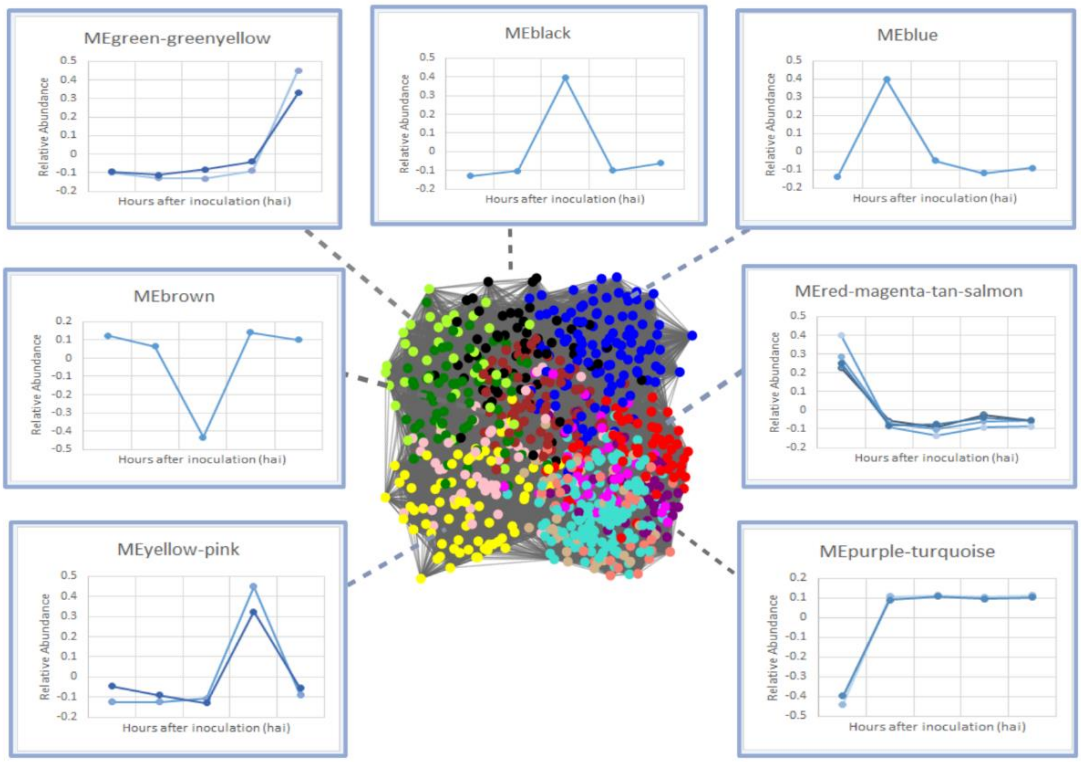

Figura 7. Susceptible network visualization, represented by their respective color-names, and respective correlated modules, grouped into one major module when responded similarly to the same metabolites and presented similar abundance pattern over time. Graphics of relative abundance over time were generated according to module eigenproteins values. (Image created using BioRender)

SUPPLEMENTARY TABLES

Table S1. List of the 115 different metabolites found in all treatments and genotypes (resistant and susceptible). Metabolites were classified according Human Metabolome Database (HMDB) classes.

ID	Derivatized Name	Common Name	Class
37234-mainlib	(Z)-Bis-1,2-(trimethylsilyloxy)ethylene	1,2-Ethenediol	Alcohols or Polyols
164513-mainlib	1-Cyclohexene-1-carboxylic acid, 3,4,5-tris[(trimethylsilyl)oxy]-, trimethylsilyl ester, [3R-(3?,4?,5?)]-	Shikimic acid	Organic acids
36897-mainlib	1-Ethenyl-3-(1-hexenyl)-4-trimethylsilylcyclopentane	1-Ethenyl-3-(1-hexenyl)-cyclopentane	Others
21693-replib	1,2-Benzenedicarboxylic acid, bis(2-methylpropyl) ester	diisobutyl phthalate	Benzenoids
9311-replib	1,2-Bis(trimethylsiloxy)ethane	Ethylene glycol	Alcohols or Polyols
207268-mainlib	1,2-Dihydroxyanthraquinone, O,O'-bis(trimethylsilyl)-	Alizarine	Benzenoids
191513-mainlib	1,2,3-Propanetricarboxylic acid, 2-[(trimethylsilyl)oxy]-, tris(trimethylsilyl) ester	Citric acid	Organic acids
37089-mainlib	1,3-Dioxolane, 2-(3-bromo-5,5,5-trichloro-2,2-dimethylpentyl)-	2-(3-Bromo-5,5,5-trichloro-2,2-dimethylpentyl)-1,3-dioxolane	Others
143937-mainlib	1,4-Butanediamine, N,N,N',N'-tetrakis(trimethylsilyl)-	Putrescine	Amines
86261-mainlib	1H-Indole-3-ethanamine, 6-fluoro-?-methyl-N,1-bis(trimethylsilyl)-	6-Fluoro-methyltryptamine (Dipterine)	Amines
116939-mainlib	2-(N-Isopropyl-N-(trimethylsilyl)amino)ethanol trimethylsilyl ether	2-(Isopropylamino)ethanol	Aminoacids derivatives
146504-mainlib	2-Allyl-1,4-dimethoxybenzene	2-Allyl-1,4-dimethoxybenzene	Benzenoids
182607-mainlib	2-Butenedioic acid (E)-, bis(trimethylsilyl) ester	Fumaric Acid	Organic acids
9303-replib	2-Butenedioic acid (Z)-, bis(trimethylsilyl) ester	Maleic Acid	Organic acids
129728-mainlib	2-Butenoic acid, 2-methyl-, trimethylsilyl ester, (E)-	2-methyl-2-butenoic acid	Organic acids
119414-mainlib	2(3H)-Furanone, dihydro-3,4-bis[(trimethylsilyl)oxy]-, trans-	Erythrono-1,4-lactone	Sugars
9299-replib	2,3,4-Trihydroxybutyric acid tetrakis(trimethylsilyl) deriv., (, (R*,R*)-)	Erythronic acid	Sugars
180081-mainlib	2,5-Dimethoxymandelic acid, di-TMS	2,5-Dimethoxymandelic acid	Benzenoids
207102-mainlib	2H-1-Benzopyran, 3,4-dihydro-2-[3,4-bis[(trimethylsilyl)oxy]phenyl]-3,5,7-	Catechine	Flavonoids

ID	Derivatized Name	Common Name	Class
	tris[(trimethylsilyl)oxy]-, (2R-trans)-		
115954-mainlib	3-Buten-2-one, 3-trimethylsilyloxy-		Alcohols or Polyols
29786-mainlib	3-Octadecyne	3-Octadecyne	Other
180080-mainlib	3,4-Dimethoxymandelic acid, di-TMS	3,4-Dimethoxymandelic acid	Benzenoids
9253-replib	3,6-Dioxa-2,7-disilaoctane, 2,2,4,7,7-pentamethyl-	1,2-propanediol	Alcohols or Polyols
37244-mainlib	4-Tris(trimethylsilyl)methylphenylisocyanate	4-tolyl isocyanate	Benzenoids
211614-mainlib	9,10-Anthracenedione, 3-methyl-1,6,8-tris[(trimethylsilyl)oxy]-	Emodin	Benzenoids
9961-replib	9,12-Octadecadienoic acid (Z,Z)-, trimethylsilyl ester	Linoleic acid	Lipids
9100-replib	?-Linolenic acid, trimethylsilyl ester	Linolenic acid	Lipids
26040-mainlib	Acetamide, 2,2,2-trifluoro-N-methyl-	N-Methyltrifluoroacetamide	Amides
180294-mainlib	Acetic acid, (3,4-dimethoxyphenyl)(trimethylsiloxy)-, methyl ester	Methyl (3,4-dimethoxyphenyl)(hydroxy)acetate	Benzenoids
38813-mainlib	Acetic acid, bis[(trimethylsilyl)oxyl]-, trimethylsilyl ester		Organic acids
1348-mainlib	Acetic acid, hydroxy-	Hydroxy-acetic acid	Organic acids
39649-mainlib	Adenosine-tetrakis(trimethylsilyl)-	Adenosine	Nucleoside
86262-mainlib	Adrenaline tetrakis(trimethylsilyl)	Adrenaline	Benzenoids
130618-mainlib	Alanine, N-methyl-n-butoxycarbonyl-, octyl ester	octyl 2-[butoxycarbonyl(methyl)amino]propanoate	Aminoacid derivative
86440-mainlib	Alanine, N-methyl-N-methoxycarbonyl-, hexyl ester	hexyl 2-[methoxycarbonyl(methyl)amino]propanoate	Aminoacid derivative
86442-mainlib	Alanine, N-methyl-N-methoxycarbonyl-, undecyl ester	undecyl 2-[butoxycarbonyl(methyl)amino]propanoate	Aminoacid derivative
39695-mainlib	Arabino-hexaric acid, 3-deoxy-2,4,5-tris-O-(trimethylsilyl)-, bis(trimethylsilyl) ester	3-Deoxy-arabino-hexaric acid	Sugars
37875-mainlib	Aucubin, hexakis(trimethylsilyl) ether	Aucubin	Terpenoids
39664-mainlib	Benzene, 1,2,3-tris[(trimethylsilyl)oxy]-	1,2,3-Trihydroxybenzene (Pyrogallic acid)	Benzenoids
39872-mainlib	Benzoic acid, 3,4,5-tris(trimethylsiloxy)-, trimethylsilyl ester	Gallic acid	Benzenoids
38436-mainlib	Butane, 1,2,3-tris(trimethylsiloxy)-	1,2,3-Butanetriol	Alcohols or Polyols

ID	Derivatized Name	Common Name	Class
119441-mainlib	Butanedioic acid, bis(trimethylsilyl) ester	Succinic acid	Organic acids
21411-replib	Butanedioic acid, methylene-, bis(trimethylsilyl) ester	Itaconic acid	Lipids
143908-mainlib	Butanoic acid, 4-[bis(trimethylsilyl)amino]-, trimethylsilyl ester	4-Aminobutyric acid (GABA)	Aminoacids
24430-replib	Cadaverine, N,N,N',N'-tetrakis(trimethylsilyl)	Cadaverine	Amines
39560-mainlib	Cinnamic acid, p-(trimethylsiloxy)-, trimethylsilyl ester	p-Coumaric acid	Phenylpropanoids
38812-mainlib	D-(-)- Erythrofuranose, tris(trimethylsilyl) ether (isomer 2)	Erythrose, furanose form	Sugars
39373-mainlib	D-(-)-Fructopyranose, pentakis(trimethylsilyl) ether (isomer 2)	Fructose, pyranose form	Sugars
170821-mainlib	D-(-)-Lyxofuranose, tetrakis(trimethylsilyl) ether	Lyxose, furanose form (Pectin)	Sugars
170816-mainlib	D-(-)-Ribofuranose, tetrakis(trimethylsilyl) ether (isomer 1)	Ribose,furanose form	Sugars
170819-mainlib	D-(+)-Talofuranose, pentakis(trimethylsilyl) ether (isomer 2)	Talose, furanose form	Sugars
9526-replib	D-Arabinonic acid, 2,3,5-tris-O-(trimethylsilyl)-, ?-lactone	Arabinonic acid, 1,4-lactone,	Organic acids
38368-mainlib	D-Erythro-Pentopyranose, 2-deoxy-1,3,4-tris-O-(trimethylsilyl)-	2-Deoxy-erythropentopyranose	Sugars
9402-replib	D-Gluconic acid, 2,3,4,5,6-pentakis-O-(trimethylsilyl)-, trimethylsilyl ester	Gluconic acid	Sugars
38783-mainlib	d-Gluconic acid, 2,3,4,6-tetrakis-O-(trimethylsilyl)-, ?-lactone	Gluconolactone	Sugars
39404-mainlib	D-Mannopyranose, 1,2,3,4-tetrakis-O-(trimethylsilyl)-, bis(trimethylsilyl) phosphate	Mannose 6-Phosphate	Sugars
38732-mainlib	Erythro-Pentonic acid, 2-deoxy-3,4,5-tris-O-(trimethylsilyl)-, trimethylsilyl ester	2-Deoxy-erythro-pentonic acid	Sugars
38695-mainlib	Ethanedioic acid, bis(trimethylsilyl) ester	Oxalic acid	Organic acids
15618-mainlib	Ethanol, 2-nitro-	2-nitro-ethanol	Others
164509-mainlib	Ethyl 2,3,4,6-tetrakis-O-(trimethylsilyl)-D-glucopyranoside	Ethyl D-glucopyranoside	Sugars
25951-mainlib	Ethylamine, 2-((p-bromo-?-methyl-?-phenylbenzyl)oxy)-N,N-dimethyl-	Embramine	Benzenoids
39403-mainlib	Glucopyranose, 1,2,3,4-tetrakis-O-(trimethylsilyl)-, bis(trimethylsilyl) phosphate	Glucose 6-Phosphate	Sugars
182910-mainlib	Glutamic acid, N-(trimethylsilyl)-, bis(trimethylsilyl) ester, L-	Glutamic acid	Aminoacids
39414-mainlib	Glycerol, tris(trimethylsilyl) ether	Glycerol	Alcohols or Polyols
164510-mainlib	Glyceryl-glycoside TMS ether	Glyceryl-glycoside	Sugars
39358-mainlib	Glycoside, methyl-trtrakis-O-(trimethylsilyl)-	Methyl glycoside	Sugars

ID	Derivatized Name	Common Name	Class
37037-mainlib	Hexadecanoic acid, 2,3-bis[(trimethylsilyl)oxy]propyl ester	1-Monopalmitin	Lipids
9118-replib	Hexadecanoic acid, trimethylsilyl ester	Hexadecanoic acid	Lipids
38761-mainlib	L-(-)-Sorbose, pentakis(trimethylsilyl) ether	Sorbose	Sugars
164512-mainlib	L-(+)-Rhamnopyranose, tetrakis(trimethylsilyl) ether	Rhamnose, pyranose form	Sugars
38907-mainlib	L-(+)-Tartaric acid, bis(trimethylsilyl) ether, bis(trimethylsilyl) ester	Tartaric acid	Organic acids
86273-mainlib	l-Alanine, N-(trimethylsilyl)-, trimethylsilyl ester	Alanine	Aminoacids
127099-mainlib	L-Alanine, N-methyl-N-(trifluoroacetyl)-, butyl ester	Butyl 2-[methyl(trifluoroacetyl)amino]propanoate	Aminoacid derivative
9234-replib	L-Asparagine, N,N2-bis(trimethylsilyl)-, trimethylsilyl ester	Asparagine	Aminoacids
39149-mainlib	L-Lysine, N2,N6,N6-tris(trimethylsilyl)-, trimethylsilyl ester	Lysine	Aminoacids
116925-mainlib	L-Norvaline, N-(trimethylsilyl)-, trimethylsilyl ester	Norvaline	Aminoacids
20907-replib	L-Proline, 1-(trimethylsilyl)-, trimethylsilyl ester	Proline	Aminoacids
129206-mainlib	L-Proline, 5-oxo-1-(trimethylsilyl)-, trimethylsilyl ester	5-oxo-Proline	Aminoacid derivative
27420-replib	L-Tyrosine, N,O-bis(trimethylsilyl)-, trimethylsilyl ester	Tyrosine	Aminoacids
39380-mainlib	Lyxose, tetra-(trimethylsilyl)-ether	Lyxose, Linear form	Sugars
38742-mainlib	Malonic acid, bis(2-trimethylsilylethyl ester	Malonic acid	Organic acids
39381-mainlib	Mannose, 6-deoxy-2,3,4,5-tetrakis-O-(trimethylsilyl)-, L-	6-deoxy-mannose, Linear form	Sugars
38855-mainlib	meso-Erythritol, tetrakis(trimethylsilyl) ether	Erythritol	Alcohols or Polyols
141919-mainlib	N,O-Bis-(trimethylsilyl)-N-methylleucine	Methylleucine	Aminoacid derivative
39552-mainlib	N,O-Bis-(trimethylsilyl)phenylalanine	Phenylalanine	Aminoacids
209278-mainlib	Octadecanoic acid, 2,3-bis[(trimethylsilyl)oxy]propyl ester	Monostearin	Lipids
9244-replib	Octadecanoic acid, trimethylsilyl ester	Octadecanoic acid (Stearic acid)	Lipids
38643-mainlib	Pentenoic acid, 4-[(trimethylsilyl)oxy]-, trimethylsilyl ester	Levulinic acid enol	Organic acids
86253-mainlib	Phenylpropanolamine, bis(trimethylsilyl)	Phenylpropanolamine (D-norephedrine or hydriatine)	Amines

ID	Derivatized Name	Common Name	Class
40201-mainlib	Phosphoric acid, bis(trimethylsilyl) 2,3-bis[(trimethylsilyl)oxy]propyl ester	Glycerophosphoric acid (BGA)	Lipids
180906-mainlib	Phosphoric acid, bis(trimethylsilyl)monomethyl ester	Methylphosphate	Others
180295-mainlib	Phthalic acid, di(3-methylphenyl) ester	di(3-methylphenyl) phthalic acid	Benzenoids
39557-mainlib	Propanetriol, 2-methyl-, tris-O-(trimethylsilyl)-	2-methyl-propanetriol	Alcohols or Polyols
38429-mainlib	Propanoic acid, 2-[(trimethylsilyl)oxy]-, trimethylsilyl ester	Lactic acid	Organic acids
119415-mainlib	Propanoic acid, 2-oxo-3-(trimethylsilyl)-, trimethylsilyl ester	Pyruvic acid	Organic acids
38809-mainlib	Propanoic acid, 2,3-bis[(trimethylsilyl)oxy]-, trimethylsilyl ester	Glyceric acid	Sugars
9203-replib	Ribitol, 1,2,3,4,5-pentakis-O-(trimethylsilyl)-	Ribitol	Alcohols or Polyols
38766-mainlib	Ribonic acid, 2,3,4,5-tetrakis-O-(trimethylsilyl)-, trimethylsilyl ester	Ribonic acid	Organic acids
205957-mainlib	Terbutaline, N-trifluoroacetyl-O,O,o-tris(trimethylsilyl)deriv.	N-trifluoroacetyl-Terbutaline	Benzenoids
9113-replib	trans-9-Octadecenoic acid, trimethylsilyl ester	Elaidic acid (Oleic acid)	Lipids
27526-replib	Trimethylsilyl 3,4-bis(trimethylsiloxy)cinnamate	Caffeic acid	Phenylpropanoids
38261-mainlib	Xylitol, 1,2,3,4,5-pentakis-O-(trimethylsilyl)-	Xylitol	Sugars
39372-mainlib	D-Xylanopyranose, TMS	Xylose, pyranose form	Sugars
9382-replib	Malic acid, TMS derivative	Malic acid	Organic acids
39387-mainlib	Galacturonic acid, TMS derivative	Galacturonic/Glucuronic acid	Sugars
39055-mainlib	L-Aspartic acid, TMS derivative	Aspartic acid	Aminoacids
51164-mainlib	L-Isoleucine, TMS derivative	Isoleucine	Aminoacids
130526-mainlib	L-Leucine, TMS derivative	Leucine	Aminoacids
38412-mainlib	L-Threonine, TMS derivative	Threonine	Aminoacids
36240-mainlib	L-Valine, TMS derivative	Valine	Aminoacids
86488-mainlib	Serine, TMS derivative	Serine	Aminoacids
39490-mainlib	Tagatofuranose/Fructofuranose	Tagatose/Fructose, furanose form	Sugars
164535-mainlib	Glucopyranose/Galactopyranose/Talopyranose	Glucose, Galactose, Talose, pyranose form	Sugars

ID	Derivatized Name	Common Name	Class
164548-mainlib	Glucose/Galactose, TMS derivative	Glucose, Galactose, linear form	Sugars
38857-mainlib	Inositol, TMS derivative	Inositol	Alcohols or Polyols

Table S2. List of principal GO terms of R-MagentaGreenPurpleSalmon resistant module ($p<0.05$), separated by biological process (P), molecular function (F) and cellular component (C). GO terms were filtered using REVIGO (0.4 similarity).

GO_acc	Term type	Term	Number in input list	Number in BG/Ref	pvalue	FDR
GO:1901135	P	carbohydrate derivative metabolic process	10	274	6.00E-05	0.0011
GO:0009056	P	catabolic process	7	244	0.003	0.031
GO:0045454	P	cell redox homeostasis	5	103	0.0014	0.018
GO:0043603	P	cellular amide metabolic process	10	408	0.0013	0.017
GO:0009987	P	cellular process	69	6925	0.0034	0.034
GO:0006091	P	generation of precursor metabolites and energy	5	90	0.00076	0.012
GO:1902600	P	hydrogen ion transmembrane transport	5	53	7.50E-05	0.0013
GO:0009141	P	nucleoside triphosphate metabolic process	10	90	4.20E-09	1.10E-06
GO:1901575	P	organic substance catabolic process	7	224	0.0019	0.022
GO:1901564	P	organonitrogen compound metabolic process	26	849	1.80E-09	9.60E-07
GO:0015979	P	photosynthesis	7	89	8.10E-06	0.00016
GO:0006457	P	protein folding	7	103	2.00E-05	0.00037
GO:0072521	P	purine-containing compound metabolic process	9	122	6.60E-07	1.60E-05
GO:0006979	P	response to oxidative stress	5	138	0.0046	0.045
GO:0044711	P	single-organism biosynthetic process	11	457	0.00085	0.012
GO:0044763	P	single-organism cellular process	31	2241	0.0007	0.011
GO:0044710	P	single-organism metabolic process	42	2807	8.50E-06	0.00016
GO:0044699	P	single-organism process	50	4462	0.0016	0.02
GO:0044281	P	small molecule metabolic process	21	610	1.10E-08	2.00E-06
GO:0016817	F	hydrolase activity, acting on acid anhydrides	12	528	0.00081	0.039
GO:0016853	F	isomerase activity	10	139	1.90E-07	3.70E-05
GO:0016667	F	oxidoreductase activity, acting on a sulfur group of donors	6	120	0.00039	0.025
GO:0003723	F	RNA binding	10	321	0.00021	0.02
GO:0005623	C	cell	35	1831	2.80E-07	6.20E-06
GO:0044464	C	cell part	35	1831	2.80E-07	6.20E-06
GO:0044444	C	cytoplasmic part	16	596	1.60E-05	0.00019
GO:0005622	C	intracellular	34	1726	2.20E-07	6.20E-06
GO:0044424	C	intracellular part	34	1649	7.60E-08	4.20E-06
GO:0032991	C	macromolecular complex	25	929	4.60E-08	4.20E-06
GO:0098796	C	membrane protein complex	10	193	3.30E-06	6.00E-05
GO:0043228	C	non-membrane-bounded organelle	12	506	0.00056	0.0039
GO:1990204	C	oxidoreductase complex	5	34	1.10E-05	0.00015
GO:0034357	C	photosynthetic membrane	5	57	0.0001	0.00088
GO:0009579	C	thylakoid	5	58	0.00011	0.00088

Table S3. List of principal GO terms of R-PinkYellowTan resistant module ($p<0.05$), separated by biological process (P), molecular function (F) and cellular component (C). GO terms were filtered using REVIGO (0.4 similarity).

GO_acc	Term type	Term	Number in input list	Number in BG/Ref	pvalue	FDR
GO:1901564	P	organonitrogen compound metabolic process	34	849	6.60E-17	3.40E-14
GO:0044281	P	small molecule metabolic process	28	610	2.30E-15	5.70E-13
GO:0044710	P	single-organism metabolic process	50	2807	4.10E-11	5.20E-09
GO:0044711	P	single-organism biosynthetic process	16	457	1.40E-07	8.90E-06
GO:0019693	P	ribose phosphate metabolic process	9	116	1.90E-07	1.00E-05
GO:0044699	P	single-organism process	56	4462	7.20E-07	2.60E-05
GO:0072521	P	purine-containing compound metabolic process	8	122	3.00E-06	5.60E-05
GO:0006807	P	nitrogen compound metabolic process	36	2383	3.30E-06	5.90E-05
GO:0008652	P	cellular amino acid biosynthetic process	6	56	4.00E-06	6.90E-05
GO:0006091	P	generation of precursor metabolites and energy	7	90	4.40E-06	7.20E-05
GO:0072524	P	pyridine-containing compound metabolic process	6	61	6.30E-06	8.80E-05
GO:0009058	P	biosynthetic process	33	2143	6.40E-06	8.80E-05
GO:0044763	P	single-organism cellular process	34	2241	6.10E-06	8.80E-05
GO:0008152	P	metabolic process	89	9388	8.80E-06	0.00012
GO:0051186	P	cofactor metabolic process	8	143	9.10E-06	0.00012
GO:0006732	P	coenzyme metabolic process	7	117	2.20E-05	0.00028
GO:0043603	P	cellular amide metabolic process	11	408	0.00014	0.0012
GO:1901135	P	carbohydrate derivative metabolic process	9	274	0.00014	0.0012
GO:1901575	P	organic substance catabolic process	7	224	0.001	0.0083
GO:0009056	P	catabolic process	7	244	0.0017	0.013
GO:0019725	P	cellular homeostasis	5	124	0.0019	0.015
GO:0044723	P	single-organism carbohydrate metabolic process	6	238	0.0065	0.049
GO:0016614	F	oxidoreductase activity, acting on CH-OH group of donors	10	140	7.80E-08	7.50E-06
GO:0016491	F	oxidoreductase activity	32	2023	5.30E-06	0.00026
GO:0048037	F	cofactor binding	14	469	5.40E-06	0.00026
GO:0003735	F	structural constituent of ribosome	10	274	2.50E-05	0.00096
GO:0005198	F	structural molecule activity	10	290	4.00E-05	0.0013
GO:0050662	F	coenzyme binding	11	361	4.80E-05	0.0013
GO:0003824	F	catalytic activity	84	9441	0.00044	0.0094
GO:0003723	F	RNA binding	8	321	0.0019	0.036
GO:0005840	C	ribosome	11	273	3.90E-06	8.20E-05
GO:0005622	C	intracellular	29	1726	5.30E-06	8.30E-05
GO:0044464	C	cell part	29	1831	1.60E-05	0.00013
GO:0005623	C	cell	29	1831	1.60E-05	0.00013
GO:0044424	C	intracellular part	26	1649	5.30E-05	0.00037
GO:0044444	C	cytoplasmic part	14	596	7.10E-05	0.00042

GO_acc	Term type	Term	Number in input list	Number in BG/Ref	pvalue	FDR
GO:0032991	C	macromolecular complex	18	929	7.40E-05	0.00042
GO:0043226	C	organelle	19	1295	0.0014	0.0064

Table S4. List of principal GO terms of R-Blue resistant module ($p<0.05$), separated by biological process (P), molecular function (F) and cellular component (C). GO terms were filtered using REVIGO (0.4 similarity).

GO_acc	term type	Term	Number in input list	Number in BG/Ref	pvalue	FDR
GO:1901575	P	organic substance catabolic process	6	224	5.40E-05	0.0047
GO:0009056	P	catabolic process	6	244	8.50E-05	0.0047
GO:0044710	P	single-organism metabolic process	18	2807	0.00074	0.017
GO:0008152	P	metabolic process	40	9388	0.00048	0.017
GO:1901564	P	organonitrogen compound metabolic process	9	849	0.00077	0.017
GO:0044281	P	small molecule metabolic process	7	610	0.002	0.037
GO:0016614	F	oxidoreductase activity, acting on CH-OH group of donors	5	140	6.40E-05	0.0019
GO:0005623	C	cell	13	1831	0.002	0.0094
GO:0005622	C	intracellular	13	1726	0.0012	0.0094
GO:0044464	C	cell part	13	1831	0.002	0.0094
GO:0044424	C	intracellular part	12	1649	0.0025	0.0094
GO:0032991	C	macromolecular complex	8	929	0.0055	0.016
GO:0043234	C	protein complex	6	616	0.0092	0.023

Table S5. List of principal GO terms of R-Cyan resistant module ($p<0.05$), separated by biological process (P), molecular function (F) and cellular component (C). GO terms were filtered using REVIGO (0.4 similarity).

GO_acc	Term type	Term	Number in input list	Number in BG/Ref	pvalue	FDR
GO:0044281	P	small molecule metabolic process	9	610	2.30E-07	1.80E-05
GO:0044711	P	single-organism biosynthetic process	8	457	3.50E-07	1.80E-05
GO:1901564	P	organonitrogen compound metabolic process	9	849	3.50E-06	8.80E-05
GO:1901566	P	organonitrogen compound biosynthetic process	8	618	3.30E-06	8.80E-05
GO:0044763	P	single-organism cellular process	13	2241	1.00E-05	0.00021
GO:0044710	P	single-organism metabolic process	14	2807	2.30E-05	0.00038
GO:0019637	P	organophosphate metabolic process	5	230	2.70E-05	0.00038
GO:0044699	P	single-organism process	16	4462	0.00026	0.0033
GO:0009058	P	biosynthetic process	10	2143	0.00095	0.0095

Table S6. List of principal GO terms of R-Red resistant module ($p<0.05$), separated by biological process (P), molecular function (F) and cellular component (C). GO terms were filtered using REVIGO (0.4 similarity).

GO_acc	Term type	Term	Number in input list	Number in BG/Ref	pvalue	FDR
GO:0015979	P	photosynthesis	6	89	4.10E-07	1.70E-05
GO:0019904	F	protein domain specific binding	5	12	1.30E-09	1.40E-07
GO:0016491	F	oxidoreductase activity	15	2023	0.00081	0.031
GO:0048037	F	cofactor binding	7	469	0.00055	0.031

Table S7. List of principal GO terms of R-Turquoise resistant module ($p<0.05$), separated by biological process (P), molecular function (F) and cellular component (C). GO terms were filtered using REVIGO (0.4 similarity).

GO_acc	Term type	Term	Number in input list	Number in BG/Ref	pvalue	FDR
GO:0006091	P	generation of precursor metabolites and energy	8	90	4.00E-09	9.60E-07
GO:1901564	P	organonitrogen compound metabolic process	17	849	2.30E-08	2.80E-06
GO:0044281	P	small molecule metabolic process	12	610	4.20E-06	0.00029
GO:0051186	P	cofactor metabolic process	6	143	2.40E-05	0.0012
GO:0006732	P	coenzyme metabolic process	5	117	0.00011	0.003
GO:0072521	P	purine-containing compound metabolic process	5	122	0.00013	0.003
GO:0006163	P	purine nucleotide metabolic process	5	120	0.00012	0.003
GO:0043603	P	cellular amide metabolic process	8	408	0.0002	0.0034
GO:0044710	P	single-organism metabolic process	23	2807	0.00028	0.0043
GO:0009058	P	biosynthetic process	18	2143	0.0012	0.013
GO:0006807	P	nitrogen compound metabolic process	19	2383	0.0015	0.016
GO:1901575	P	organic substance catabolic process	5	224	0.0019	0.019
GO:0044723	P	single-organism carbohydrate metabolic process	5	238	0.0025	0.024
GO:0009056	P	catabolic process	5	244	0.0028	0.026
GO:0044249	P	cellular biosynthetic process	16	1984	0.0035	0.031
GO:0008152	P	metabolic process	48	9388	0.0045	0.037
GO:0005975	P	carbohydrate metabolic process	8	673	0.0047	0.037
GO:0043232	C	intracellular non-membrane-bounded organelle	8	506	0.00081	0.024

Table S8. List of principal GO terms of R-BlackBrownGreenyellow resistant module ($p<0.05$), separated by biological process (P), molecular function (F) and cellular component (C). GO terms were filtered using REVIGO (0.4 similarity).

GO_acc	Term type	Term	Number in input list	Number in BG/Ref	pvalue	FDR
GO:0015979	P	photosynthesis	15	89	2.10E-16	8.70E-14
GO:0044281	P	small molecule metabolic process	26	610	5.10E-14	1.10E-11
GO:0044710	P	single-organism metabolic process	51	2807	1.90E-12	2.60E-10
GO:1901564	P	organonitrogen compound metabolic process	27	849	1.20E-11	1.20E-09
GO:0006091	P	generation of precursor metabolites and energy	11	90	5.80E-11	4.80E-09
GO:0019684	P	photosynthesis, light reaction	8	34	2.60E-10	1.80E-08
GO:0008152	P	metabolic process	94	9388	3.30E-09	1.70E-07
GO:0044712	P	single-organism catabolic process	8	91	2.80E-07	8.90E-06
GO:1901605	P	alpha-amino acid metabolic process	7	66	4.90E-07	1.40E-05
GO:0009056	P	catabolic process	11	244	9.30E-07	2.40E-05
GO:0044237	P	cellular metabolic process	61	5625	5.30E-06	8.90E-05
GO:0044699	P	single-organism process	52	4462	5.90E-06	9.50E-05
GO:0044711	P	single-organism biosynthetic process	13	457	1.30E-05	0.00017
GO:0019693	P	ribose phosphate metabolic process	7	116	1.60E-05	0.00021
GO:0006979	P	response to oxidative stress	7	138	4.70E-05	0.00047
GO:0043603	P	cellular amide metabolic process	11	408	9.70E-05	0.00082
GO:1901135	P	carbohydrate derivative metabolic process	9	274	0.0001	0.00085
GO:0044763	P	single-organism cellular process	30	2241	0.00011	0.00094
GO:0009987	P	cellular process	66	6925	0.00014	0.0012
GO:0006807	P	nitrogen compound metabolic process	29	2383	0.00075	0.0056
GO:0009058	P	biosynthetic process	25	2143	0.0033	0.023
GO:0016491	F	oxidoreductase activity	32	2023	2.20E-06	0.00044
GO:0016209	F	antioxidant activity	8	148	8.60E-06	0.00088
GO:0016853	F	isomerase activity	7	139	4.90E-05	0.0033
GO:0016684	F	oxidoreductase activity, acting on peroxide as acceptor	6	133	0.00031	0.012
GO:0016614	F	oxidoreductase activity, acting on CH-OH group of donors	6	140	0.0004	0.014
GO:0003735	F	structural constituent of ribosome	8	274	0.00054	0.016
GO:0005198	F	structural molecule activity	8	290	0.00077	0.02
GO:0016829	F	lyase activity	7	229	0.00093	0.021
GO:0004601	F	peroxidase activity	5	131	0.002	0.037
GO:0034357	C	photosynthetic membrane	8	57	9.90E-09	3.00E-07
GO:0009579	C	thylakoid	8	58	1.10E-08	3.00E-07
GO:0032991	C	macromolecular complex	21	929	8.80E-07	1.40E-05
GO:0044424	C	intracellular part	27	1649	8.90E-06	0.0001
GO:0005622	C	intracellular	27	1726	2.00E-05	0.0002
GO:0044464	C	cell part	27	1831	5.60E-05	0.00045
GO:0005623	C	cell	27	1831	5.60E-05	0.00045
GO:0044444	C	cytoplasmic part	12	596	0.00064	0.0037
GO:1990904	C	ribonucleoprotein complex	8	314	0.0013	0.0065

Table S9. List of principal GO terms of S-RedTanMagentaSalmon susceptible module ($p<0.05$), separated by biological process (P), molecular function (F) and cellular component (C). GO terms were filtered using REVIGO (0.4 similarity).

GO_acc	Term type	Term	Number in input list	Number in BG/Ref	pvalue	FDR
GO:1901564	P	organonitrogen compound metabolic process	26	849	6.80E-11	3.60E-08
GO:0044281	P	small molecule metabolic process	20	610	4.80E-09	1.20E-06
GO:0015979	P	photosynthesis	8	89	2.40E-07	2.50E-05
GO:0072524	P	pyridine-containing compound metabolic process	7	61	3.00E-07	2.60E-05
GO:0044710	P	single-organism metabolic process	40	2807	1.10E-06	6.40E-05
GO:0006096	P	glycolytic process	5	41	1.20E-05	0.00028
GO:0044711	P	single-organism biosynthetic process	13	457	1.30E-05	0.00028
GO:1901607	P	alpha-amino acid biosynthetic process	5	43	1.50E-05	0.00032
GO:0019637	P	organophosphate metabolic process	9	230	2.80E-05	0.00051
GO:0006091	P	generation of precursor metabolites and energy	6	90	4.00E-05	0.00061
GO:0051186	P	cofactor metabolic process	7	143	5.90E-05	0.00083
GO:0072521	P	purine-containing compound metabolic process	6	122	0.0002	0.0021
GO:0055086	P	nucleobase-containing small molecule metabolic process	7	181	0.00024	0.0026
GO:1901135	P	carbohydrate derivative metabolic process	8	274	0.00054	0.0048
GO:0006457	P	protein folding	5	103	0.00072	0.0063
GO:0044763	P	single-organism cellular process	27	2241	0.0014	0.011
GO:0006807	P	nitrogen compound metabolic process	28	2383	0.0016	0.013
GO:0043603	P	cellular amide metabolic process	9	408	0.0017	0.013
GO:0044699	P	single-organism process	43	4462	0.0039	0.029
GO:0009056	P	catabolic process	6	244	0.0061	0.044
GO:0048037	F	cofactor binding	11	469	0.00032	0.022
GO:0016853	F	isomerase activity	6	139	0.00038	0.022
GO:0050662	F	coenzyme binding	10	361	0.00016	0.022
GO:0034357	C	photosynthetic membrane	8	57	9.90E-09	3.40E-07
GO:0009579	C	thylakoid	8	58	1.10E-08	3.40E-07
GO:0032991	C	macromolecular complex	18	929	4.40E-05	0.00079
GO:0005622	C	intracellular	26	1726	5.60E-05	0.00084
GO:0044424	C	intracellular part	25	1649	7.20E-05	0.00093
GO:0044464	C	cell part	26	1831	0.00015	0.0015
GO:0005623	C	cell	26	1831	0.00015	0.0015
GO:0098796	C	membrane protein complex	7	193	0.00035	0.0032
GO:0044444	C	cytoplasmic part	11	596	0.0021	0.016
GO:0005737	C	cytoplasm	12	733	0.0036	0.025
GO:0043232	C	intracellular non-membrane-bounded organelle	9	506	0.0068	0.041
GO:0043228	C	non-membrane-bounded organelle	9	506	0.0068	0.041

Table S10. List of principal GO terms of S-PurpleTurquoise susceptible module ($p<0.05$), separated by biological process (P), molecular function (F) and cellular component (C). GO terms were filtered using REVIGO (0.4 similarity).

GO_acc	Term type	Term	Number in input list	Number in BG/Ref	pvalue	FDR
GO:1901564	P	organonitrogen compound metabolic process	27	849	2.60E-11	8.60E-09
GO:0044281	P	small molecule metabolic process	21	610	1.50E-09	2.40E-07
GO:0044710	P	single-organism metabolic process	43	2807	1.20E-07	1.30E-05
GO:0006520	P	Cellular amino acid metabolic process	8	148	1.10E-05	0.00045
GO:1901575	P	organic substance catabolic process	9	224	2.90E-05	0.0011
GO:0009056	P	catabolic process	9	244	5.60E-05	0.0019
GO:0006412	P	translation	11	383	7.50E-05	0.0023
GO:0006807	P	nitrogen compound metabolic process	32	2383	0.00011	0.0025
GO:0008152	P	metabolic process	85	9388	0.00012	0.0025
GO:0043603	P	cellular amide metabolic process	11	408	0.00013	0.0025
GO:0044699	P	single-organism process	49	4462	0.00017	0.0032
GO:0015979	P	photosynthesis	5	89	0.00044	0.0061
GO:0006457	P	protein folding	5	103	0.00083	0.011
GO:0045454	P	cell redox homeostasis	5	103	0.00083	0.011
GO:0044763	P	single-organism cellular process	28	2241	0.0011	0.013
GO:0009987	P	cellular process	63	6925	0.0027	0.029
GO:0051186	P	cofactor metabolic process	5	143	0.0033	0.033
GO:0044237	P	cellular metabolic process	53	5625	0.0037	0.036
GO:0009117	P	nucleotide metabolic process	5	149	0.0039	0.037
GO:0016491	F	oxidoreductase activity	29	2023	8.50E-05	0.009
GO:0048037	F	cofactor binding	12	469	0.0001	0.009
GO:0005622	C	intracellular	30	1726	1.50E-06	8.00E-05
GO:0032991	C	macromolecular complex	20	929	5.60E-06	8.00E-05
GO:0044464	C	cell part	30	1831	4.90E-06	8.00E-05
GO:0005623	C	cell	30	1831	4.90E-06	8.00E-05
GO:0044424	C	intracellular part	29	1649	1.80E-06	8.00E-05
GO:0044444	C	cytoplasmic part	13	596	0.00025	0.0028
GO:0043228	C	non-membrane-bounded organelle	10	506	0.0026	0.02
GO:1990904	C	ribonucleoprotein complex	7	314	0.0062	0.035

Table S11. List of principal GO terms of S-Blue susceptible module ($p<0.05$), separated by biological process (P), molecular function (F) and cellular component (C). GO terms were filtered using REVIGO (0.4 similarity).

GO_acc	Term type	Term	Number in input list	Number in BG/Ref	pvalue	FDR
GO:0044281	P	small molecule metabolic process	16	610	1.90E-09	7.70E-07
GO:0009141	P	nucleoside triphosphate metabolic process	7	90	1.00E-07	2.00E-05
GO:1901564	P	organonitrogen compound metabolic process	16	849	1.80E-07	2.40E-05
GO:0044710	P	single-organism metabolic process	29	2807	3.40E-07	3.40E-05
GO:1901657	P	glycosyl compound metabolic process	7	132	1.20E-06	6.80E-05
GO:0006091	P	generation of precursor metabolites and energy	6	90	2.10E-06	7.40E-05
GO:0072521	P	purine-containing compound metabolic process	6	122	1.10E-05	0.00019
GO:1901135	P	carbohydrate derivative metabolic process	8	274	1.40E-05	0.00024
GO:0015979	P	photosynthesis	5	89	3.40E-05	0.00046
GO:0044711	P	single-organism biosynthetic process	9	457	8.30E-05	0.001
GO:0044699	P	single-organism process	32	4462	0.00017	0.0021
GO:0044763	P	single-organism cellular process	20	2241	0.00032	0.0037
GO:1901575	P	organic substance catabolic process	5	224	0.002	0.023
GO:0009056	P	catabolic process	5	244	0.0029	0.031
GO:0016614	F	oxidoreductase activity, acting on CH-OH group of donors	6	140	2.30E-05	0.00088
GO:0016853	F	isomerase activity	6	139	2.20E-05	0.00088
GO:0016491	F	oxidoreductase activity	20	2023	8.00E-05	0.0023
GO:0003735	F	structural constituent of ribosome	6	274	0.0008	0.015
GO:0005198	F	structural molecule activity	6	290	0.0011	0.017
GO:0044424	C	intracellular part	21	1649	1.00E-06	6.40E-05
GO:0005622	C	intracellular	21	1726	2.10E-06	6.60E-05
GO:0044464	C	cell part	21	1831	5.30E-06	7.20E-05
GO:0005623	C	cell	21	1831	5.30E-06	7.20E-05
GO:0032991	C	macromolecular complex	13	929	6.60E-05	0.0007
GO:0044444	C	cytoplasmic part	10	596	0.00012	0.0011
GO:0005840	C	ribosome	6	273	0.00078	0.0062
GO:0043226	C	organelle	11	1295	0.012	0.048

Table S12. List of principal GO terms of S-Brown susceptible module ($p<0.05$), separated by biological process (P), molecular function (F) and cellular component (C). GO terms were filtered using REVIGO (0.4 similarity).

GO_acc	Term type	Term	Number in input list	Number in BG/Ref	pvalue	FDR
GO:0015979	P	photosynthesis	8	89	6.40E-10	1.70E-07
GO:0006091	P	generation of precursor metabolites and energy	7	90	2.10E-08	2.70E-06
GO:0019684	P	photosynthesis, light reaction	5	34	1.30E-07	1.10E-05
GO:0019693	P	ribose phosphate metabolic process	6	116	2.20E-06	0.00014
GO:0055086	P	nucleobase-containing small molecule metabolic process	6	181	2.50E-05	0.00046
GO:0072521	P	purine-containing compound metabolic process	5	122	4.70E-05	0.00068
GO:0008152	P	metabolic process	44	9388	9.50E-05	0.0011
GO:1901135	P	carbohydrate derivative metabolic process	6	274	0.00023	0.0026
GO:1901564	P	organonitrogen compound metabolic process	10	849	0.0003	0.0032
GO:0044281	P	small molecule metabolic process	8	610	0.00064	0.0066
GO:1901575	P	organic substance catabolic process	5	224	0.00074	0.0073
GO:0009056	P	catabolic process	5	244	0.0011	0.01
GO:0044710	P	single-organism metabolic process	18	2807	0.0018	0.017
GO:0044711	P	single-organism biosynthetic process	6	457	0.0032	0.028

Table S13. List of principal GO terms of S-Black susceptible module ($p<0.05$), separated by biological process (P), molecular function (F) and cellular component (C). GO terms were filtered using REVIGO (0.4 similarity).

GO_acc	Term type	Term	Number in input list	Number in BG/Ref	pvalue	FDR
GO:1901564	P	organonitrogen compound metabolic process	11	849	3.20E-06	0.00049
GO:1901566	P	organonitrogen compound biosynthetic process	9	618	1.20E-05	0.0009

Table S14. List of principal GO terms of S-YellowPink susceptible module ($p<0.05$), separated by biological process (P), molecular function (F) and cellular component (C). GO terms were filtered using REVIGO (0.4 similarity).

GO_acc	Term type	Term	Number in input list	Number in BG/Ref	pvalue	FDR
GO:1901564	P	organonitrogen compound metabolic process	20	849	1.50E-09	5.30E-07
GO:0044710	P	single-organism metabolic process	35	2807	6.90E-09	1.20E-06
GO:0044281	P	small molecule metabolic process	15	610	1.30E-07	1.50E-05
GO:0006091	P	generation of precursor metabolites and energy	7	90	2.90E-07	2.60E-05
GO:0044712	P	single-organism catabolic process	6	91	5.20E-06	0.00028
GO:0051186	P	cofactor metabolic process	7	143	5.40E-06	0.00028
GO:0006732	P	coenzyme metabolic process	6	117	2.10E-05	0.00067
GO:0009056	P	catabolic process	8	244	1.90E-05	0.00067
GO:0009167	P	purine ribonucleoside monophosphate metabolic process	5	87	6.20E-05	0.0011
GO:0008152	P	metabolic process	61	9388	6.00E-05	0.0011
GO:0006979	P	response to oxidative stress	6	138	5.00E-05	0.0011
GO:0044699	P	single-organism process	36	4462	0.00015	0.002
GO:0009058	P	biosynthetic process	21	2143	0.00055	0.0054
GO:0044711	P	single-organism biosynthetic process	8	457	0.0012	0.011
GO:0006412	P	translation	7	383	0.002	0.017
GO:0006807	P	nitrogen compound metabolic process	21	2383	0.0021	0.018
GO:0043603	P	cellular amide metabolic process	7	408	0.0028	0.021
GO:0044237	P	cellular metabolic process	38	5625	0.0035	0.026
GO:0044763	P	single-organism cellular process	19	2241	0.0055	0.039
GO:0016491	F	oxidoreductase activity	25	2023	2.70E-06	0.00033
GO:0016614	F	oxidoreductase activity, acting on CH-OH group of donors	6	140	5.40E-05	0.0022
GO:0003735	F	structural constituent of ribosome	7	274	0.00029	0.0091
GO:0005198	F	structural molecule activity	7	290	0.00041	0.01
GO:0003824	F	catalytic activity	58	9441	0.00089	0.019
GO:0005737	C	cytoplasm	12	733	0.00013	0.002
GO:0005840	C	ribosome	7	273	0.00029	0.0033
GO:0044444	C	cytoplasmic part	10	596	0.00042	0.0038
GO:0032991	C	macromolecular complex	12	929	0.0011	0.0083
GO:0044464	C	cell part	17	1831	0.0036	0.021
GO:0005623	C	cell	17	1831	0.0036	0.021
GO:0005622	C	intracellular	16	1726	0.0049	0.025

Table S15. List of principal GO terms of S-GreenGreenyellow susceptible module ($p<0.05$), separated by biological process (P), molecular function (F) and cellular component (C). GO terms were filtered using REVIGO (0.4 similarity).

GO_acc	Term type	Term	Number in input list	Number in BG/Ref	pvalue	FDR
GO:1901564	P	organonitrogen compound metabolic process	17	849	9.80E-08	1.70E-05
GO:0006091	P	generation of precursor metabolites and energy	6	90	3.20E-06	0.00028
GO:0009205	P	purine ribonucleoside triphosphate metabolic process	5	88	4.60E-05	0.0016
GO:1901575	P	organic substance catabolic process	7	224	5.50E-05	0.0016
GO:0044710	P	single-organism metabolic process	26	2807	6.40E-05	0.0017
GO:0009056	P	catabolic process	7	244	9.30E-05	0.0021
GO:0044711	P	single-organism biosynthetic process	9	457	0.00015	0.0025
GO:0072521	P	purine-containing compound metabolic process	5	122	0.0002	0.0029
GO:0006508	P	proteolysis	9	634	0.0015	0.017
GO:0008152	P	metabolic process	53	9388	0.0023	0.024
GO:0055114	P	oxidation-reduction process	16	1849	0.0045	0.045
GO:0032991	C	macromolecular complex	12	929	0.00057	0.031

SUPPLEMENTARY FIGURES

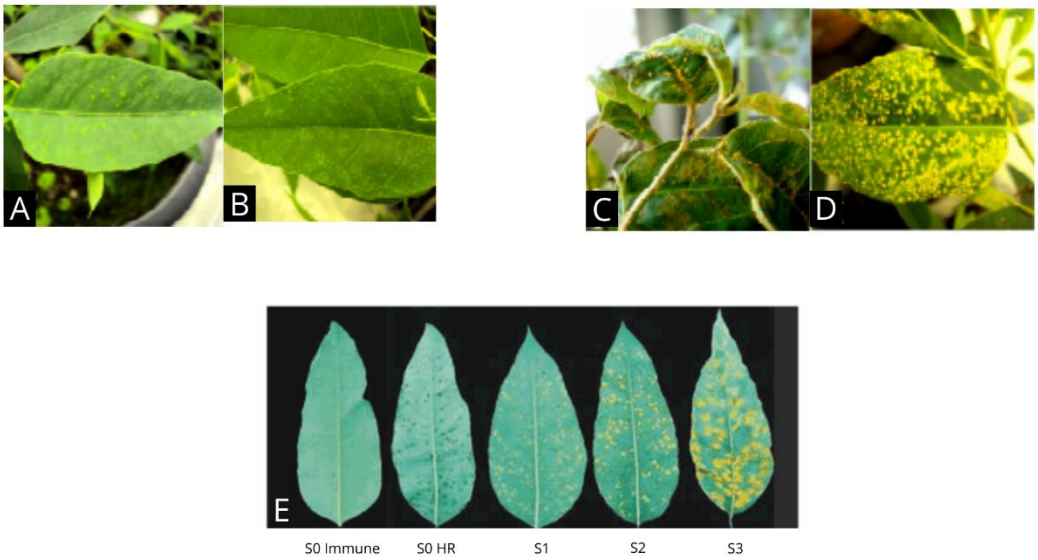

Figure S1. Characterization of symptoms at 11days after inoculation (dai) of *A. psidii* infection in rust-resistant (B) R3 selected genotype, in comparison with (A) resistant genotype BRASUZ clone, both displaying only chlorotic spots. (D) Rust-susceptible selected genotype S4 and (C) previously known susceptible genotype M09D1 used as comparison, both displaying characteristic yellow pustules on adaxial and abaxial leaf surfaces R3 genotype was identified as S0 HR and S4 genotype as S3, according to JUNGHANS et al (2003) scale (E).

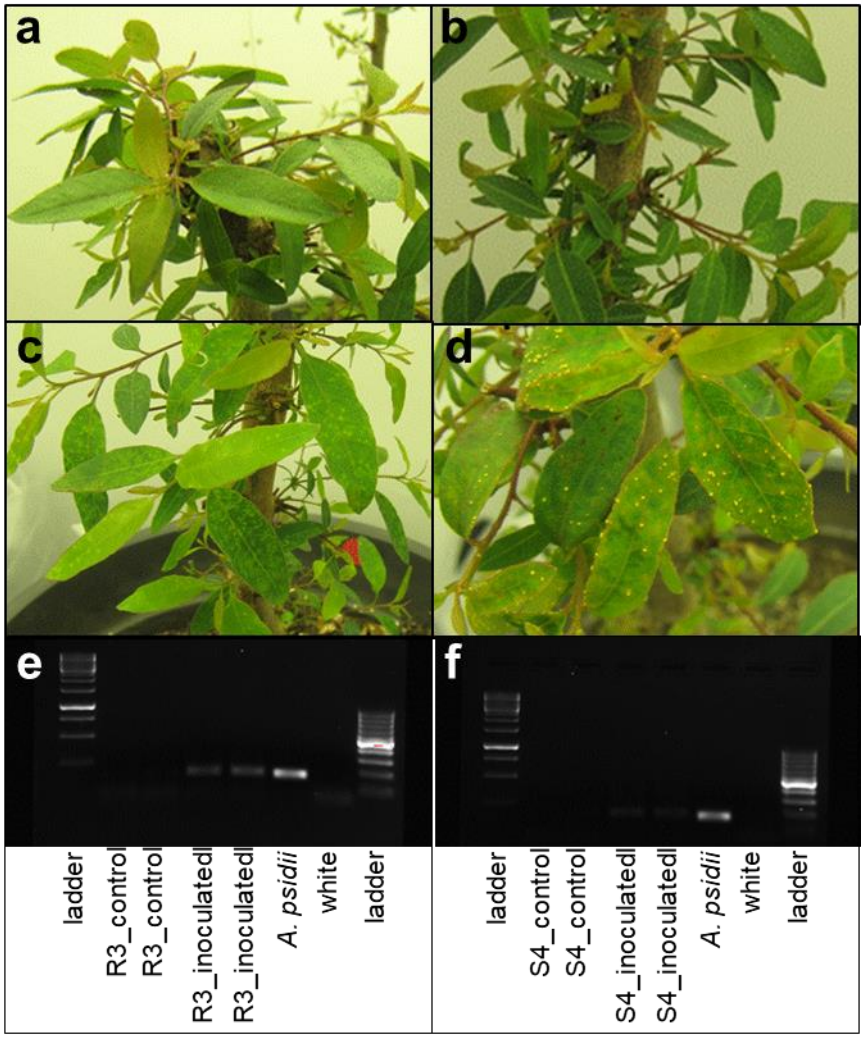

Figure S2. Confirmation of inoculation and mock-inoculation of control plants at 11 days after inoculation. (a) Mock-inoculated resistant plants. (b) Mock-inoculated susceptible plants. Both without any visual symptoms. (c) Inoculated resistant plants displaying symptoms of hypersensitive reactions. (d) Inoculated S4 plants with characteristic yellow pustules. Presence or Absence of *A. psidii* was confirmed using an agarose gel containing amplified DNA fragments produced using specific *A. psidii* primers, for (e) resistant and (f) susceptible genotype (SEKIYA, 2020).

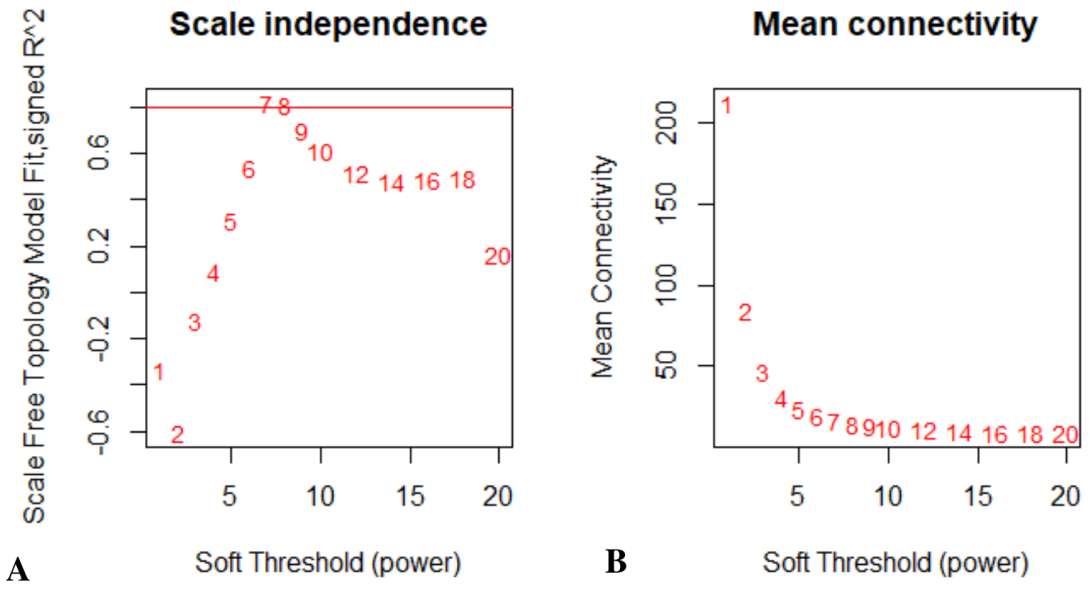

Figure S3. Graphical parameters utilized to construct WGCNA network by choosing a soft thereshold. (A) Scale independence and (B) mean connectivity for resistant proteins. Soft threshold of 7 were used.

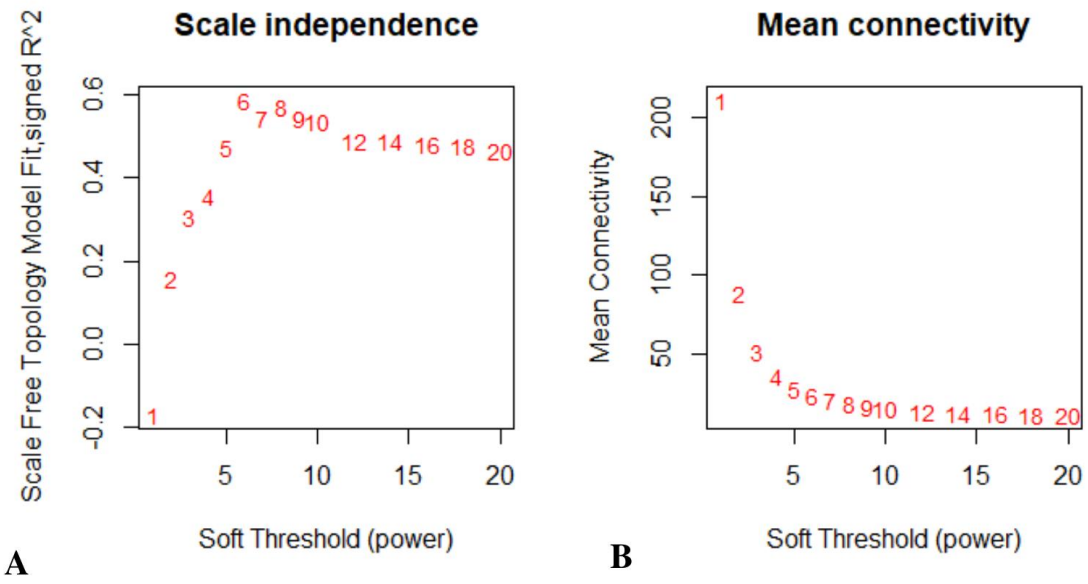

Figure S4. Graphical parameters utilized to construct WGCNA network by choosing a soft thereshold. (A) Scale independence and (B) mean connectivity for susceptbile proteins. Soft threshold of 6 were used.

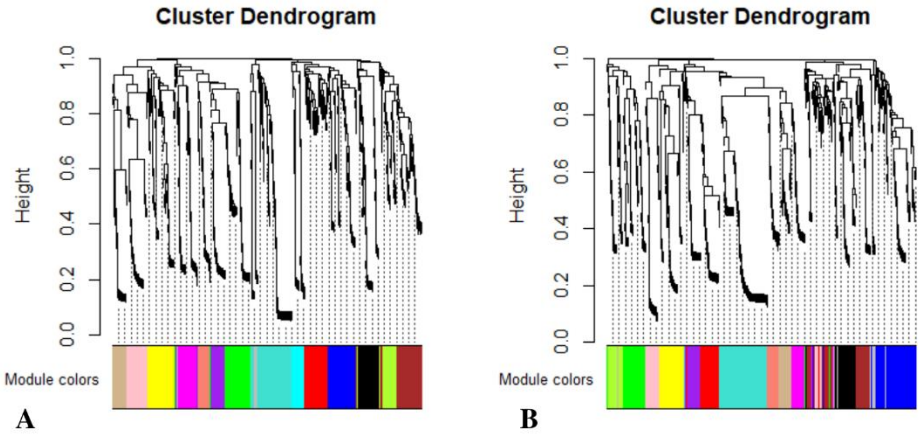

Figure S5. Cluster Dendrogram of protein modules of both resistant (A) and susceptible (B) genotypes, initially generated with WGCNA. There were obtained 13 and 14 protein modules.